University of Pavia

Department of Molecular Medicine

PhD course in Translational Medicine

XXXIV cycle

PhD thesis on

Development of *ex vivo* bone marrow model for platelet production and drug testing

Tutor:

Prof. Alessandra Balduini

Candidate:

Dr. Paolo Maria Soprano

Academic year 2020-2021

Introduction

The Bone Marrow

The human bone marrow is a soft and viscous tissue located in the hollow space of the bones where it hosts the multipotent hematopoietic stem cells (HSCs), responsible for the regulation of blood cell production.

Structurally, the bone marrow is mainly composed of the vasculature enclosed in a mesh of Extracellular Matrix (ECM) components and soluble factors.

In adults, the bone marrow is hosted in the mid-diaphyseal portion of peripheral bones which consist of irregular interconnected spaces by bone trabeculae. The osseous tissue of bone trabeculae and the marrow are separated by a layer of connective tissue, the endosteum, covered by osteoblasts (OBs) and osteoclasts which play a pivotal role in remodeling the surface of the bone and providing an anatomical location for immature HSCs, defined as the endosteal region.

The cellular compartment of the bone marrow includes HSCs, blood cell progenitors, and randomly distributed stromal cells. The assessment of bone marrow functionality is strictly related to its cellularity, defined as the percentage of bone marrow volume occupied by HSCs. In general, the bone marrow cellularity decreases with aging.

The hematopoietic process is strongly affected by the interaction between the HSCs and the stromal cells which contributes to determining the stem cell fate, namely quiescence, differentiation, or mobilization. The HSC is a multipotent stem cell and is defined by its ability to self-renew as well as give rise to all blood cells progenitors, that can differentiate into mature blood cell types. These cells are $CD34^+$, $Thy-1^+$, Lin^-, c-kit^{low}, and $CD38^-$ (Shin et al, 2014). HSCs reside in a specific niche environment, closely associated with endosteum, in a condition of relative hypoxia. In this niche, HSCs remain in a non-replicative and quiescent state, mainly regulated by the interaction with OBs, and probably sustained by a quite stiff matrix (>35 kPa) (Buxboim et al, 2010; Nelson et al, 2016). On the other side, HSCs can be associated with sinusoidal endothelium, where Endothelial Cells (ECs), Perivascular Mesenchymal Stem cells (MSCs), CXCL12-abundant reticular cells, and macrophages contribute to the differentiation in mature blood cells. In this context, cell-cell interaction, released factors (CXCL12, SCF, E-Selectin, Leptin, Nestin), and a quite soft matrix (0.3 kPa in the marrow, 0.5-2 kPa in endothelium, 5-8 kPa in the vessels) determine a specific environment to foster HSC differentiation (Chatterjee et al, 2021)(**Figure 1**).
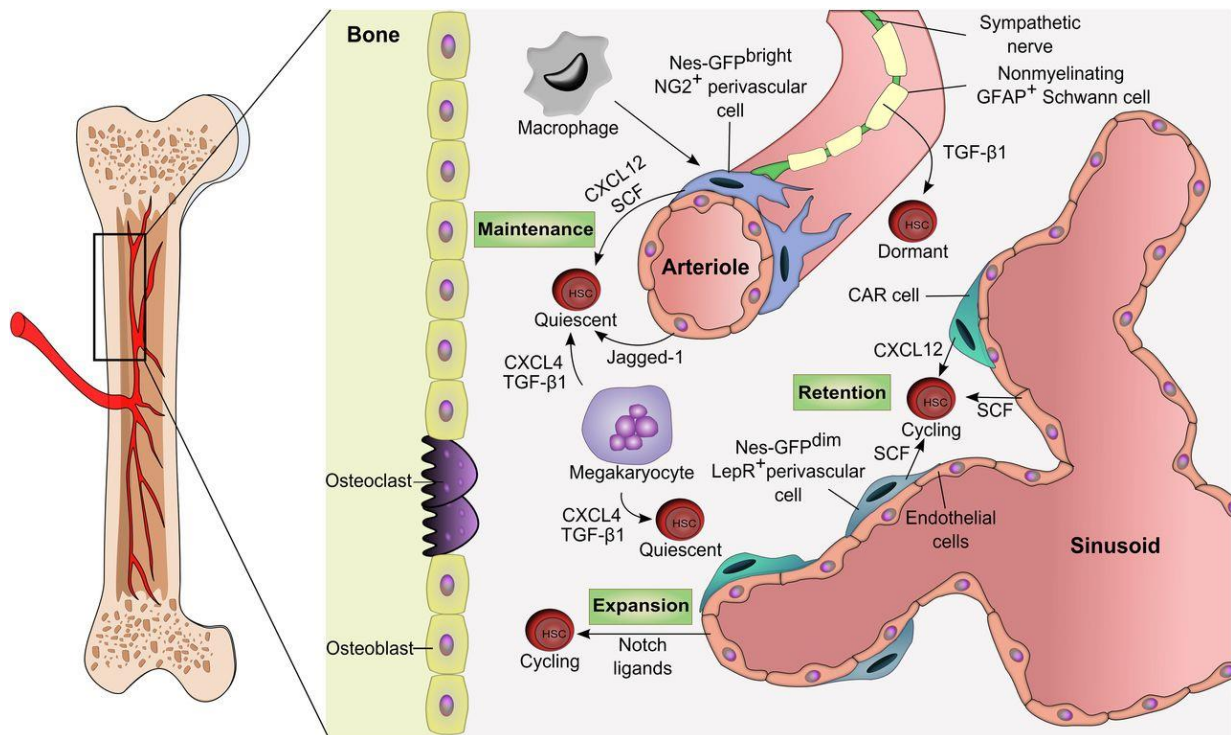
Fig.1 Haematopoietic Stem Cell (HSC) niches in the adult bone marrow. In adult Bone marrow, HSCs mainly reside in the perivascular areas, containing macrophages, megakaryocytes, neurons, Schwann Cells, and CAR cells. In the vascular /periarteorialar niche, HSCs maintenance is positively regulated from Nes-GFP[bright] NG2^{+} cells, Schwann cells, and endothelial cells. The perisinusoidal niche influences the HSC self-renewal, while megakaryocytes lead HSC quiescence through the secretion of CXCR4 and TGF-β1. Source: Boulais et al., 2015.

OBs are bone-lining cells, involved in the bone remodeling dynamics with osteoclasts (OCs), which resorb the bone. The major functions of OBs in bone remodeling are the secretion of unmineralized bone matrix proteins, but recent studies revealed the role of OBs in regulating also the HSC fate (Calvi et al, 2003; Zhang et al, 2003). Zhang *et al*. (Zhang et al, 2003) demonstrated how the increased number of N-cadherin-positive osteoblasts (SNO cells) was correlated with the increasing number of HSCs, that remain attached to the SNO cells in association with N-Cadherin. Simultaneously, Calvi's work (Calvi et al., 2003) identified the role of parathyroid hormone/parathyroid hormone-receptor (PPRs) in increasing the number of HSCs via Notch signaling and the relative connection with Jagged 1-expressing OBs to amplify the signal. However, the role of OBs in HSC maintenance remains controversial. It was noted that OBs can

regulate positively the HSC function by the secretion of angiopoietin-1, thrombopoietin, and Jagged-1, while osteopontin and dikkopf1 showed a negative regulation.

Mesenchymal Stem Cells (MSCs), the multipotent stromal cells and progenitors of osteoblastic lineage, adipocytes, and fibroblasts, are active components of HSC regulation in the bone marrow. In particular, Nestin[+]-MSCs express a high level of genes involved in HSC maintenance, and their depletion results in bone marrow dysfunction. According to recent studies, it is very likely that HSCs and MSCs are intimately associated with one another and coordinate activities of the niches (Kanazawa et al, 2021; Woods et al., 2021). Several works highlighted the close interaction between MSCs and HSCs, demonstrating how these stromal cells support the engraftment of HSCs after transplantation. Besides cellular interaction, MSCs release several HSC-supportive molecules, such as fibronectin, osteopontin, CXCL12, Ang-1, thrombospondin (Shiozawa et al, 2008). Recent advances in single-cell RNA sequencing revealed the presence of different subsets of MSCs which can be classified into "less differentiated" and "more stem-like" features, depending on gene set signatures (Woods et al., 2021). Moreover, Triana's work mapped a large bone marrow cell population and demonstrated the presence of a small amount of heterogenous MSCs expressing high levels of CXCL12, and this result was validated after FACS based isolation and analysis with other MSCs signatures genes (Triana et al., 2021). In this regard, Zhang and colleagues brilliantly classified human bone marrow MSCs into different clusters, such as adipo, osteo, and chondrogenic subpopulations, and two terminal clusters, representing senescent cells (Zhang et al. 2003).

HSCs are widely distributed in the bone marrow regions and several data suggest a significant regulation of perivascular districts, where they establish constant relations with endothelial lineages. Given the massive vascularization of the bone marrow, it is likely that resident vessels can promote the regulation of both expansion and differentiation of the hematopoietic compartment. To date, two distinct vascular niches have been identified in the mouse model: the arteriolar niches, mainly associated with the endosteal region and composed by sympathetic nerve fibers, Nestin-GFP, and NG2 cells; and the sinusoidal niche, where HSCs interact with CXCL12-abundant reticular cells, Nestin-GFP and LepR cells. In this context, arterioles are closely associated with both quiescent NG2^{+} niche cells and HSC and are structurally different from sinusoids, translating into distinct functions with endothelial cells. Frenette and

colleagues revealed the role of the arteriolar niche in HSCs quiescence (Kunisaki et al. 2013), and, in particular, periarteriolar Nestin$^+$ cells regulate the stem cell dormancy with a still unknown mechanism.

Endothelial cells, lining the sinusoidal blood vessels, may also contribute to HSC regulation. The bone marrow structure is largely enriched in vasculature and arterioles branch with sinusoids, which identifies the perivascular niche. Itkin's work (Itkin et al., 2016) showed how endothelial cells contribute to forming a distinct environment that can regulate HSCs behavior, and it seems strictly related to vessels permeability. Arteriolar bone marrow vessels reveal a lower permeability compared to sinusoids that represent the site for HSCs trafficking and mobilization. Consequently, the different levels of permeability reflect distinct levels of Reactive Oxygen Species (ROS) nearly the vasculature sites, affecting HSCs fate. The less permeable vasculature promotes a lower ROS microenvironment, where HSCs are maintained in a quiescent state, while the more permeable sinusoids foster the HSCs activation via ROS exposure. Along with the concentration gradient of ROS levels, strong evidence suggests the role of cell adhesion molecules, such as Endothelial Selectins, in HSCs fate. Particularly, in the perivascular niche, endothelial cells express E-Selectin, the main driver of HSC proliferation, and it has been demonstrated, in mouse models, how HSCs can detect the signal of E-Selectin by glycosphingolipids (Winkler et al., 2012). Other several factors are involved in HSCs maintenance, including SCF, CXCL12, angiopoietin 1, and Thrombopoietin which can be released by several cell sources, but recent findings sustain that the effect of these molecules on HSC fate is spatially-dependent and cell-dependent. Morrison's work clarified that HSCs require SCF released in the perivascular niche, in particular from Lepr expressing perivascular cells and endothelial cells, but they may not be its exclusive source on that side (Ding et al., 2012). Endothelial cells and perivascular cells are also the main source of CXCL12, required for HSC maintenance and retention in the bone marrow, confirming the pivotal role of the perivascular niche in the regulation of hematopoiesis (Ding et al., 2013).

Despite all this knowledge, the cellular composition and spatial distribution of the bone marrow components remain still unclear. Baccin et colleagues first characterized the cellular composition of the bone marrow using droplet-based, single-cell RNA-sequencing, with a focus on the major hematopoietic and stromal cell lineages. After the microdissection of bone marrow niches and an integrated RNA-seq, they established that CAR (CXCL12-abundant reticular) cells form a three-dimensional

network supporting bone marrow vessels, in collaboration with other components of the perivascular niche. They also showed the presence of particular subsets of CAR cells, Adipo-CAR and Osteo-CAR, with a distinct pattern of localization and functions (Baccin et al., 2020).

Besides the humoral factors, bone marrow niche cells produce and release components that form matrices of various stiffness in the bone marrow microenvironment. As previously described, the osteoblastic niche is characterized by very high stiffness, while in the perivascular niches MSCs release a soft matrix. Specifically, bone marrow cells secret structural proteins such as collagen I and IV, glycoproteins, such as fibronectin (FN), laminin (LN), and glycosaminoglycans (GAG). The distribution and composition of ECM components in the bone marrow affect its stiffness and, then, cell behavior and fate. In 1998, Nillson (Nilsson et al., 1998), first described the ECM composition of the bone marrow, localizing type I and type IV collagens and fibronectin in the endosteal region, while the marrow vessels seem surrounded by laminin and type IV collagen in mice femora. However, the softness of marrow is also the result of ECM protein density: FN is ubiquitous but denser close to the endosteum. In this context, HSCs localize close to the osteoblastic niche, with an elasticity >30 kPa (Shin et al., 2014). However, the extracellular microenvironment undergoes remodeling by the action of proteolytic enzymes, belonging to the metzincin family, that can degrade ECM components and affect biomechanical characteristics of the bone marrow. The metzincins family comprises secreted and membrane-bound matrix metalloproteinases (MMPs) membrane-bound ADAMs, and secreted ADAMTs. The most expressed MMPs in the bone marrow are the MMP-2, MMP-9, and MMP-14, widely present in the bone marrow, while the MMP-8 seems to be more restricted to specific immune lineage. Only in the last decade, the recent studies on mechanobiology showed how cells feel the different components of the extracellular environment and its mechanical forces, and also HSCs are sensitive to physical signals. Several groups tested different types of hydrogels to demonstrate the mechanosensitivity of HSCs and how they modulate their behavior on softer rather than stiffer matrices. If stiffer collagen gels seem to foster cytoskeletal development and spreading, HSCs showed greater viability on softer matrices (Choi et al., 2012). ECM signals are sensed and transmitted by integrins, as they recognize many of the ECM molecules, but other receptors are known to be mechanosensitive, such as adherent junctions proteins, G protein-coupled receptors, or ion channels, that

integrate the signal from outer to the inner of the cell. In these last years, many works are investigating the role of transcriptional cofactors YAP/TAZ, which seem to be involved in the sensing of biophysical forces transmitted by blood flow.

Megakaryocytes

Megakaryocytes are giant cells closely located to sinusoids vessels and, once mature, undergo several cycles of endomitosis, elongate long cytoplasmatic extension, called proplatelets, in blood vessels lumen, and release platelets assembled at their termination (Italiano et al.,1999) (**Figure 2**).

During hematopoiesis, quiescent HSC, Long Term-HSC (LT-HSC), are recruited to differentiate in Short Term-HSCs (ST-HSCs) that give rise to the closely committed progenitor, the multipotent progenitor (MPP) (Yang et al., 2005). Subsequently, the common progenitor is forced to switch to the myeloid lineage by which the common myeloid progenitor (CMP) and megakaryocyte-erythroid progenitor (MEP) differentiate in megakaryocytes. Nevertheless, there is growing evidence that LT-HSCs are reasonably heterogeneous. In recent work, Yamamoto and coworkers surprisingly figured out the presence of a subset of restricted-myeloid HSC population with long-term repopulating activity (MyRPs), committed to erythro-megakaryocyte lineage, bypassing the conventional model (Yamamoto et al, 2013). These data seem to correlate with Sanjuan-Pla's study with whom it has been identified a von Willebrand Factor[+] platelet-biased population of HSCs, with a primed gene expression for megakaryocyte/platelet lineage (Sanjuan-Pla et al., 2013). On the other hand, megakaryocytes play a role in the maintenance of the quiescence of HSCs in the bone marrow niche, considering that *in vivo* megakaryocytes ablation gives rise to HSC proliferation, due to a loss of regulation mediated by megakaryocyte-derived CXCL4 (Bruns et al., 2014).

The purification of the pivotal cytokine driver of thrombopoiesis, Thrombopoietin (TPO), in 1994, allowed to better elucidate the mechanism of HSC differentiation.

Besides its effect on HSC self-renewal and quiescence (Qian et al., 2007), the interaction of TPO with its receptor, c-Mpl, promotes the *in vivo* megakaryopoiesis and platelet production (Kaushansky et al., 1994) but, to date, little is known about the mechanisms underlying this activity.
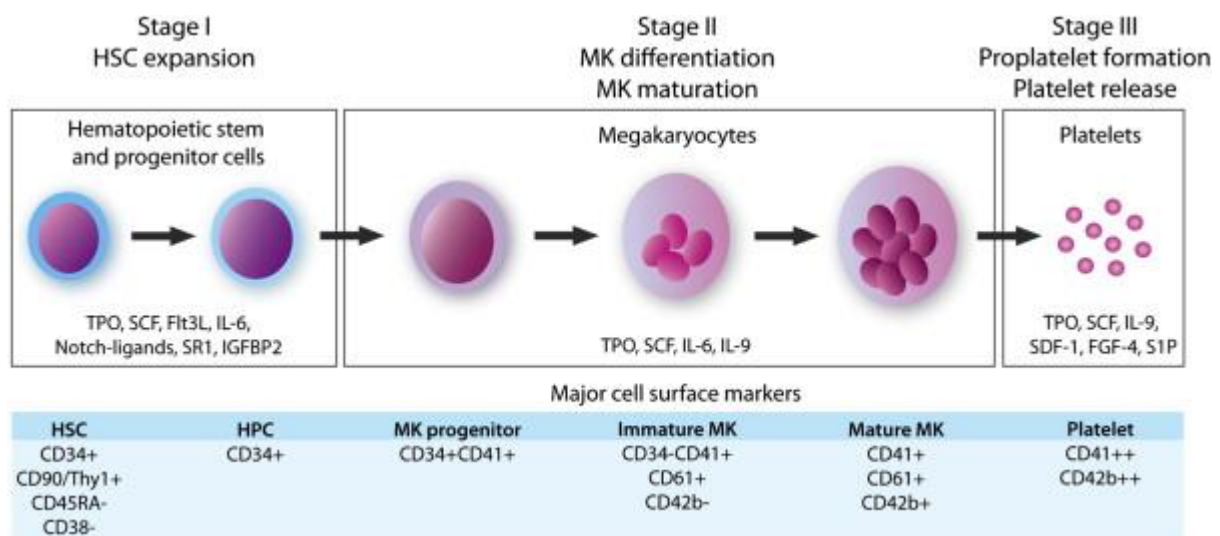
Fig.2 The main steps of megakaryocyte maturation and differentiation. The first stage of Megakaryopoiesis involves the expansion of CD34+ HSC and multipotent progenitors. Subsequently, Megakaryocytes' differentiation and maturation (CD41+ CD61+) is mainly characterized by the increase of cell size and DNA replication without cytokinesis (endomitosis). Upon completion of maturation, polyploid megakaryocytes extend cytoplasmic processes (proplatelets) into the blood vessels lumen, where they release platelets. Source: Lee et al., 2014

Interestingly, Nakamura-Ishuzu and his team (Nakamura-Ishizu et al., 2018) contributed to clarifying some aspects of the subcellular pathway involved in this process. Particularly they highlighted how the TPO-mediated stimulation is accompanied by upregulation of mitochondrial activity and mass in activated HSCs, associated with translocation of non-nuclear p-STAT3 in mitochondria and relative activation of complexes I and II of electron transport chain.

Moreover, it has been demonstrated the involvement of TPO in endomitosis, the process with which megakaryocyte becomes polyploid through cycles of DNA replication without cell division, accumulating DNA content up to 128N in a single poly-lobulated nucleus (Ebbe, 1976; Gurney et al., 1994). This intriguing process seems to be related to supporting the large quantities of mRNA and protein packaged into platelet granules and a work by Mazharian *et al.* (Mazharian et al., 2013) discovered the role of the protein-tyrosine phosphatases Shp1 and Shp2 in endomitosis. Knocking out the expression of Shp1 and Shp2 in animal models, they found defects in endomitosis, observing 2-4N immature megakaryocytes, probably due to an impaired c-Mpl-related signaling and defective cytokinesis.

The maturation of megakaryocytes is also characterized by the formation of a membrane system, called Demarcation Membrane System (DMS). Its main function is to provide a membrane reservoir for proplatelet formation, relying on actin fiber assembly via WASp/WAVE pathways in response to PI-4,5-P$_2$ signaling (Schulze et al., 2006) and the interaction of CDC42 interacting protein 4 (CIP4) with WASP in promoting actin reorganization (Chen et al., 2013).

In the terminal stage of differentiation, megakaryocytes extend long and branched processes, called proplatelets, in the lumen of sinusoidal bone marrow vessels. Observation of long cytoplasmic process from megakaryocyte bodies was theorized and observed for a long time (Becker et al.,1976; Radley et al.,1980), and reproduced *in vitro* in 1995 by Hunt's group (Choi et al., 1995). With this work, they established an *in vitro* culture system to differentiate CD34$^+$ cells, selected from leukapheresis, in megakaryocytes that spontaneously form proplatelets structure in culture.

The process origins from a single site on the plasma membrane and it's strictly dependent on microtubules assembly and remodeling. Mainly composed of dimers of alpha/beta-tubulin, microtubules assemble from the centrosomes and extend toward the edge of the cell, where they polymerize in both directions of proplatelets. These pseudopodia extensions initiate the formation of 100-500 μm long protrusions (proplatelet shafts) filled with microtubular linear bundles. Next, these structural filaments form a loop at the terminal ends of proplatelets, giving rise to bulbous tips 3-5 μm in diameter. Interestingly, the rate of growth of proplatelets is quite variable and depends on the maturation state of megakaryocytes (from 5 μm/min to 14 μm/min) (Italiano et al., 2007).

However, mechanisms underlying proplatelet extension don't seem to be correlated with microtubule polymerization. The actin cytoskeletal forces are regulated by dynein, a microtubule molecular protein, and RhoA, a Rho GTPase: if Dyneyn seems to play a role in microtubule sliding, RhoA is implicated in stress fibers formation and regulates actomyosin contractility (Suzuki et al., 2013)(**Figure 3**).
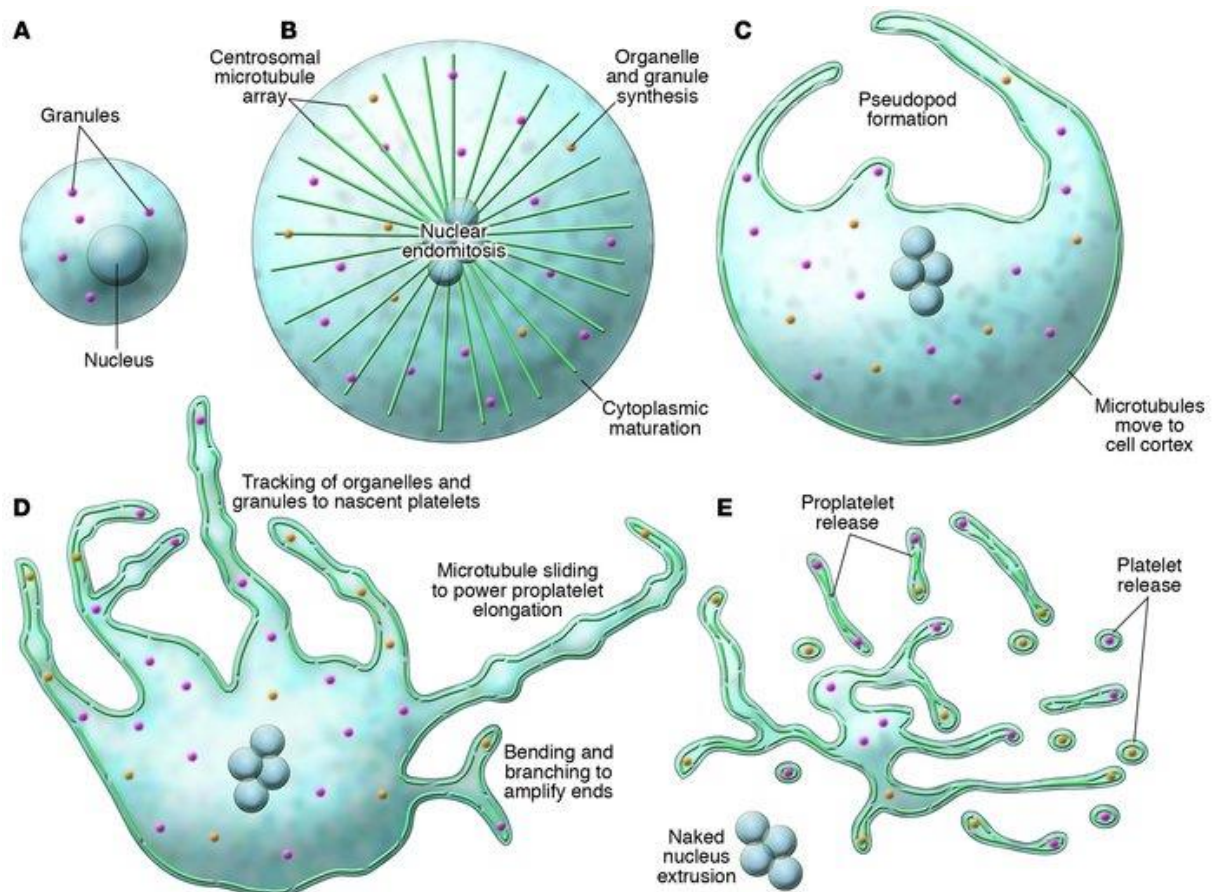
Fig. 3. Platelets originate from megakaryocytes in the bone marrow. Megakaryocytes give raise from HSCs (**A**) and undergo nuclear endomitosis, organelle synthesis, and cell size expansion (**B**). Microtubules translocation to the cell cortex (**C**) enhances pseudopods formation and their elongation promotes proplatelet branching and shedding (**D**). In the last step of this intriguing process, proplatelets and their terminal ends (platelets) are *in vivo* detached from blood flow. Source: Patel et al., 2005.

Finally, platelets are released in the blood flow from the terminal ends of proplatelets, according to the prevalent model of thrombopoiesis. This flow model was proposed by several groups studying the *in vitro* mechanisms of platelet production, but it was unclear whether platelets originated from entire detached proplatelets or their terminal tips. In this regard, Junt demonstrated the pivotal role of blood flow in platelet release from megakaryocytes. Along with *in vivo* observations, in which blood flow-induced shear stress (1.3 to 4.1 dynes/cm^2 in bone marrow sinusoids) helps platelets detachment, megakaryocytes release more proplatelet-like fragments when they were agitated with the respect to static conditions (Junt et al., 2007). These data were confirmed by the brilliant work of Koji Eto's team, which produced a new microfluidic system with appropriate levels of shear stress to induce a massive production of

platelets in an innovative model of bioreactor. In his VerMES, a vertical tank bioreactor, a turbulent flow is generated by blades repeating an up-and-down reciprocal motion. They found an increasing generation of $CD41^+CD42b^+$ platelets from an immortalized megakaryocytic cell line (imMKCL) when turbulent energy of 0.002-0.014 m^2/s^2 and shear stress 0.4-3.0 Pa were applied.

Beyond TPO-mediated priming mechanisms, little is known about the regulators of thrombopoiesis. However, Rafii's work points out the attention to the interaction between progenitors and bone marrow endothelial cells (BMECs), mediated by Stromal Derived Factor-1 (SDF-1) and fibroblast growth factor-4 (FGF-4) secretion, suggesting the importance of the vascular niche in promoting the maturation of megakaryocytes (Avecilla et al., 2004).

Interestingly, ECM structure and stiffness can determine megakaryocyte maturation. Recent data from Leon's team offer a new perspective on the role of mechanotransduction in the regulation of hematopoiesis, showing how megakaryocyte maturation and proplatelet formation have been promoted by a softer environment (30-60 Pa) due to the involvement of MLK1 and myosin IIA (Aguilar et al., 2016). Recent work from Abbonante *et al*. remarks on the involvement of mechanical stress on megakaryocyte functionality (Abbonante et al., 2017), reporting that silk-based softer films (≤10 MPa) positively regulate megakaryocyte maturation via activation of mechano-sensitive TRP channel, transient receptor potential cation channel subfamily V member 4 (TRPV4).

In the last years, the new whole-organ imaging techniques are opening unexplored scenarios, overcoming the difficulties to study *in vivo* processes in the bone marrow. In this context, Junt and colleagues firstly observed *in vivo* thrombopoiesis by intravital two-photon microscopy (2P-IVM) in mouse skull bone marrow. This work confirmed that megakaryocytes are mainly located close to bone marrow sinusoids and extend proplatelets in their lumen, where platelets are detached by blood hydrodynamic fluid shear (Junt et al., 2007).

With this approach, Stegner observed the *in vivo* distribution of megakaryocytes in mouse skull bone marrow in steady-state conditions. Briefly, *in vivo* imaging did not show megakaryocyte migration but a wide distribution of mature megakaryocytes and progenitors into the organ, with a prominent localization along sinusoids. Overall, these data seem to doubt the concept of two separable niches and suggest that megakaryocyte behavior and function are strongly shaped by their spatial location in

the bone marrow (Stegner et al., 2017). *In vivo* platelet release was brilliantly observed and measured in bone marrow from the scalps of eGFP mice by Koji Eto's group, integrating two-photon microscopy and particle image velocimetry (PIV). This system allowed the analysis of the effect of dynamic blood flow on megakaryocyte function, demonstrating the importance of turbulence on the activation of megakaryocytes and platelet production (Ito Y et al., 2018).

It is certainly arousing plenty of interest the platelet biogenesis in the lung, where it has been estimated 50% of total platelet production (Lefrançais et al., 2017). The pulmonary vascular bed showed evidence to support *in vivo* thrombopoiesis when *ex vivo* megakaryocytes were infused in animal models (Fuentes et al., 2010), probably due to the similarities with bone marrow microenvironment and blood shear stress. Interestingly, unveiling ECM composition, the lung seems to reflect the structural features of bone marrow. The spongy lung parenchyma is sustained by type I and type III collagens and elastic fibers, composed of elastin and microfibrils which are mostly fibrillin and fibulin, embedded in a matrix of glycosaminoglycans heparin sulfate and chondroitin sulfate (Suki et al.,2008). Because of the high heterogeneity of ECM protein content, normal human lung parenchyma shows a wide elastic modulus range, from 0.44 to 7.5 kPa (White et al.,2015), depending on the measured anatomical district. Despite these similarities with bone marrow, little is known about mechanisms leading to thrombopoiesis in the lung but, recently, Lefrançais contributed to elucidate several aspects of this elusive process. Lefrançais revealed the medullar origin of intravascular megakaryocytes in the lung, that migrate from bone marrow and release platelet in the pulmonary bloodstream. Although the lung was widely known as a source of platelets, imaging of lung thrombopoiesis has been challenging. Using 2PIVM, they imaged for the first time in *vivo* megakaryocyte releasing platelets in the lung of fluorescently labeled mice, less mature than bone marrow megakaryocyte but able to produce more than 10 million platelets per hour. Moreover, they also showed the presence of a high HSCs content in the extravascular space of the lung, capable to migrate to the bone marrow and restore functional defects. Taken together, these data suggest the presence of new extramedullary HSCs niche in mice but need to be translated in humans. Previous studies provided evidence of intravascular megakaryocyte in human lungs, probably released from the marrow and retained in pulmonary vessels because of their cell size. Nevertheless, which mechanisms are

involved in megakaryocytes migration to the lung, and what promotes platelet production in this site remain still unexplained.

Moreover, emerging evidence in the last years has demonstrated both megakaryocyte and platelets heterogeneity in morphology, function, and ontogeny. Recently, single-cell RNA sequencing has permitted to dissecting the cellular heterogeneity of several cell populations, including megakaryocytes (Wang et al., 2021). These studies elucidated unexpected functions of megakaryocytes as regulators of HSC quiescence, immune response, and bone metastasis. To better investigate megakaryocyte behavior during the development, Liu and colleagues (Liu et al., 2021) isolated megakaryocytes from the yolk sac, the fetal liver, and the adult bone marrow of mice and performed a transcriptomic analysis through single-cell RNA sequencing, showing significant differences in morphology and molecular signature in different stages. Megakaryocyte displayed a greater proportion of the polyploid population in adults (>16N) but immature megakaryocyte was observed in both fetal and adult mice. The transcriptional analysis demonstrated the presence of two megakaryocyte subpopulations with possible niche supporting an immune functions, distinct from platelet-biased megakaryocytes, both in embryonic and adult stages. These immune populations were isolated through the expression of specific markers (CD53 in embryos, CD48 in adults) and provided evidence of the heterogeneity of different subpopulations in megakaryocytes, as demonstrated by Sun and colleagues (Sun et al., 2021).

Growing evidence also sustains how this megakaryocyte heterogeneity may be inherited in platelet. In fact, in a recent work, Battinelli *et al.* (Battinelli et al., 2019) observed that individual megakaryocytes could allocate different RNAs or proteins to specific platelets, and this different composition in alpha-granules composition can reflect the multiple functions of these cells and open new perspectives in understanding the mechanisms of platelet dysfunctions.

Platelets

Platelets are anucleated blood cells (2-4 mm diameter), mainly involved in hemostasis and coagulation, circulating in the blood for 7-10 days and cleared in the spleen and liver. Given their short lifespan, millions of platelets are produced every day, sustaining a physiological count range of 150 – 400.000 platelet/microL of blood (Lu et al., 2011).

They are primarily produced in the bone marrow from megakaryocytes, branching numerous cytoplasmatic protrusions called proplatelets. This intriguing process, defined as Thrombopoiesis, has also been reported in mice lungs, as described above (Lefrançais et al., 2017). After elongation of the cytoplasmatic protrusions in the vessel lumen of bone marrow sinusoids, immature platelets (or reticulated platelets) are released into the blood flow.

These small cell fragments are involved in many physiological processes, especially hemostasis through their ability to aggregate and form clots in response to activation, but growing evidence highlights their involvement in inflammation (Linden et al., 2005). They circulate in laminar blood flow, in close contact with the endothelium, and after activation, they undergo structural changes to spread and adhere to the endothelial damaged surface, where release granules and aggregate with leukocytes and other platelets (Hartwig, 2002). It's widely recognized that platelets activation is mediated by the von Willebrand Factor (vWF) receptor complex GPIb-IX-V, and the collagen receptor GPVI, leading to integrin activation and integrin-dependent stable platelet adhesion and aggregation (Woulfe et al, 2002). Platelet adhesion is fostered by the exposure and activation of integrins, such as activated αIIbβ3 to its ligands (fibrinogen, vWF, and RGD sequences containing proteins). Through this mechanism, platelets are induced to leak their granular content. Alpha-granules contain chemokines, coagulation factors, and adhesion molecules, while Dense granules are characterized by the presence of ionic calcium, magnesium, nucleotides (ATP, GTP, ADP, GDP), and serotonin. Their release triggers the amplification of platelet activation and recruits other circulating platelets into aggregates (Li et al., 2010) (**Figure 4**).
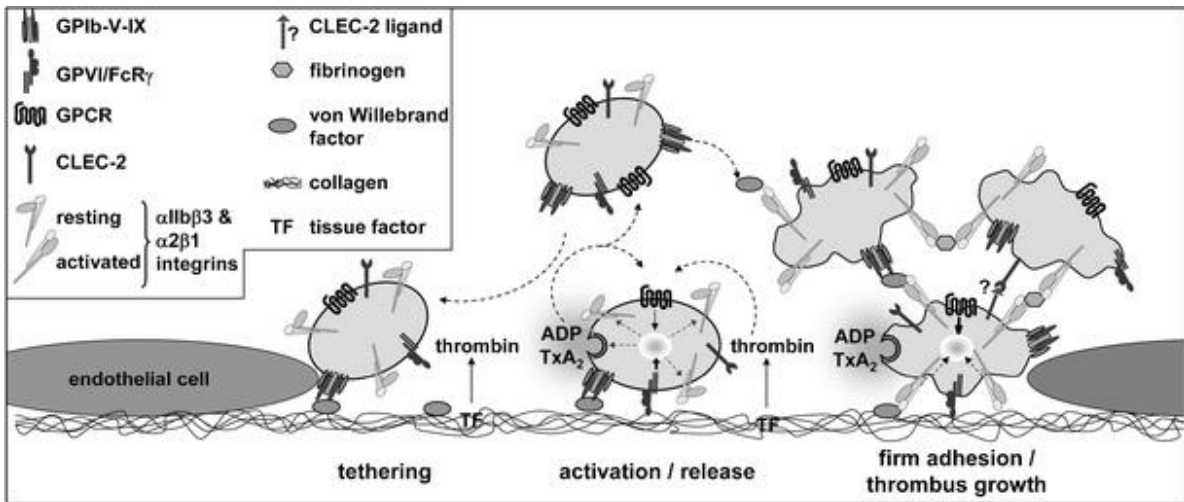
Fig. 4 Schematic Model of platelet adhesion and thrombus formation. After initial tethering, (GPIb-vWF), the cellular activation is induced by GPVI-collagen interaction. The exposure of high-affinity integrins and ADP, ATP, and TxA$_2$ release triggers the final activation. The adhesion mediated by $\alpha2\beta1$ and αIIb$\beta3$ enhanced the release of agonists with procoagulant activity. Source: Stegner D et al., 2011.

Next-generation sequencing technology (NGST) is facilitating the knowledge of new genes responsible for both qualitative and quantitative defects in platelets. Inherited disorders of platelet function are relatively rare and are characterized by mild or severe clinical symptoms. For instance, platelets fail to aggregate for CD41/αIIb$\beta3$ dysfunction (Glanzmann's thrombasthenia) or to adhere to vascular endothelium due to mutations in GPIb/IX/V complex (Bernard-Soulier syndrome). Notably, platelets can display defects in granules content, as in the case of dense granule deficiency (δ-SPD), or coagulant function (Scott syndrome).

Inherited Thrombocytopenias

A platelet count that falls recurrently below the lower limit of 150.000/microL is defined as thrombocytopenia. The relevance of thrombocytopenia in the individual patient is variable and depends on the clinical presentation. Because platelets play an essential role in preserving vessel wall integrity, thrombocytopenia is associated with a defect of primary hemostasis. Clinically significant spontaneous bleeding does not usually occur until the platelet count is less than $10\text{-}20\times10^9$/L. The causes of thrombocytopenia can be subdivided into decreased platelet production, increased platelet destruction,

increased splenic sequestration, and dilution. Investigation requires consideration of patient age, baseline platelet count, medical and surgical history, including any bleeding or thrombotic manifestations, family history, medication history, results of any pertinent laboratory testing, and physical examination findings. Thrombocytopenic symptoms may include petechiae, fatigue, purpura, spontaneous bleeding from gums or nose, jaundice, enlarged spleen (splenomegaly), DVT (deep vein thrombosis), but the clinical phenotype could be widely heterogeneous. Although platelet numbers are decreased in thrombocytopenia, their function often remains completely intact.

In this context, Inherited Thrombocytopenias (ITs) represent a heterogeneous group of disorders characterized by the low platelet count, but clinical manifestation may vary depending on age, gender, and ethnic background. Severe ITs can present in the newborn period, while mild IT may remain undiagnosed until incidental detection on routine blood testing in adulthood. Some ITs show only hematologic manifestations, such as a difference in platelet size or distinctive granulocyte inclusions, while other ITs can be correlated with additional non-hematologic manifestations or predispose to acute myelogenous leukemia or myelodysplastic syndromes. To date, ITs encompass 45 disorders with different degrees of complexity of the clinical picture and very wide variability in the prognosis. They include forms characterized by thrombocytopenia alone, forms that present with other congenital defects, and conditions that predispose to acquire additional diseases throughout life. The development of genetic technologies, such as whole-exome sequencing (WES) and whole-genome sequencing (WGS) led to the discovery of new mutations and the identification of genes responsible for ITs.

ITs can be classified based on platelet size, which is greatly variable, and the presence of additional defects to lower platelet count (Noris et al., 2017). In the last years, several classification methods were adopted, based on the inheritance transmission model, platelet size (micro-, macro-thrombocytopenia), and pathogenic mechanisms impairing megakaryocyte differentiation. According to Prof. Carlo Balduini's criteria (Balduini et al., 2012), IT can be divided into 3 groups:

- Forms characterized by only platelet defect,
- Forms associated with additional congenital defects (syndromic forms),
- Forms characterized by an increasing risk of acquiring additional diseases.

The key mechanism of some ITs is the defective transition of hematopoietic progenitor cells to megakaryocytes, resulting in the absence or severe reduction in the number of bone marrow megakaryocytes (Balduini et al., 2017). The most frequent and studied form of IT with defective megakaryocyte differentiation is the Congenital Amegakaryocytic Thrombocytopenia (CAMT), characterized by MPL biallelic mutations that abrogate TPO-MPL signaling. The role of MPL is widely recognized in bone marrow cells development and patients with residual activity of this receptor result in less severe thrombocytopenia. Other rare forms (TAR, RUSAT) are caused by alterations in RBM8A and HOXA11, involved respectively in JAK2-STAT signaling and megakaryocyte precursor differentiation.

Megakaryocyte maturation is altered in several different forms of IT, showing a normal or increased number of immatures, dysmorphic, and dysfunctional megakaryocytes (**Figure 5**).
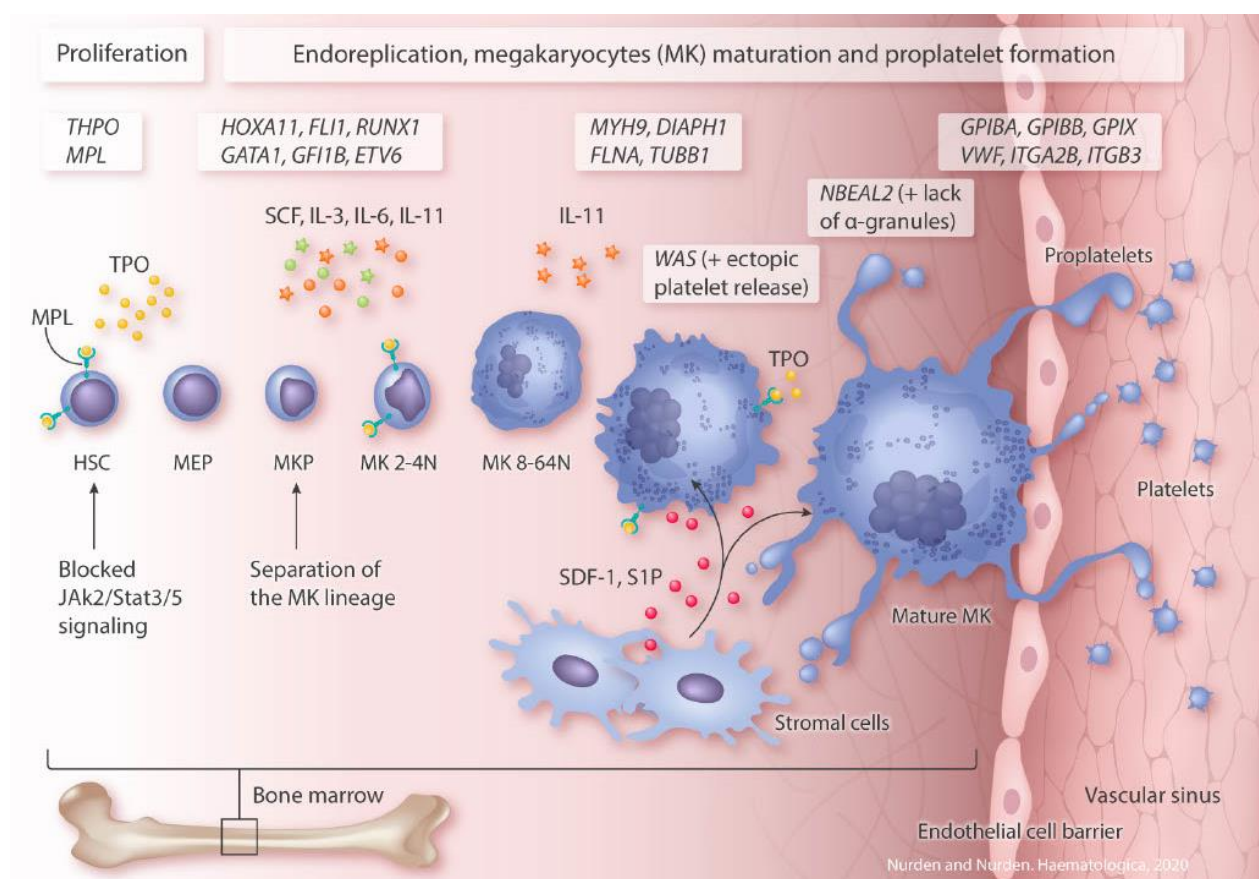

Fig.5 Main megakaryocyte genetic alterations associated with Inherited Thrombocytopenia: This image resumes the major steps of megakaryopoiesis highlighting how inherited defects of selected genes may cause a defect of megakaryocytes differentiation and maturation and platelet production. Source: Nurden et al., 2020.

This group of alterations strikes the main transcription factors of megakaryopoiesis, e.g. *RUNX1, FLI1, GATA1, GFI1b,* and *ETV6*, causes defects in the formation of megakaryocyte cytoskeleton (*MYH9, MYL9, MYH10* genes), proteins involved in alpha and dense granules development (*PF4, PLDN*), and members of megakaryocyte signaling (*ANKRD26, MPL, PRKCQ, ALOX12, PCTP*). In three cases (*FPD*-AML, *ANKRD26*-RT, *ETV6*-RT) the mutations can predispose to hematological malignancies. The molecular mechanisms involved in *ANKRD26* and *FPD*-AML might be related to RUNX1, resulting in impaired megakaryocyte maturation. Other gene alterations (*FLI1*) can alter the transactivation of genes involved in megakaryocyte maturation (*MPL, GP9, GP1BA, ITGA2, PF4*) and alpha-granules content.

In the third group, defects of proplatelet formation and extension are observed and mainly characterized by macrothrombocytopenia, caused by mutations in genes encoding components of cytoskeleton or microtubule system (*MYH9, ACTN1, FLNA, TPM4, TRPM7, TUBB1*). Pathological mechanisms underlying the development of macrothrombocytopenia involve mutations of genes for megakaryocyte glycoprotein complexes, GPIb/IX/V and GPIIb/IIIa, such as in biallelic and monoallelic BSS and ITGA2B/ITGB3-related thrombocytopenia.

IT's characterized by thrombocytopenia as the main symptoms derive from mutations in 19 genes. The clinical manifestations are mainly defined by reduced platelet count, with different severity of bleeding correlated with the degree of thrombocytopenia. In some cases (monoallelic and biallelic BSS) thrombocytopenia can be associated with severe platelet functional defects, while *ACTN1*, *GP1BB-BA* mutations don't correlate with significant reduction and dysfunction in platelets. ITs can also associate with other congenital diseases (e.g., Jacobsen Syndrome) or predispose to other malignancies, such as hematological and non-hematological diseases. The recently discovered *ANKRD26*-RT represents one of the highest prevalent IT and shows a strong propensity to acquire malignancies (10% of reported patients). FDP-AML and *ETV6*-RT are also reported with a high risk of acquiring hematological malignancies (respectively 45% and 30%). ITs could evolve in bone marrow aplasia, as observed in CAMT and RUSAT diseases, often characterized by absent or reduced megakaryocytes in the bone marrow. Lastly, *MYH9*-RD is the most common form of IT

(25% of total cases) and is associated with macrothrombocytopenia age-related (often relieved in adulthood) and extra-hematological disorders (nephropathy, hearing loss).
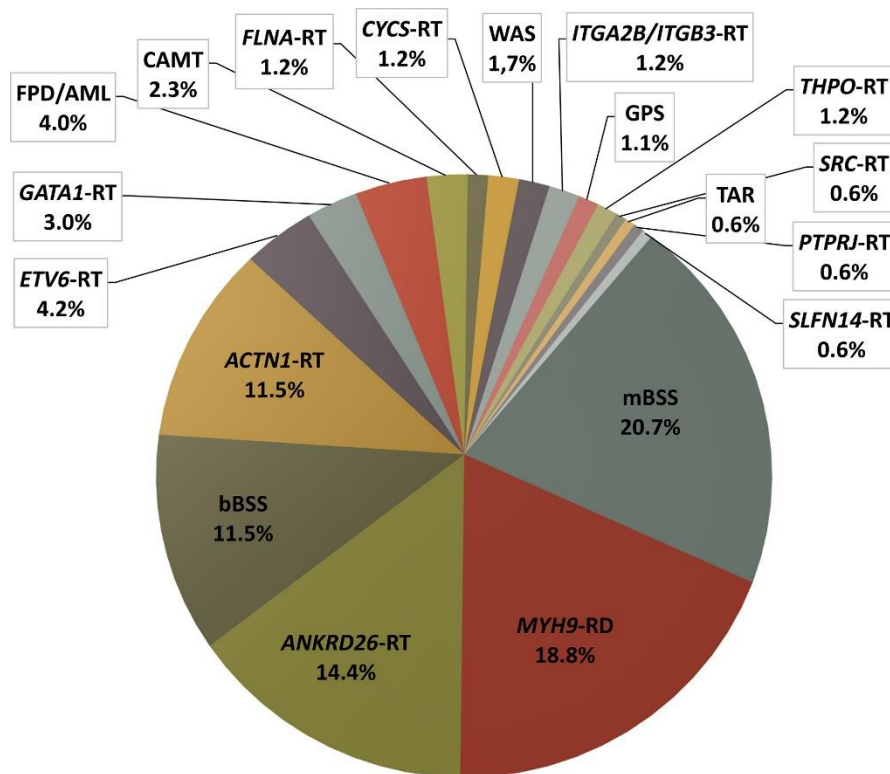

Fig. 6. **Relative frequency of different forms of ITs in our case series of 335 consecutive Italian families.** Source: Pecci et al., 2021

Given its high variability and heterogeneity, the management of ITs requires the evaluation of peculiar clinical parameters to better design the therapeutic strategy. For instance, the first therapeutic approach is focused on the management of the bleeding (Bolton-Maggs et al, 2006). IT patients generally have no or mild spontaneous bleeding, and treatment of hemorrhages, usually mucocutaneous, is based on local measures and platelet transfusions. These are effective in stopping bleeding episodes but expose patients to the risk of acute reactions, transmissions of infectious disease, and alloimmunization. For these kinds of reasons, they should be limited to long bleeding episodes. Hemostatic agents are recommended in some bBSS cases, treated with recombinant activated factor VII (rFVIIa). To prevent hemorrhagic events during surgery or other invasive procedures, it should be important to know the history of bleeding as a major predictive factor for the intervention. The indication for prophylactic platelet transfusion before surgery depends on the type of procedure and bleeding risk. Generally, a platelet count of at least 50×10^9/L is suggested for most major surgery,

while prophylactic platelets are required for ITs associated with platelet dysfunction. Finally, several clinicians recommend the anti-fibrinolytic drug, such as Tranexamic Acid, Desmopressin, to cover low-risk procedures. The Thrombopoietin-receptor agonists (TPO-RAs) approach will be extensively treated in the following sections.

ANKRD26-Related Thrombocytopenia

Thrombocytopenia 2 (THC2 [MIM 188000]) represents one of the rarest forms of autosomal-dominant thrombocytopenia. Patients affected by THC2 show mild to severe thrombocytopenia, resulting in mild bleeding diathesis and poor bleeding events (Noris et al., 2011). The THC2 locus was mapped to chromosome 10p11.1-p12, with two missense changes in different linked genes: c.501G>C (p.Glu167Asp) of MASTL (Ghandi et al.2003), and c.22C>T (p.His8Tyr) of ACBD5 (Punzo et al., 2010).

These two gene mutations, found in two different families, contribute to the onset of THC2 but are also associated with mutations in a third gene, *ANKRD26*. Specifically, in 2011, Peppucci and colleagues (Pippucci et al., 2011) observed different heterozygous single nucleotide substitutions within the 5′ UTR of *ANKRD26* in several individuals showing a clinical phenotype consistent with THC2, harbouring mutations in MASTL or ACBD5. After a wide screen in additional families, six different *ANKRD26* mutations were associated with thrombocytopenia, and they were all located in a stretch of 19 nucleotides of the 5'UTR.

ANKRD26 (*Ankyrin Repeat Domain Containing 26*) is the ancestor of a family of primate-specific genes termed POTE (Prostate-, Ovary-, Testis-, and placenta-Expressed genes) and its expression is also reported in megakaryocytes (Macaulay et al., 2007). This gene encodes for a 192 kDa protein, highly enriched with spectrin helices and ankyrin repeats, both protein domains with confirmed interactions with the cytoskeletal and signaling protein.

Despite pieces of evidence suggesting its involvement in several metabolism pathways (Raciti et al., 2011; Fei at al., 2011), its role has to be clarified. The function of POTE genes is still elusive but recent studies suggest the involvement of ANKRD26 in cytoskeletal actin organization and localization (Bera et al, 2002), proapoptotic process (Liu et al., 2009), and tumor progression (Bera et al., 2008). Moreover, the disruption of *Ankrd26* in mice could explain certain forms of obesity, gigantism, and diabetes

(Bera et al., 2008; Dong et al., 2005), due to likely deregulation in the modulation of signaling pathways.

Overall, very distinct mutations in *ANKRD26* have been linked to different human cancers. In 2017, Marconi and coworkers studied 250 consecutive, non-familial, adult Acute Myeloid Leukemia (AML) patients and screened the first exon of *ANKRD26*, including 5'UTR. Briefly, they found variants in four patients and most of them were associated with the synthesis of N-terminal truncated *ANKRD26* isoforms with a strong ability to stimulate MAPK/ERK signaling pathway. This mechanism could explain the increased risk of myeloid malignancies in THC2 patients (Marconi et al., 2017). Furthermore, the cancer-linked Ankrd26 mutations include a C terminal Ankrd26 truncation and fusion with a part of the protein product of the protooncogene RET (Staubitz et al, 2019), a tyrosine kinase signaling component.

All these mutations include deletion of a more C-terminal part of Ankr26, resulting in disruption of the site of binding to PIDD1, a component of the multi-protein complex PIDDosome. This complex is composed of three proteins, Caspase-2, PIDD1, and RAIDD, and its activation leads to p21-dependent cell cycle arrest due to an increase in the number of mature centrosomes after disrupting cytokinesis or forcing centrosome overduplication (Fava et al., 2017) (**Figure 7**). Therefore, it could speculate a role of this altered mechanism in the reduction of megakaryocyte ploidy observed in THC2 patients.
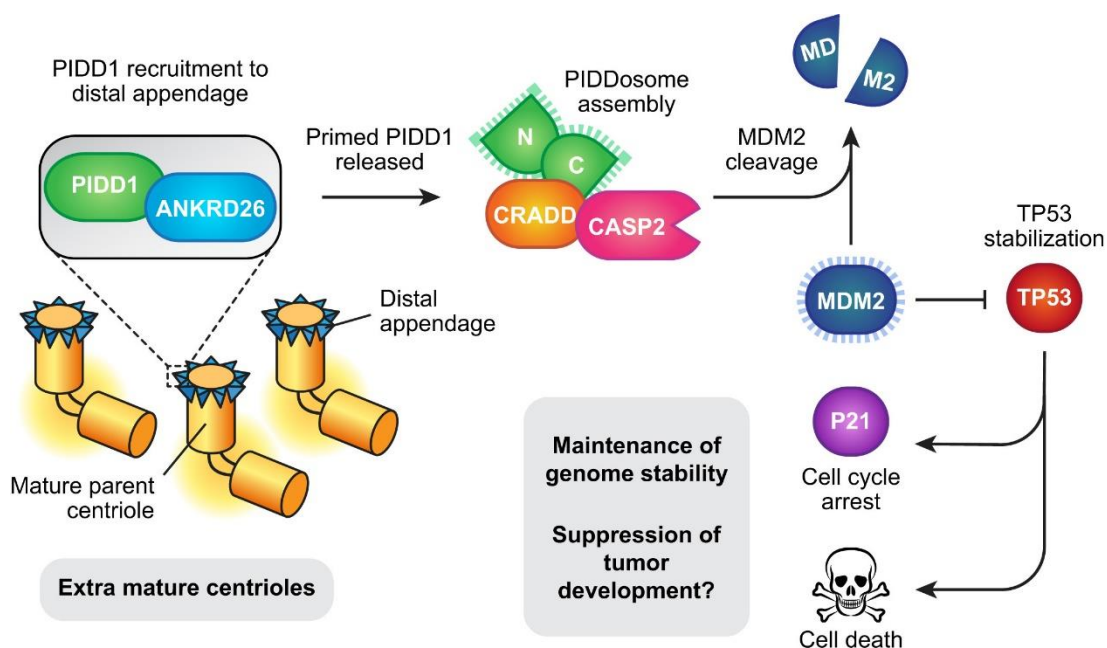
Fig. 7 Model of PIDDosome activation in cells with extra centrosomes. PIDD1 is recruited by ANKRD26 in the distal appendage. When extra mature parent centrioles are present, PIDD1 is released and activates PIDDosome assembly and caspase-2 activation, which leads to cell cycle arrest via p53. Source: Evans et al., 2021.

Mechanisms affecting megakaryocyte function and platelet-related count in *ANKRD26*-RT are still unknown. Pecci and coworkers suggested the involvement of PaCS, novel particulate ubiquitin/proteasome-rich cytoplasmic structures, largely present in *ANKRD26*-RT megakaryocytes and platelets (Necchi et al., 2012). Moreover, it has been observed that *ANKRD26* expression in healthy individuals decreases during the megakaryopoiesis, but *ANKRD26*-RT patients display a persistent expression in mature megakaryocytes (Bluteau et al., 2014).

The same group demonstrated that mutations in 5'UTR of *ANKRD26* resulted in the loss of binding of two main transcription factors, runt-related transcription factor 1 (RUNX1) and friend leukaemia integration 1 transcription factor (FLI1), and in *ANKRD26* overexpression in megakaryocytes. The *in vitro* analysis of megakaryopoiesis also evidenced a normal profile of maturation but a decreased formation of proplatelets, in terms of percentage of proplatelet forming-megakaryocytes and number of proplatelets branches per megakaryocyte.

This accumulation of ANKRD26 in the inner part of the cell membrane may also alter the TPO/MPL signaling. ANKRD26 could act as a mediator between the receptors and the signaling pathways, and this hypothesis was confirmed by the over-activation of TPO/MPL downstream pathways (JAK/STAT, PI3K, MAPK/ERK) observed in patients' megakaryocyte (**Figure 8**) (Bluteau et al., 2014).
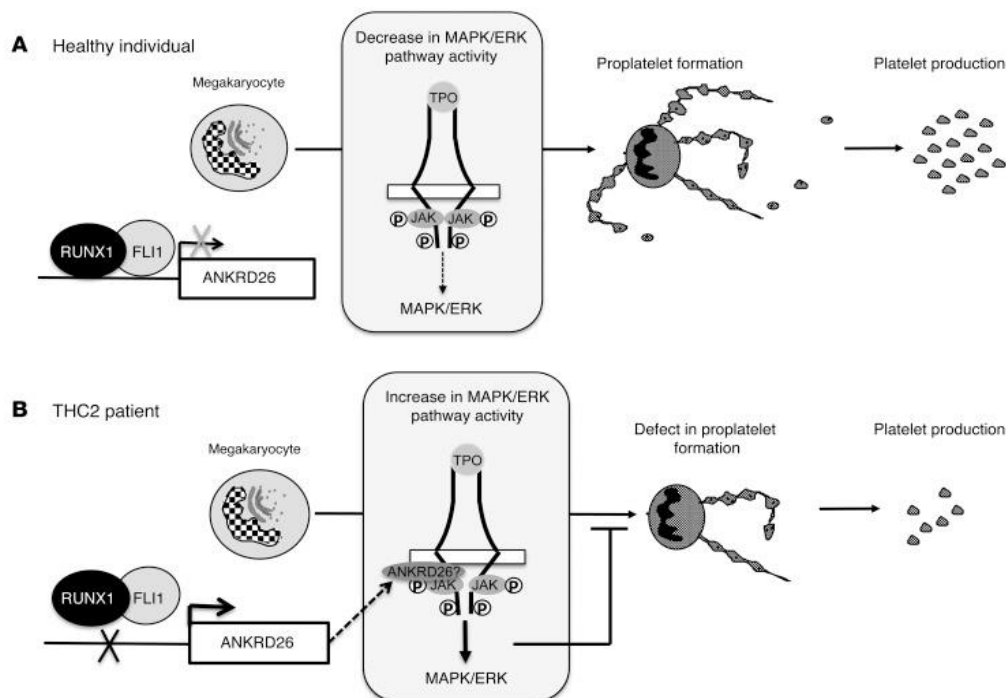
Fig.8 Schematic representation of pathogenic mechanism in ANKRD26-RT. In healthy subjects, RUNX1/FLI1 deregulates the ANKRD26 gene expression, leading to a decrease in TPO/MPL/MAPK/ERK activity (**A**). In THC2 patients, mutations prevent RUNX1/FLI1 inhibition, resulting in overexpression of ANKRD26, its accumulation in the inner part of the cell membrane, and altered TPO/MPL cascade signaling. MAPK/ERK overactivation leads to a defect in proplatelet formation. Source: Bluteau et al., 2014.

To date, *ANKRD26*-RT represents one of the most frequent forms of ITs (Pecci et al., 2020) and presents non-syndromic thrombocytopenia, dominant inheritance, mild to moderate reduction of platelet count, and normal platelet size. However, it can predispose to myeloid neoplasms: it was observed an incidence of acute myeloid leukemia (AML), MDS, and chronic myeloid leukemia was increased by 24, 12, and 21 fold, respectively, compared to the general population (Noris et al., 2013).

MYH9-related disease

Mutations of *MYH9* in humans cause a syndromic, autosomal-dominant disorder called *MYH9*-related disease (*MYH9*-RD) (Kelley et al., 2000), resulting in congenital

thrombocytopenia, platelet macrocytosis, and inclusions of NMHC IIA in the cytoplasm of neutrophil granulocytes (Pecci et al., 2018).

MYH9 gene encodes the heavy chain of non-muscle myosin of class II, isoform A (NM IIA), involved in cell contractility, migration, and adhesion. In mammals, three isoforms of class II non-muscle myosin (NM IIA, IIB, IIC) were found, encoded by MYH9-10 and -14, but only NM IIA is expressed in platelets. NM IIA is a hexameric molecule, characterized by a homodimer of heavy chains (230 kDa), two regulatory light chains (20 KDa), and two supplementary light chains (17 kDa). Functionally, the N-terminal head domain represents the globular motor domain, responsible for actin binding, while the neck domain acts as the lever arm that amplifies the movement induced by the conformational changes of the motor domain. Moreover, the tail domain facilitates the dimerization of the heavy chains and formation of NM IIA functional filaments, a long alpha-helical coiled-coil rod constituted of typical heptad repeats (**Figure 9**).
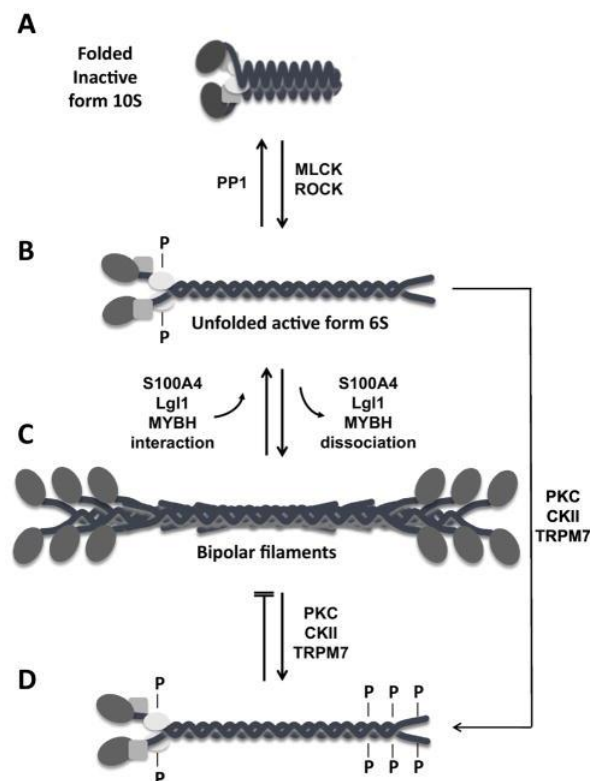

Fig. 9. Molecular Structure of non-muscle myosin IIA. The folded, inactive 10S form on NM IIA (**A**) assumes an unfolded form after specific phosphorylation (**B**) and assembles into bipolar filaments (**C**). Phosphorylation of residues at the C-terminus by different kinases disassemblies the bipolar filaments. Source: Pecci et al, 2018

The folded (inactive) and unfolded (active) forms of NM IIA are regulated by the action of specific kinases (myosin light chain, MLCK and Rho Kinase) that remove the inhibition through the phosphorylation of 20kDa light chain on serine 19 (S-19) and threonine 18 (T-18). This mechanism triggers the bipolar filament formation and increases the actin-activated MgATPase activity (Craig et al., 1983). On the other hand, Protein Kinase C (PKC) can decrease the activity of NM IIA through the phosphorylation of Serine 1,2 and Threonine 9.

NM II isoforms are widely expressed in different tissues and are associated with specific functions. In this context, it's not rare to reveal the co-presence of NM IIA and NM IIB in complex tissue with different cell types, but some isoforms (NM IIA) are exclusively found in some cell types (Spleen cells, platelets). Several groups are still investigating the role NM IIA in megakaryocytes and platelets, and specifically which mechanisms required the involvement of this isoform. In recent work, Catherin Leon (Pertuy et al., 2014) analyzed the myosin IIA deficiency in a Myh9 -/- mouse model and in MYH9-RD patients. Results evidenced that the absence of myosin affects the F-actin organization in megakaryocytes, with critical alteration of organelle motility during proplatelets elongation (**Figure 10**). In particular, F-Actin distribution in Myh9 -/- model doesn't appear localized in the peripheral region of megakaryocytes, as observed in WT megakaryocytes. Based on this model, the organelle distribution is strongly affected in megakaryocytes and this alteration reflects impaired trafficking of these structures along proplatelets in native platelets.
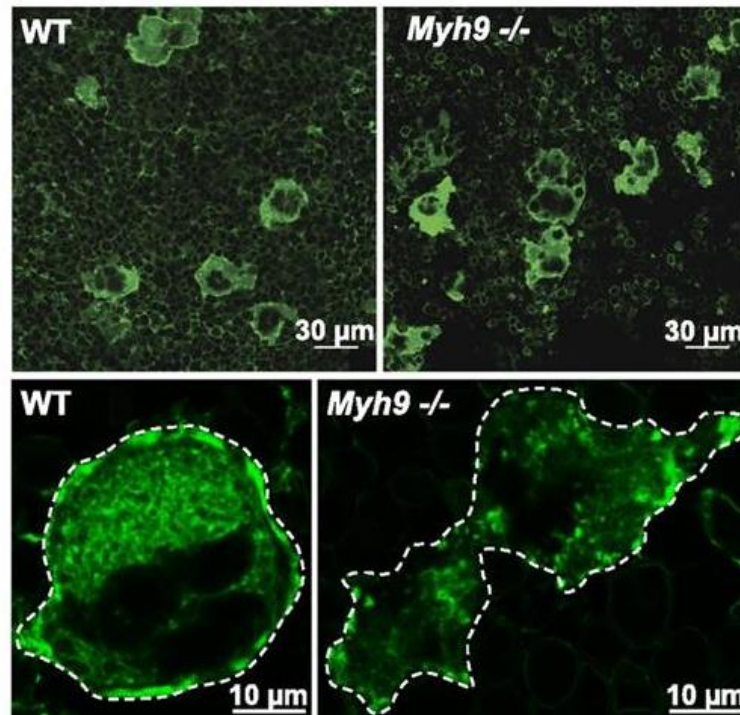
Fig. 10. Defective actin organizations in Myh9 [-/-] Details of impaired organization of F-Actin distribution in bone marrow Myh9 [-/-] megakaryocyte, stained with AF-488 phalloidin. Source: Pertuy et al., 2014.

MYH9-RD is the most frequent form of ITs (Pecci et al., 2021), and its clinical manifestations range from mild reduction of platelet count to severe thrombocytopenia. From a diagnostic point of view, *MYH9*-RD is characterized by platelet macrocytosis and inclusions of the NMHC IIA proteins in the blood smear of patient samples (Seri et al., 2003).

Cellular and functional alterations involve megakaryocyte maturation, which presents defects in proplatelets branching and increased diameter of tips (Pecci et al., 2009). In this study, Alessandra Balduini and coworkers analyzed the *in vitro* megakaryocyte maturation and differentiation of *MYH9*-RD patients samples, belonging to four unrelated *MYH9*-RD pedigrees carrying the p.D1424N or the p.R1933X mutants. Briefly, results showed that there was a comparable maturation between patients and controls, but the proplatelets extended by *MYH9*-RD presented an altered morphology, in terms of the reduced number of bifurcations and larger size of tips compared to the healthy controls.

Recently, Fowler's work suggested a new pathogenic mechanism sustaining megakaryocyte defect in proplatelet formation and function in *MYH9*-RD mouse models. Using three models with different point mutations located in NM IIA, he demonstrated that *MYH9*-RD megakaryocyte distribution in bone marrow is generally altered, due to compromised contractility and adhesion (Kasturi et al.,2020).

TPO AND c-Mpl

Since the cloning of c-Mpl (Vigon et al., 1992) and purification of its ligand TPO (Kaushansky et al., 1994), respectively 1992 and 1994, a new era of research on megakaryopoiesis and thrombopoiesis was opened and new paths in developing therapeutic strategies for thrombocytopenia were mapped. Human TPO is a 353-amino acid glycoprotein (85 kDa), compose of two subdomains: a 153-residue N-terminal receptor-binding-domain (RBD) and a 179-residue C-terminal domain. Similar to Erythropoietin (EPO), TPO has high- and low-affinity ligand-binding sites and binds to the receptor with a 1:2 stoichiometry. In contrast to EPO and GH, TPO possesses an additional, predicted intrinsically disordered C-terminal domain, which is heavily glycosylated (six N-linked and four O-linked sites). The glycan domain plays a role in the correct trafficking of the cytokine through the secretory system (Hoffman et al, 1996) (**Figure 11**).
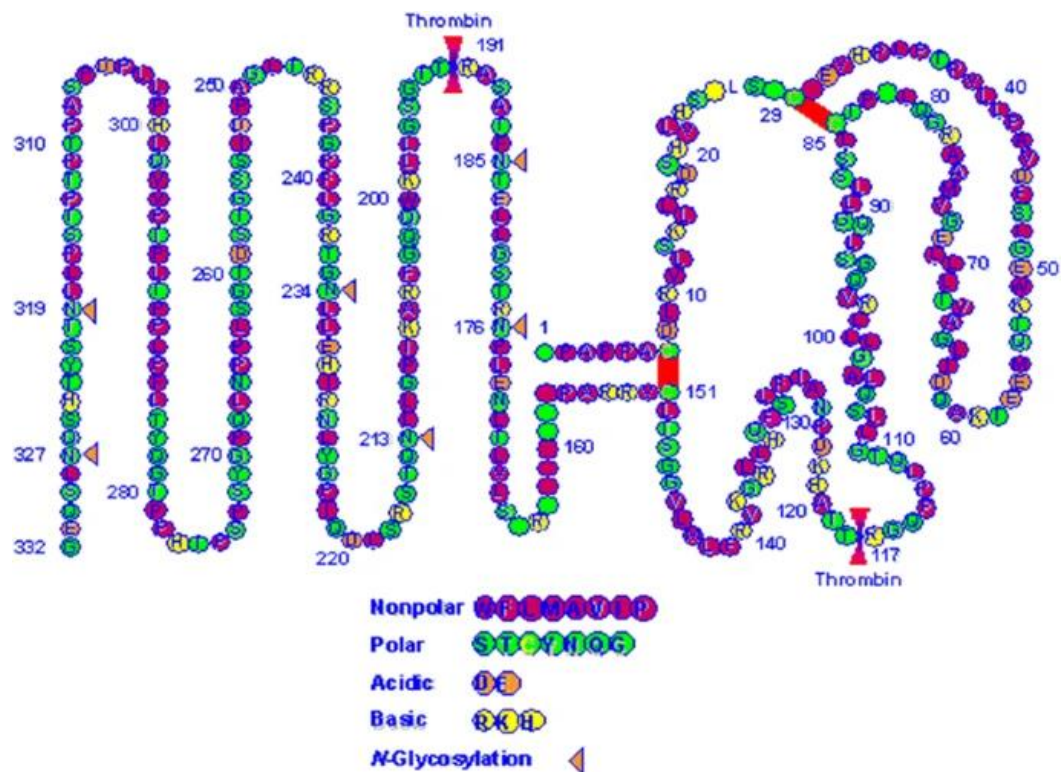
Fig.11. Structure of Thrombopoietin. Thrombopoietin (TPO) displays two main functional domains: an EPO-like domain (residues 1-153) which binds the TPO receptor, and a carbohydrate-rich domain (residues 154-332) responsible for its stability. Source: Kuter, 2013.

TPO is mainly produced in the liver (60% of total), but other sources are represented by kidney proximal tubes cells and bone marrow stromal cells. Its physiological concentration in serum is around 50-150 pg/ml, inversely related to megakaryocyte and platelet count. TPO is cleared from the circulation through receptor-mediated uptake and degradation by megakaryocytes and platelets, and a decreased count of both cells leads to reduced TPO binding and clearance, increasing the circulating TPO. In many thrombocytopenic conditions, TPO levels are up to 20-fold above normal, in inverse relationship with platelet count (Kuter et al, 2009). Conversely, in patients with thrombocytosis, the TPO production is overwhelmed by platelet-mediated TPO metabolism, and then its circulating concentration is very low. Further, in the last years, several teams are focusing attention on the diagnostic value of TPO levels to discriminate between the different forms of thrombocytopenia. Porcelijn's study measured the level of plasma TPO in 178 clinically well-defined thrombocytopenic patients and observed how all patients with depressed platelet production had elevated

TPO levels, whereas TPO levels were in the normal range in patients with immune-mediated thrombocytopenia (Porcelijn et al., 1998).

The TPO receptor, c-Mpl, is primarily expressed in HSCs, megakaryocytes, and platelets. This protein is made up of 635 amino acids and belongs to the hematopoietic growth factor receptor superfamily. Unlike the other members, it shows two cytokine receptor modules (CRM) in the extracellular domain, while the cytoplasmatic domain is composed of two 60-amino acids acid regions. Finally, the membrane-proximal region includes two conserved sequence motifs (box 1 and box 2), essential for binding to Janus Kinase 2 (JAK2) to lead signal transduction (**Figure 12**).
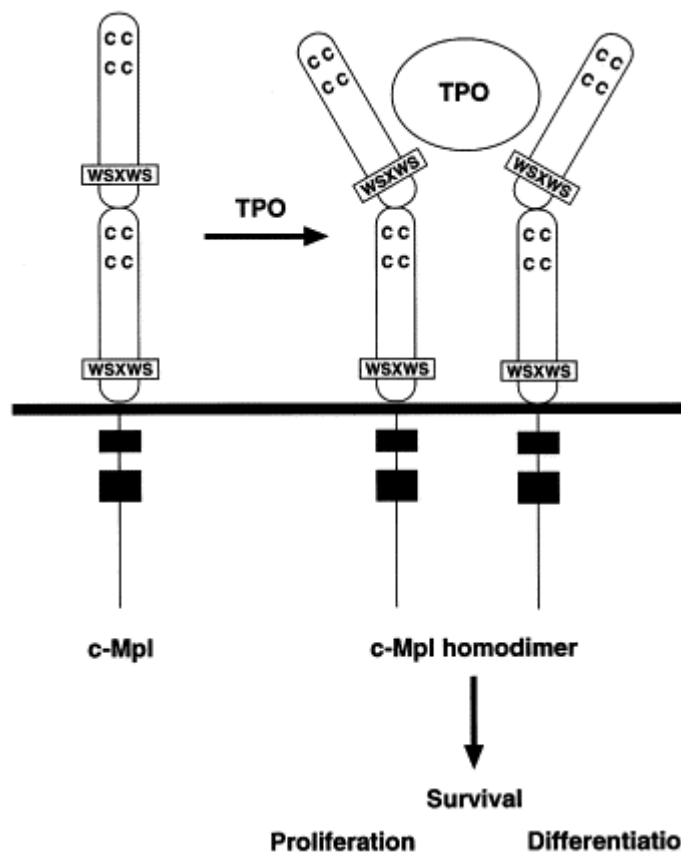
Fig.12 Schematic representation of Thrombopoietin receptor, c-Mpl. Thrombopoietin (TPO) binding stimulates c-Mpl homodimerization and activation of signaling pathways cascade. Notably, the extracellular domains conserve cysteine pairs and WSXWS motifs. Source: Alexander et al., 1999.

To further understand the mechanisms of interaction c-Mpl/TPO, Luoh's team (Luoh et al., 2000) analyzed the contribution of the different regions (cytoplasmic and distal) in the stimulation of megakaryopoiesis. They knocked out the carboxy-terminal 60 amino acid of the c-Mpl intracellular domain in mouse models, observing normal platelet and

megakaryocyte counts but an impaired response to exogenous TPO. Further analysis (Drachman et al., 1997) on truncated forms of murine c-Mpl identified subdomains necessary for activation of TPO-induced signal transduction. In particular, the TPO receptor can be phosphorylated at either Y112 or Y117, but Y112 is necessary for phosphorylation of Shc and Shc-associated p145(SHIP). Y112 also represents a STAT5 recruitment site, and STAT5 phosphorylation is partially phosphorylated in absence of tyrosine residues in the c-Mpl cytoplasmic domain.

According to several studies, megakaryocytes and platelets express a huge number of c-Mpl receptors on their cell surface, respectively 12000 and 25-200, and that seems modulated by TPO binding and receptor internalization (Fielder et al., 1997; Li et al., 1999). This latter process is believed to play a role in the regulation of circulating TPO and involves two distinct regions of interest: the primary site of c-Mpl tyrosine phosphorylation and the box2 motif. Particularly, this study (Debra et al., 2003) demonstrated that two dileucine motifs in the cytoplasmatic domain drive the internalization and this mechanism occurs also in absence of JAK2 activation.

After binding of TPO, the receptor homodimerize, and this lead to phosphorylation and activation of JAK2, which activates the phosphorylation cascade and triggers multiple signaling pathways, in particular transducers and activation of transcription (JAK2, STAT3, STAT5), the mitogen-activated kinase (MAPK), such as ERK, p38 kinase, or the phosphatidylinositol-3-kinase (PI3K) pathway. Briefly, homodimerization of c-Mpl allows JAK2 kinases to cross-phosphorylate and activate each other. Activated JAK2 kinase phosphorylates tyrosine residues on the distal portion of the c-Mpl receptor which leads to the recruitment of various proteins to the receptor via their Shc homology (SH2) or phosphotyrosine-binding (PTB) motifs. JAK2 also activates STAT family and dimerization of STAT proteins cause their translocation to the nucleus and transcription of genes, such as BCL2L1, CYCLIN D1, and c-MYC. TPO can also activate the phosphatidylinositol-3-kinase (PI3K) pathway and the mitogen-activated protein kinase (MAPK) pathways. In PI3K pathway, it leads to phosphorylation and activation of AKT, which promotes cell cycle progression inhibiting FOXO3 translocation in the nucleus and activation of BAD-mediated apoptosis signal. In MAPK pathway, SOS1 (guanine nucleotide exchange factor) activates RAS that sustains MAPK cascade, regulating cell cycle regulatory genes (CDK4/6, ELK1, CREB1).

The mechanism which triggers megakaryopoiesis became clear after the cloning of TPO in 1994 (Kaushansky et al., 1994). Different *in vitro* approaches demonstrated how TPO was able to drive differentiation and megakaryocyte differentiation, increasing the number of megakaryocyte colony-forming units, cell size and ploidy, and expression of lineage-specific markers GPIb and GPIIb/IIIA (Kaushansky et al., 1994). Gurney's and Sauvage's (Gurney et al., 1996; de Sauvage et al., 1994) *in vivo* studies also revealed how the KO of the two genes determine a 67% lower platelet count in animal models, showing the key role of TPO as the only key regulator of platelet production. Interestingly, these animals also showed a reduction of erythroid (BFU-E) and myeloid (CFU-GM) colonies, suggesting that TPO also served the growth and viability of cells of all lineages.

TPO is widely recognized as a regulator of megakaryopoiesis and thrombopoiesis, supporting HSCs survival and expansion and megakaryocyte progenitor cells. It promotes the proliferation, maturation, and differentiation of megakaryocytes, but it doesn't seem involved in the last step of proplatelet formation and platelet release in blood. However, several studies demonstrated its fundamental role in bone marrow functionality and HSC development: congenital absence of c-Mpl is related to CAMT progression, and experimental deletion of TPO/c-Mpl leads to severe Thrombocytopenia.

Several studies support the hypothesis that the level of serum TPO may help distinguish between various causes of thrombocytopenia and predict treatment response to pharmacological treatment, e.g. TPO Receptor Agonists (TPO-Ras). Kuter's team (Makar et al., 2013) assessed the serum TPO concentration in patients with haematological malignancies to determine the normal range of TPO levels and find a likely correlation between TPO levels and different platelet production. Serum TPO concentration in consumptive thrombocytopenia (e.g. Immune Thrombocytopenia) was significantly lower than hyperproliferative, with an inverse correlation with overall platelet count. Eligible patients were treated with TPO-RAs (Romiplostim, Eltrombopag) and subsequently, the clinical response was correlated with serum TPO levels. From obtained data, patients with serum TPO levels <95pg/ml showed a positive response (a sustainable increase of platelet count) to the treatment, suggesting a diagnostic utility to predict response to treatment with TPO mimetics. Through a receiver operating characteristics (ROC) analysis, the same group further identified optimal TPO thresholds in ITP patients for response to TPO-RAs treatment,

respectively ≤ 136 pg/ml for eltrombopag and ≤209 pg/ml for romiplostim (Al-Samegakaryocyteari et al, 2018).

Thrombopoietin receptor agonists (TPO – RAs)

The cloning and purification of TPO in the early '90s sustained the development of recombinant proteins, such as recombinant human TPO (rhTPO) and pegylated megakaryocyte growth and development factor (PEG-rHuMGDF), to assess their potential use to treat pathologies affecting platelet production, in particular Thrombocytopenia. Their administration in cancer patients with thrombocytopenia helped platelet recovery (Basser et al., 2000) but, despite initial promising results, they didn't prove effective in ameliorating ITP. Moreover, the administration of PEG-rHuMGDF to healthy volunteers to enhance platelet collections after apheresis, caused cross-reactive thrombocytopenia in several cases These conflicting results have prompted the scientific community to develop novel thrombopoietin agents. These "second-generation" molecules have little sequence homology with TPO, avoiding cross-reactivity, and include peptide and small molecule mimetics and c-Mpl agonistic antibodies (**Figure 13**).
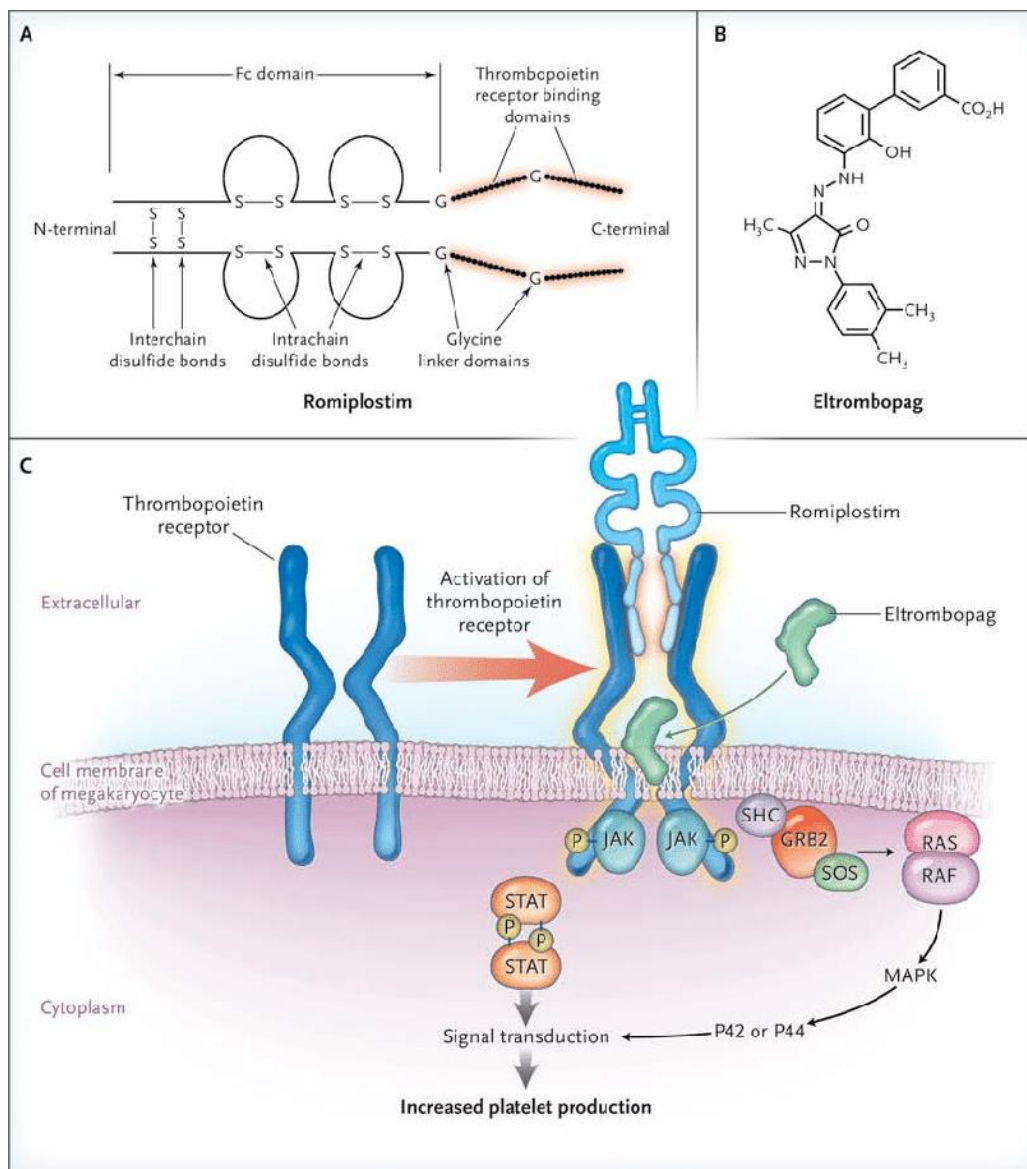
Fig.13 Thrombopoietin Mimetics: Eltrombopag and Romiplostim. Chemical structures of Romiplostim (**A**) and Eltrombopag (**B**) that stimulate the Thrombopoietin Receptor, c-Mpl, with different mechanisms of action (**C**). Source: Imbach et al., 2011

1. TPO Peptide Mimetics: Romiplostim

In 1997, Cwirla's group (Cwirla et al., 1997) identified two families of small peptides binding the TPO receptor from a recombinant peptide library. One of these families, characterized by a specific 14-amino acid peptide sequence, showed its ability to bind the receptor with high affinity and stimulate the proliferation of the TPO-responsive cell line. After peptide dimerization, it also drives the *in vitro* proliferation and maturation of megakaryocytes from human

bone marrow. However, given its intrinsic instability *in vivo*, various strategies were employed to increase their shelf-life, such as the generation of fusion with stable protein (e.g. Fab59, Peg-TPOmp).

Romiplostim (AMG 531, Nplate) represents a new class of therapeutics called "peptibodies", which identifies the fusion of the component peptide and the FC portion of an immunoglobulin. This structure allows this molecule to interact and stimulate the c-Mpl and stabilize the complex for *in vivo* treatment. This molecule is made as a recombinant protein in *E. Coli* and the Fc fragment is derived from the human IgG1 heavy chain (**Figure 14**).
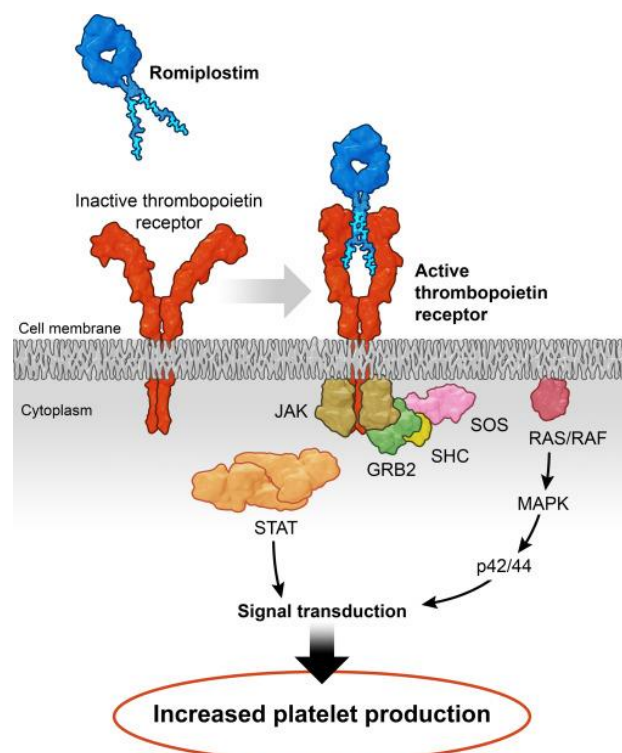
Fig.14. Mechanism of action of Romiplostim. This "peptibody" mimics the action of Thrombopoietin (TPO) inducing the dimerization of c-Mpl and its activation. Romiplostim competes with TPO for the extracellular binding site and triggers the activation of AKT, STAT, and ERK pathways, involved in megakaryocyte differentiation and platelets production. Source: Kuter et al., 2021

Since the first *in vitro* evidence (Broudy et al., 2004), Rompilostim was able to stimulate CFU-Meg growth and maturation of megakaryocytes in a concentration-dependent manner. Interaction of Romiplostim with c-Mpl seems to activate tyrosine phosphorylation and subsequent activation of Mp1, JAK2-STAT5, ERK1/2, and AKT downstream signaling pathways (Currao et al.,

2013). *In vivo* studies showed that Romiplostim was active in different species, well-tolerated, and induced dose-dependent response, tough the data obtained from nonhuman primates was variable.

After *in vivo* administration in healthy human volunteers, romiplostim demonstrated its effectiveness to increase platelet number with a lower dose compared to nonhuman primates (1-3 ug/kg, i.v.), reaching the peak count 12-16 days after administration (Wang et al., 2004). A second double-blind, phase 1 study (Kumagai et al.2007), demonstrated the good tolerability of Romiplostim in healthy volunteers and non-significant side effects, but some aspects involving the clearance and the optimal dose remain unanswered.

A large body of evidence supports the use of romiplostim to safely and effectively increase platelet counts in adults and children with ITP. Two-phase 1-2 clinical trials in patients with chronic ITP were completed, in the U.S. (dose:0.2-10 ug/kg) and Europe (dose: 300-500 ug). In both cases, Romiplostim was well tolerated and able to induce platelet increase (endpoint: platelet count between $50-450x10^9/L$) (Bussel et al., 2006; Newland et al., 2006). Lastly, two studies were completed in adult chronic ITP (splenectomized/non) and, even in this case, Romiplostim sustained a durable platelet response, respectively in 38% and 61% of overall cases (Kuter et al., 2008). Safety and long-term efficacy have been evaluated in chronic ITP patients: after up to 156 weeks (mean=69) of treatment, serious adverse events were reported in 9% of patients, severe bleeding in 9%, and thrombotic episodes in 5%(Bussel et al., 2009). Kuter and coworkers (Kuter et al., 2010) reported the results of a Phase III trial of 234 adult patients with ITP who had not undergone splenectomy, compared romiplostim treatment with standard of care – glucocorticoids being the most common standard-of-care treatment noted. They found that the rate of response was 2.3-times higher, and the incidence of treatment failure was lower (romiplostim, 11%; standard of care, 30%; P,0.001). Overall this data suggests an acceptable safety profile of the drug.

Romiplostim is, then, approved for ITP with an insufficient response to corticosteroids, immunoglobulins, or splenectomy, but positive responses were obtained in clinical studies on CIT; aplastic anemia patients in which the risk/benefit ratio has to be assessed.

2. TPO Small Molecules Mimetic: Eltrombopag

Small molecule compounds (< 500 Da) are developed as alternative sources of TPO mimetic. They can bind the c-Mpl in different sites with respect to TPO and show a heterogeneous potency and more restricted species specificity. For instance, AKR-501 promotes megakaryocyte differentiation, but it's 30-1000-fold less potent than recombinant human TPO. The species restriction of many TPO nonpeptide mimetics is a peculiar characteristic that limits their preclinical evaluation only on toxicology testing.

Eltrombopag (Promacta® or SB-497115) is a first-class, orally active, small molecule (MW=564 Da). Structurally, it belongs to the (5-oxo-1,5-dihydropyrazol-4-ylidene)hydrazines family, modified in byphenyl carboxylates to improve bioavailability. This class of compounds elicits signal transduction response (JAK2 and STAT5 activation) through TPO receptor stimulation, promoting megakaryocyte differentiation (**Figure 15**).
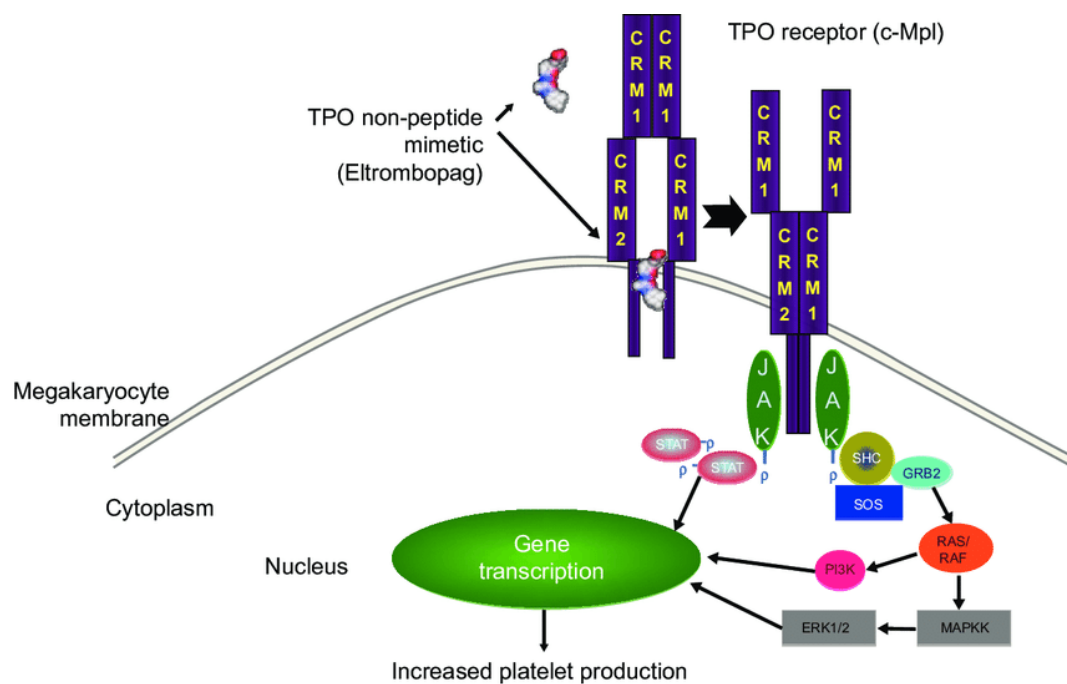
Fig.15 Putative mechanism of action of Eltrombopag. This molecule binds the c-Mpl in its transmembrane region and activates JAK/STAT and MAPK pathways, stimulating platelet production. Source: Giannini et al., 2009

Compared to other TPO-RAs, Eltrombopag has a unique transmembrane binding site and does not compete with TPO, allowing additive effects even in patients with increased endogenous TPO levels (Kuter, 2007). Particularly,

Eltrombopag interacts with a Histidine residue (His 499) in the transmembrane domain and two C -terminal residues (Leu504, Ala506, Gly509, and Leu511– Leu-513). Recently, it has been revealed the iron-chelation action of Eltrombopag (Roth et al., 2012), but there is no evidence suggesting a therapeutic role in patients with ITP. However, chelation of Zn^{2+} seems to play a role in interaction with His499 and presumably increases the binding affinity for the TPO receptor, c-Mpl (Kim et al., 2007).

For these reasons, SB-497115 was selected for clinical studies for its efficacy (EC_{50}=30-100 nM) and oral bioavailability (Luengo et al., 2004). In Phase-1 Clinical Trial, Eltrombopag was administered to 73 healthy male subjects as once-daily oral capsules for 10 days at doses of 5,10,25,30,50 e 75 mg, and prompted a dose-dependent platelet count increase, with no differences in adverse events with respect to placebo. Further, *in vitro* evidence demonstrated how SB-497115 doesn't mimic the ability of rhTPO to enhance ADP-induced aggregation of platelets (Erhardt et al., 2004), whereas *in vivo* administration in chimpanzees confirmed the increase of platelet count and good tolerability (Sellers et al., 2004). Safety and tolerability of Eltrombopag were also sustained from results obtained by 3 Phase-1 trials, in which ITP patients were treated for 6 weeks at doses of 30-75 mg, with no evidence of correlation with drug administration (Provan et al., 2006). Given that, Bussel's team conducted a trial in which 118 adults with chronic ITP, refractory to an approved treatment, received 30, 50, and 75 mg/day. The platelet response increase was linear, dose-dependent, with a significant response after 15 days of treatment, and reduction of bleeding events (Bussel et al., 2007).

Finally, in Phase2-3 clinical trials, Eltrombopag was administered to 73 ITP patients and the study group achieved platelet counts of 50 000/µL within 2 weeks. In conjunction with the rise in platelet count, a prospective assessment showed a significant reduction in bleeding events both during and at the end of the study. From these results, it has been concluded that Eltrombopag is an effective and safe treatment for patients with chronic ITP, at doses of 50mg, and could be safely increased to 75 mg in Non-Responders (Bussel et al., 2009).

Encouraging results were also obtained from Phase-3 Clinical Trials in thrombocytopenic patients correlated to Hepatitis C. Briefly, this study showed that Eltrombopag increased platelet count to $100000/mm^3$ in a dose-dependent

manner, even after the suspension of the treatment (McHutchinson et al., 2007). Other clinical studies (Afdhal et al., 2012) confirmed the effectiveness of Eltrombag in raising the platelet count in a numerous, correlated group of patients. Currently, Eltrombopag is FDA and EMA-approved as second-line treatment of patients with ITP or thrombocytopenia associated with chronic hepatitis C infection but plans for testing the safety and thrombopoietin potential of eltrombopag in the treatment of thrombocytopenia in MDS are underway.

In this context, new TPO-RAs small molecules with high structural and chemical similarities to Eltrombopag have been developed in the last years.

Lusutrombopag and Avatrombopag are orally bioavailable drugs that interact with the transmembrane portion of TPO-Rs on megakaryocytes, and subsequently, stimulate the proliferation and differentiation of megakaryocytes from bone marrow progenitor cells leading to increased production of platelets. Specifically, Avatrombopag (Doptelet®) interacts with the transmembrane domain of the TPO receptor and provides several advantages over other drugs, such as less immunogenicity, oral routes of administration, and potentially reduced production costs (Fukushima et al., 2009). However, its bioactivity is restricted to humans and chimpanzees, resulting in unsatisfactory pre-clinical data. Like Eltrombopag and Lusotrombopag, Avatrombopag interacts with a specific His499 in the transmembrane domain but doesn't show any chelation of cation properties and requires no dietary restrictions. From a pharmacological point of view, Avatrombopag has a similar half-life (19 hours) compared to Eltrombopag (21-32 hours), satisfactory *in vivo* response, and a safety profile. Finally, it's currently approved for the treatment of thrombocytopenia in patients with chronic ITP who don't respond to previous therapeutic options (Dova Pharmaceuticals Inc; Doptelet: Prescribing information. FDA).

Given the different pharmacodynamic and pharmacokinetic properties of Eltrombopag and Romiplostim, patients' response to TPO-RA treatment can result in refractoriness or resistance due to intrinsic biological variability. In this regard, several clinal studies reported TPO-RAs switching, from eltrombopag to romiplostim and vice versa, in patients with ITP who don't respond to the first treatment. In clinical practice, TPO-RAs switching could be due to: lack of efficacy, platelet fluctuations, safety and tolerability, and adverse effects. From a retrospective analysis (González-Porras et al., 2019), the

primary reason for switching was identified in lack of efficacy (58%) and, in summary, 75% of patients who switched to the alternate TPO-RA maintained or achieved a response.

Inherited Thrombocytopenia and TPO-RAs

Most patients with IT have no or mild spontaneous bleeding and treatment of haemorrhages, usually mucocutaneous is based on locale measures and platelet transfusions. Beyond local measures (e.g.nasal packing, cauterization), platelet transfusion is currently considered the standard measure to stop bleeding. Its use is limited by the risk of HLA alloimmunization, enhancing refractoriness, but it remains the first-line treatment of life-threatening bleeding. In some cases, antifibrinolytic agents can help to recover the hemostatic function (desmopressin, Recombinant Factor VIIa) (Nurden et al., 2020).

To achieve a long-term increase in platelet count, splenectomy and Hematopoietic Stem Cells Transplant (HSCT) are the non-pharmacological treatments of choice. Splenectomy was demonstrated to raise the platelet count in patients with WAS/XLT but it's associated with the onset of infections. HSCT should be considered for severe clinical manifestations and poor prognosis.

To summarize, only two significant therapeutic options (platelet transfusion and HSCT transplant) are available for increasing the platelet count in ITs, unfortunately carrying little transient efficacy or risk of life-threatening side effects

TPO-RAs are currently opening new prospects in the treatment of ITs, providing new potential pharmacological options to increase the platelet count of these patients.

Experience in the treatment of IT with Romiplostim was reported only in a few case studies. In 2012, a patient with Fechtner syndrome (*MYH9*-RD) was included in an AMG531 (Romiplostim) clinical trial (1 to 10 ug/kg body weight). The treatment resulted in an increase in platelet count from 7.000/uL to 66.000/uL after 7 months, followed by a decrease in long-term administration. The reason for treatment failure was unclear, probably due to stem cell depletion during therapy (Gröpper et al., 2012). A short-term treatment (6 weeks) with Romiplostim (1 to 5 ug/kg) involved an *MYH9*-RD patient eligible for a surgical procedure. Romiplostim was able to raise platelet count (84

x10^9/L), but an increase in platelets (giant platelets) was also observed (Yamanouchi et al., 2015).

However, several groups are investigating the effect of Eltrombopag on IT patients. In a Phase-2, multicenter, open-label, dose scalation trail (Pecci et al., 2010), *MYH9*-RD thrombocytopenic patients (<50x109/L) received Eltrombopag (50 mg to 75 mg) for a short period (up to 6 weeks). The treatment was able to restore the platelet count in 11/12 patients, with remission of spontaneous bleeding. Subsequently, given the positive response, TPO-RAs were investigated for the treatment of other forms of ITs. In 2019, the same group has treated patients with *MYH9*-RD and severe thrombocytopenia, elected for surgery, with a short-term course of Eltrombopag (Zaninetti et al., 2019). Briefly, Eltrombopag was used at the dose of 75 mg/day for 3 weeks before the surgery and continued 3 to 7 days after the surgery, obtaining an increase in pre-operative platelet count (75-180 x 10^9 /L) with no significant safety issue.

Zaninetti and coworkers (Zaninetti et al., 2020) also conducted a Phase-2 trial in which Eltrombopag was administered to patients with five different types of ITs (*MYH9*-RD, *ANKRD26*-RD, X-linked/Wiskott-Aldrich syndrome, monoallelic Bernard Soulier syndrome, *ITGB3*- RD). Patients received an escalating dose of Eltrombopag for several weeks (6 to 16 weeks) and a positive response was achieved in 48% of cases. In 2016, Viallard's team reported successful use of Eltrombopag (50 mg/day for 4 weeks) on a 67-year-old man harbouring *ANKRD26* mutation, restoring the platelet count and allowing surgery procedure (Fiore et al., 2016).

Despite all, there are 45 different genes associated with ITs and, at a glance, it cannot predict whether a patient with other gene mutations will respond to the TPO-RAs in the same way. Some concern is, also related to long-term treatment with TPO-RAs: several studies seem to exclude a malignant progression but rare cases of bone marrow fibrosis are reported.

From 2D to 3D culturing

Two Dimensional (2D) cell culture has been the method used to culture cells for decades, providing the most common platforms for screening drugs, testing cellular toxicity, and assessing cellular behaviour in experimental conditions. In this model,

cells are seeded in a liquid medium where they get in contact with nutrients, cytokines, and other soluble factors, in a monolayer. In the last years, the field of mechanobiology highlighted the central role of physical forces in cell development and physiology, completely absent in 2D culture. In answer to these limitations, several three-dimensional have been developed for different kinds of tissues in which cells take into account the spatial organization of the environment. However, to better resemble the complexity and the composition of native tissues, several parameters should be considered before approaching 3D cultures, such as the choice of material for the scaffold, the source of cells, and the method of culture, according to the tissue of study. To date, several 3D models (organotypic explant cultures, cell spheroids, microcarrier cultures, tissue-engineered models, hydrogels, scaffolds) were achieved and opened new perspectives for biomedical research (**Figure 16**).
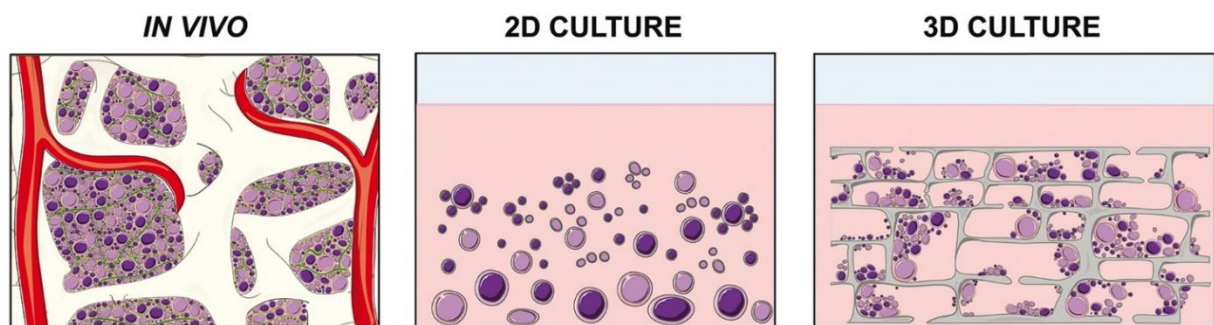
Fig.16. From In Vivo to 3D culture approach. *In vivo* cell behavior is deeply impacted by cell-cell interaction and microenvironment structure and composition. The 2D cultures can ensure cell contacts but environmental cues still represent a limitation. To date, 3D cultures are ameliorating the knowledge of biological mechanisms through the mimicking of the native microenvironment. Source: Adapted from Di Buduo et al., 2021

For instance, cellular spheroids, typically based on the tendency of cells to aggregate, provided a useful tool for studying solid tumor growth and metastasis. However, the need for a more complex and sizeable model determined the development of scaffolds, porous structures mimicking the architecture of tissue or organ and taking into account other parameters, such as cell shape, cell adhesion site, and the flow of gases, nutrients, and metabolites. In this context, the choice of bulk materials is fundamental to fabricating a scaffold and includes metals, glasses, polymers, and ceramics. Their main characteristics are relative to the ability to reproduce the extracellular

microenvironment, along with biocompatibility and plasticity. In this regard, a fundamental requirement for biomaterials is to resume the physical and chemical features of ECM for supporting cell growth and viability, including the possibility to entrap bioactive molecules, modulate a specific range of stiffness and determine the organization and morphology.

Scaffold-based techniques, such as hydrogel-based support or organoids, provide an array of advantages. Hydrogels are a group of polymeric materials, capable of holding large amounts of water in their 3D networks. Both natural (fibrinogen, collagen, Matrigel) and synthetic hydrogels (polyethylene glycol (PEG), polylactic acid (PLA), or poly(vinyl acetate) (PVA)) are largely used in biomedical research. Its intrinsic features allow encapsulating cells into a transparent scaffold, that can be functionalized with active factors and is easy to analyze through microscopic observation. From natural material-based scaffolds, the most used hydrogel type for *in vitro* 3D model is Matrigel, which forms a randomly weaved mesh of fibers that withholds a large amount of fluid, and is useful to establish different types of 3D organoids and 3D spheroids (Ferreira et al., 2018). Organoids can be cultured from embryonic stem cells (ESCs), adult stem cells (AdSCs), induced Pluripotent Stem Cells (iPSCs), and tissue fragments embedded into extracellular matrix 3D scaffold designed with natural or synthetic components. However, these processes don't allow for a specific and regular distribution of cells or matrices, but this limitation has been overcome by 3D bioprinting. With this approach, cells or biomolecules are printed directly onto a substrate in a specific pattern such that the cells can hold together to build the normal 3D structure of a complex tissue. This automatized process enhances a precise and controlled pattern of ECM organization and can also improve the perfusion of gas and nutrients, as well as inter-and intercellular communications (Knowlton et al., 2018). This technique is based on the use of bioink, a material made of biomaterials, cells, and other curing agents, used for the fabrication of functional human tissues, organs, and *in vitro* scaffolds (Guillemot et al., 2011). To date, there has been considerable progress in the bioprinting domain, with various types of tissue being printed and tested, but several issues are still being addressed, such as the use of primary cells, long-term evaluation of post-printing cell viability, and deeper characterization of cell-bioink interactions (Vijayavenkataraman et al., 2018). In this regard, FDA has recently issued a guide, "Techincal considerations for Additive Manufactured Devices"

(fda.gov/media/97633), providing the guidelines for the regulation of additive manufacturing, including 3D bioprinting.

3D cultures have shown differences in drug response, morphology and proliferation rate in static conditions, while under flow conditions, response and functions showed increasing reliability. For this purpose, multiple microfluidic devices were introduced to establish dynamic conditions for cell culture systems. Polydimethylsiloxane (PDMS) is the most used material for making microfluidic devices, due to its gas permeability, biocompatibility, and cost-effectiveness. Along with other thermoplastic and glass scaffolds, PDMS strongly improved microfluidic platforms and the development of a dynamic condition for 3D culture. For instance, Beebe's group has incorporated 3D hydrogel culture, through the use of passive pumping in microchannel arrays. In that system, the pressure difference moves the solutions through the microchannel to the outlet reservoir until the pressure of the droplet remaining at the inlet equals that formed at the outlet (Walker et al., 2002). Chung et al reported a PDMS device to test the migration of endothelial cells through three channels separated by a collagen scaffold (Chung et al., 2009). In the last years, several culture methods include fiber scaffolds, made of natural (collagen, gelatin, silk fibroin) or synthetic (polycaprolactone, polyurethane, polystyrene) fibers. They can be tuned to sizes ranging from microns to nanometers in diameter, and they show strong stability over a wide range of temperatures. Lee and colleagues explored the possibility to incorporate a fiber scaffold in a (polydimethylsiloxane) PDMS microfluidic device. They fabricated PDMS scaffolds, made of two components, in which the bottom layer of the scaffold hosted the inlet port and the outlet port, and the upper part covered the polyurethane fibers scaffold (Lee et al., 2009)

Silk fibroin from *Bombyx Mori*

The scientific community is constantly seeking more sustainable and reliable materials to satisfy the growing demand in different research areas, including biomedical applications. As concerns clinical and biotechnological points of view, natural polymers have attracted the attention of researchers that consider several key factors when designing a scaffold, such as biocompatibility, biodegradability, mechanical properties, structure, and fabrication methods. Promising results were obtained from the use of

alginate, cellulose, and chitosan, useful to resemble the biological and mechanical features of ECM components, but they also showed some limitations that include high cost and batch to batch high variability. Therefore, finding a material combining the biological properties of natural polymers and the mechanical proficiency of synthetic compounds has become the most fascinating challenge over the last decade.

In this context, silk fibroin from silkworm *Bombyx Mori* cocoons has recently gained success as biomaterials due to its several desirable properties. Native *Bombyx Mori* silk is mainly composed of silk fibroin embedded in a coat of sericin proteins. While sericins are adhesive proteins (25-30% of total cocoon weight), fibroin consists of a light chain (MW=26 kDa) and heavy chain (MW=390 kDa) linked by disulfide bonds (Vepari et al., 2007). Structurally, silk fibroin is composed of hydrophobic beta-sheets, linked by small hydrophilic disulfide bonds, while the polypeptide chain includes glycine-X repeats where X is alanine, serine, threonine, or valine. This high content in Beta-sheets results in a hydrophobic protein with strong mechanical properties and ultimate tensile strength (UTS) of 740 MPa.

This strength but elastic protein is biocompatible, having low immunogenicity and low thrombogenicity, and it has been already extensively used in clinical and biomedical applications (as sutures) and bioengineering approaches to create films, gels, sponges, or tubes in bone regeneration and vessels engineering (Lovett et al., 2007). Biocompatibility is a key factor for reliable and successful data from *in vitro* biological tests and *in vivo* scaffold implantation. Silk Fibroin is biologically inert and several studies were conducted to test *in vivo* biocompatibility. Since 1989, this molecule showed blood compatibility during *in vivo* experiments (Sakabe et al., 1989), and in 1993, its use was approved by FDA as a biomaterial for sutures. Moreover, *in vitro* studies demonstrated that silk fibroin film and fibres don't activate an inflammatory response, in terms of macrophage response (Santin et al., 1999; Panilaitis et al., 2003). More concerns regard the use of Sericine in biomedical applications for its inflammation-inducing effects, allergenicity, and immunogenicity. Firstly, Dewair's team (Dewair et al., 1985) measured the immune response (IgE and IgG antibodies titer) in silk-sensitive persons after exposure to silk products. The results revealed an increase in IgE antibody titers in silk-sensitive subjects, with a prominent allergenic activity belonging to the sericin group of silk proteins. These data were confirmed by Zaoming' study in which 90% of the patient population (n=41) developed an allergic reaction to silk extract (sericin) (Zaoming et al., 1996). Other adverse reactions were

observed in ophthalmology (Soong et al., 1984) when some patients experienced severe inflammation with sericin containing raw silk sutures, but fewer reactions with sericin-free silk. However, the biosafety of sericin remains still controversial and some recent *in vivo* studies (Jiao et al., 2017) seem to confute previous hypotheses and results, re-evaluating the likely applications of this silk component as biomaterial (Cao et al., 2016).

Fibrous proteins, like silk fibroin, are characterized by a highly repetitive primary sequence that leads to homogeneity in secondary structure and then, significant mechanical properties for biological and biomedical applications. Silk fibers can be processed following a well-established protocol (**Figure 17**) (Rockwood et al., 2011) to extract a silk fibroin solution, that can be further processed into several formats (sponges, tubes, films) with controlled stiffness and shape.

To obtain a silk fibroin solution*, Bombyx Mori* silk cocoons are boiled for 30 min in 0.02M Na2CO3 to remove the glue-like and adhesive protein, Sericin (*degumming*). Subsequently, the fibroin fibers are rinsed and washed three times in bidistilled water and dried. Then, fibroin fibers are dissolved in 9.3 M LiBr solution at 60°C and finally dialyzed against water (Rockwood et al., 2011).
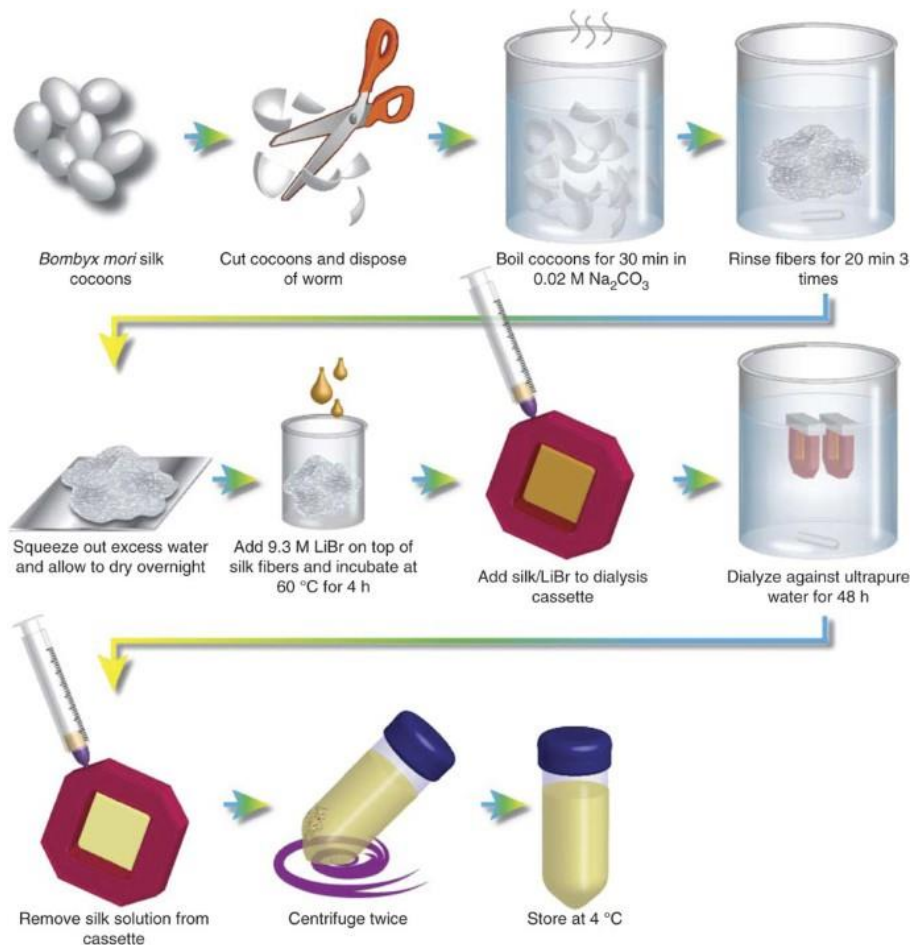
Fig. 17. Schematic representation of Silk Fibroin extraction procedure. This scheme resumes the main steps for silk fibroin extraction from Bombyx Mori cocoons. After boiling in Na2CO3 solution, silk fibres are dissolved in 9.3 M LiBR and dialyzed in a dialysis cassette. The silk fibroin solution is then removed and centrifuged to remove particulates. Source: Rockwood et al., 2011.

Silk fibroin offers versatility in matrix scaffold design, with mechanical and biological performances comparable to extracellular matrix proteins extracts. As mentioned before, this protein can be shaped in several formats for a wide range of applications, deeply investigated in clinical and biomedical applications (**Figure 18**).

Fig.18. Schematic resume of material fabricated from Silk Cocoons processing. Silk fibroin can be processed to obtain a wide range of scaffolds and supports with a large field of applications. Source: Rockwood et al., 2011.

Prof. Kaplan from Tuft University first pioneered the ability of silk fibroin to support cell viability and function, when silk fibroin films were decorated with RGD peptides to promote interaction and adhesion of OB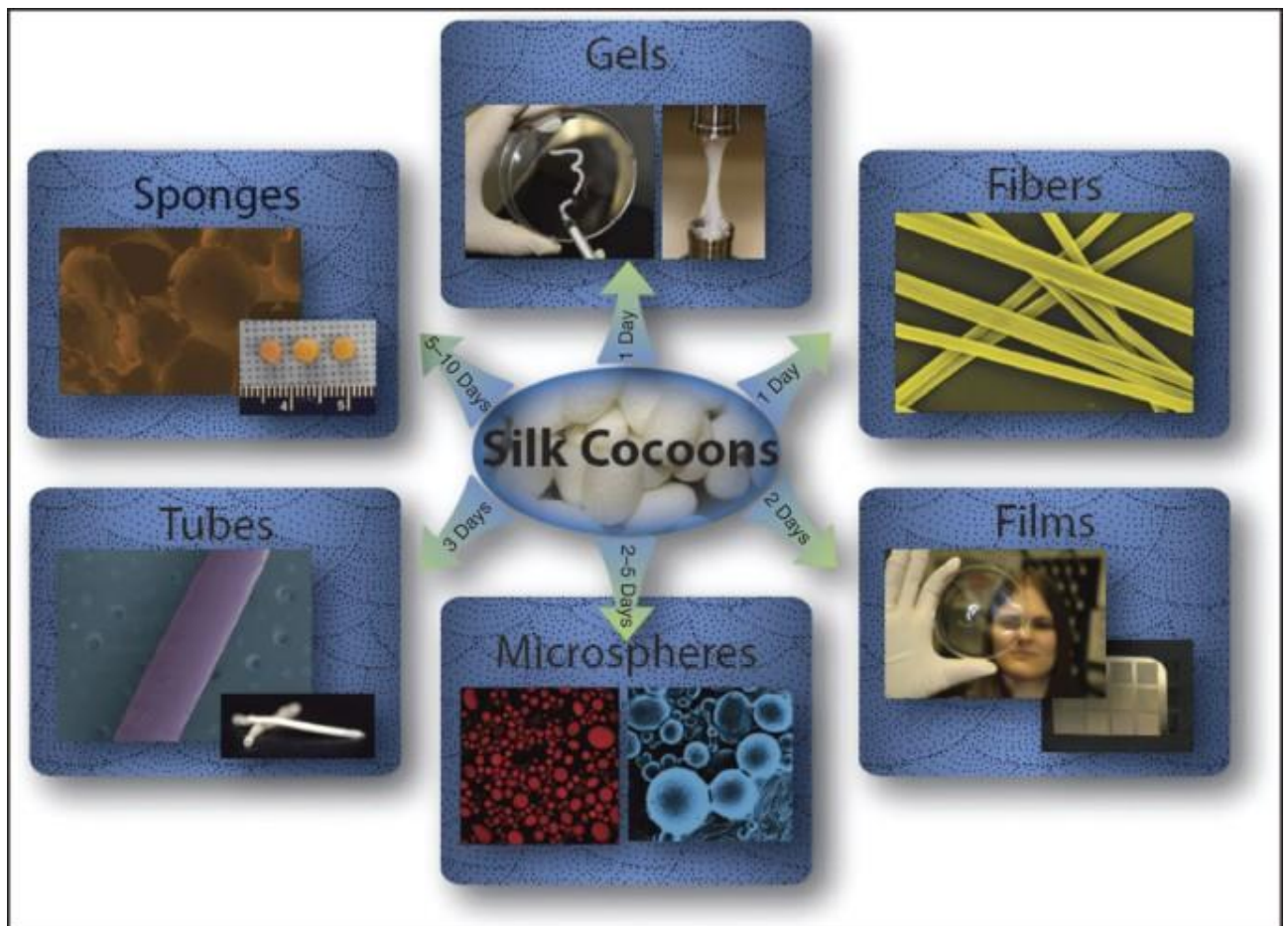s (Sofia et al., 2001). The tunable properties of silk fibroin allow engineering artificial vessels, small tubes (0.1 to 6.0 mm) with controlled pore sizes and robustness. These microtubes exhibit peculiar features, such as permeability, burst pressures, barrier function for both protein diffusion and cell migration, and show the advantage of being functionalized with Extracellular Matrix proteins and Endothelial cells (Lovett et al., 2007; Di Buduo et al., 2015).

Porous sponge scaffolds are important for tissue engineering applications for cell attachment, proliferation, and migration, as well as for nutrient and waste transport. These structures have been utilized in several studies to test the impact of 3D microenvironment on cell behaviour. In 2004, Meinel *et al.* seeded an RGD coupled silk sponge with human MSCs in an osteogenic medium and resulting in osteoblastic

49

differentiation, evaluated by deposition of hydroxyapatite and bone marker upregulation (Meinel et al., 2004). In this regard, silk fibroin sponges can reproduce the architecture of soft and spongy tissues, providing an *ex vivo* model to recreate their complex microenvironment. Alessandra Balduini's group developed several silk-based bone marrow models able to support megakaryocyte function and platelet production and release. In these bioreactors, as described below, functionalized silk sponges are used as a scaffold for seeding megakaryocytes and produce platelets *ex vivo* (Di Buduo et al., 2015; Di Buduo et al. 2017).

3D models of megakaryopoiesis

3D cell cultures deeply improved the knowledge underlying the physiological and pathological mechanisms regulating cellular function. In this context, some groups explored the possibility to apply this model of culture to megakaryopoiesis and thrombopoiesis, to better elucidate some undiscovered aspects of megakaryocyte maturation and platelet production.

Currao and colleagues fabricated a hyaluronan-based hydrogel mixed with different ECM components to evaluate the impact of different matrices on megakaryocyte maturation and function (Currao et al., 2016). The incorporation of different ECM proteins by photo-crosslinking demonstrated that platelet production is mainly enhanced by a soft environment (type-IV collagen) rather than a stiffer matrix (type-I collagen). The involvement of structural cues in megakaryopoiesis and Thrombopoiesis paved the way for the study of the impact of mechanical factors and forces in megakaryocyte maturation and Platelet formation and release. Abbonante's work (Abbonante et al., 2017) demonstrated that megakaryocytes extended more proplatelets on type I and type IV collagens coated on soft silk fibroin film (<10 MPa) compared to stiffer film (>90 Mpa), elucidating the role of mechanical factors. This mechanism seems to be mediated by the activation of TRPV4 (Transient Receptor Potential cation channel subfamily V member 4), a membrane mechano-sensitive cation channel, that regulates mechanotransduction pathways and controls thrombopoiesis on soft substrates. Furthermore, Aguilar and colleagues have proved that 3D cultures using methylcellulose hydrogel with established stiffness (<10 kPa)

better mimic the bone marrow mechanical cues and improve megakaryocyte maturation compared to 2D liquid culture (Aguilar et al., 2016).

3D bone marrow models

Over the years, evidence has accumulated that mechanical and biochemical networks of ECM, soluble factors, and cellular interactions drive cellular functions and viability. Simplified 2D *in vitro* models have been unquestionably useful to obtain basic information for cellular behavior and function but it shows huge limitations in replying to the impact of the complexity of the environment of an organ or tissue. 3D cultures deeply improve the reliability and effectiveness of the data derived from experimental studies, but there is a pressing need to validate more complex and realistic models to bridge the gap with *in vivo* models. In this scenario, scientists have been trying to build laboratory platforms able to mimic bone marrow environments and support the *ex vivo* study of megakaryopoiesis and thrombopoiesis. The first approaches included microfluid chips, in which cells were seeded in a microfluidic device (organ-on-a-chip) that recreates the main characteristic of the native organ. To study cell behavior and evolution of the bone marrow environment during drug screening, Torisawa and colleagues proposed the first bone marrow-on-a-chip (Torisawa et al., 2014). This micro-fluidic model consisted of bone marrow containing both artificial bone and living marrow. The system was made of a hollow cylinder of polydimethylsiloxane (PDMS) filled with a type I collagen gel containing bone-inducing materials. The model was first implanted subcutaneously in mice, and then harvested and cultured inside a microfluidic PDMS platform. The perfusion chamber was separated from overlying and underlying microfluidic channels by porous PDMS membranes. The system was continuously perfused for a week with a syringe pump and irradiation toxicity tests were performed enabling the study of cell responses underflow. In a subsequent study, the device was demonstrated to maintain mouse hematopoietic stem and progenitor cells in normal proportions for at least 2 weeks in the perfused culture and to produce mature blood cells. The first microfluidic chip for specifically making platelets was established by Thon *et al*. The device was made of transparent PDMS and supported high-resolution live-cell microscopy and quantification of platelet production. The device consisted of an upper and a lower microfluidic channel separated by a 2 μm fenestrated barrier. Human iPSCs-derived megakaryocytes were seeded in the upper

channel and extended proplatelets through the slits. This channel was filed with matrigel or alginate hydrogel, while the lower channel was coated with endothelial cells to mimic the vascular network. The perfusion was performed through a syringe pump and fluid shear rates experienced by megakaryocytes were studied in silico and could be regulated across the bioreactor as a function of flow rate (Thon et al., 2014). Moreover, an intriguing challenge for biomedical researchers is represented by combining the 3D cultures system with flow bioreactors. New bioengineering approaches offer 3D scaffolding for bone marrow mimic, proposing the use of biomaterials that allow the realization of a porous microenvironment with interconnected pores allowing cell seeding, cell-cell interaction, cell differentiation, ECM deposition, or coating, and diffusion of oxygen, nutrients, and growth factors. The first platelet bioreactor was presented by Sullenbarger et colleagues. It was composed of a polycarbonate chamber for 3 disks of woven polyester or colloidal crystal hydrogel. These 3 disks could be studied independently. Medium flow passed under and over the disks but not through them, thus limiting the shear stress. The cell chamber was isolated from gas exchange chambers under and over by gas-permeable membranes (Sullenbarger et al., 2009). CD34$^+$ cells derived from cord blood were injected by syringe in the medium flow, then a regular flow was applied. During the culture was possible to collect nonadherent cells or platelets element via a harvest port. The culture of CD34$^+$ cells in this bioreactor allowed a long-term production of platelets (10 days in 2D vs more than 30 days in the bioreactor) and a higher number of collected platelets. Interestingly, when low oxygen concentration (5%) was imposed within the device, enhanced HSC expansion but decreases platelet production were observed; on the opposite, the culture at high oxygen tension (20%) increased the production of platelets but lowered HSC expansion (Lasky & Sullenbarger, 2011; Mostafa et al., 2000).

In the last decade, several bioreactors were developed to satisfy the high demands of platelets supply for regenerative medicine. Computational Fluid Dynamics simulations and a microfluidic device approach were proposed by William Miller's group to obtain a bioreactor with uniform shear stress and an increased yield of proplatelet/megakaryocyte ratio (21± 3) (Martinez et al., 2016) (**Figure 19-a**). Baruch's group designed, in 2016, a microfluidic chip bioreactor with vWF micropillar that allows megakaryocyte entrapment e proplatelet elongation (Blin et al., 2016) (**Figure 19-c**).

Mimicking the bone marrow vascular shear stress is the most intriguing challenge in modeling bioreactors to increase the platelet production yield. To date, several groups are attempting to validate dynamic bone marrow models, as suggested by the rotary cell culture system (RCCS) (speed=20 rpm) that improves megakaryocyte maturation and differentiation from CD34$^+$ umbilical cord blood, also significantly leading the platelet yield in the system (Yang et al., 2016). To finally further improve the system, many researchers are exploiting the possibility to introduce *in vitro* generated megakaryocytes, derived from human iPSC, to provide new clinical perspectives for transfusion therapy (Eicke et al., 2018) and to improve platelet production (Ito et al., 2018). Particularly, Koji Eto's model of the bioreactor, VemMES, recreates a turbulent flow (120 to 300 mm/s) in 2.4 L tank through the use of rotating blades, deeply ameliorating the platelet release (up to 100 billion) from imMKCL cell model line (**Figure 19–e**)
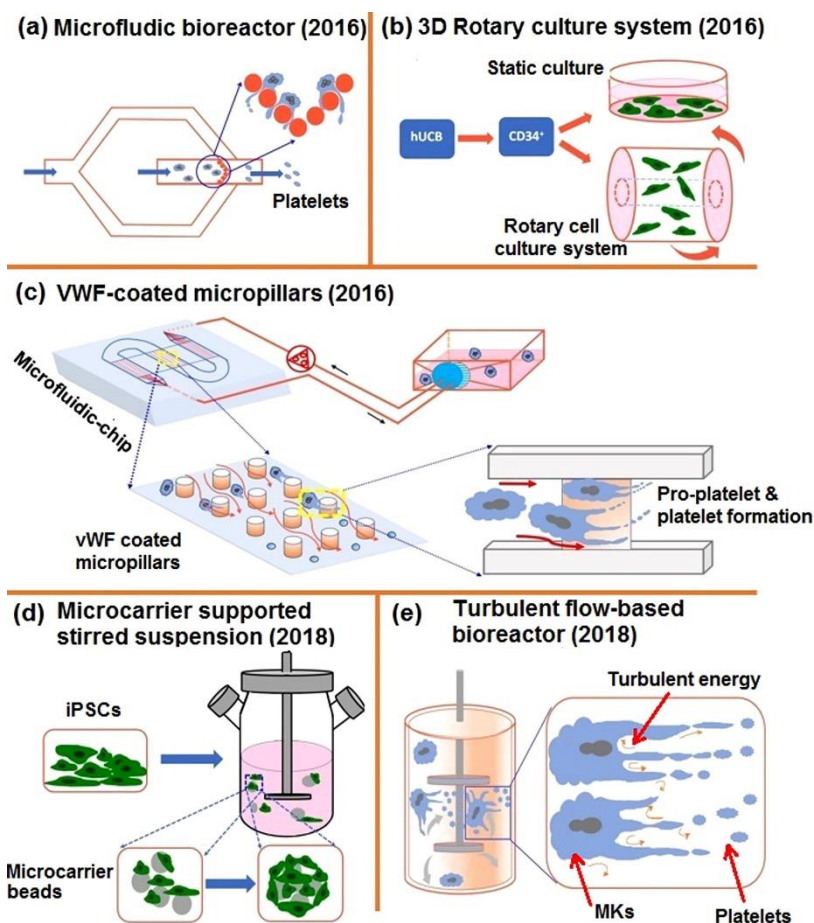

Fig. 19. Scaling-up *in vitro* platelet production. Recent advances in platelet production. Different approaches to designing bioreactors are improving the platelet yield achievement,

paving the way for a future application in therapeutics and transfusions. Source: Ingavle G et al., 2019.

Several groups are exploiting the benefit of using biomaterials able to be chemically and mechanically tailored to entrap bioactive molecules, such as growth factors and ECM components. Silk fibroin from *Bombyx Mori* silk cocoons has extensively demonstrated unique characteristics for biomedical applications, in terms of elasticity, biocompatibility, and low immunogenicity and thrombogenicity (Di Buduo et al., 2017; Omenetto & Kaplan, 2010). In the last decade, Alessandra Balduini's group designed 2D and 3D silk-based platforms to elucidate the hidden cellular mechanisms of megakaryocyte maturation and platelets release (Abbonante et al., 2017; Di Buduo et al., 2017; Di Buduo et al., 2015). In the case of platelets production, the group designed a silk tube functionalized with ECM proteins (fibronectin, type IV collagen, laminin) and SDF-1α, surrounded by a type I collagen hydrogel and Matrigel or by a silk sponge (Di Buduo et al., 2015; Di Buduo et al., 2017; Pallotta et al., 2011). The structure of the silk sponge was closer to the medullar topography and enhanced the adhesion and migration of cells within the structure (Di Buduo et al., 2015; Di Buduo et al., 2017). In the vascular compartment, the presence of SDF-1α directed the migration of mature megakaryocytes toward the silk tube. Then, the composition in ECM of the silk tube improved proplatelets elongation in the luminal side, and medium flow through the silk tube facilitated platelet release. The scaffold was placed in a PDMS bioreactor chamber that was perfused via a syringe pump, the flowrate generated a physiological shear rate of 60 s^{-1} inside the silk vascular tube. Platelets collected with flow passing through the tube were functional and still alive 4 days after collection. It was also shown that the perfusion of red blood cells in the medium during platelet production did not increase the yield of platelets, while co-culture with a monolayer of endothelial cells or functionalization of silk tube with VEGF and VCAM did. This model could be easily adapted for studying mechanisms of normal and pathological megakaryopoiesis and for drug screening (Di Buduo et al., 2016); while in an attempt to scale up platelet production for transfusions, multi-porous silk sponges have been tested (Di Buduo et al., 2017; Tozzi et al., 2018). These sponges were cultured within new modular flow chambers with flow passing through the different channels/pores and megakaryocytes in direct contact with the flow. This enhanced the capacity of platelet production, because of the biggest volume of the perfused area which allowed to increase the

concentration of cells in the sponge, and of the softer environment functionalized with ECM components that support proplatelet formation.

Induced Pluripotent Stem Cells (iPSCs): where do we stand in platelet production?

The study of blood diseases has always been encouraged and supported by the wide accessibility of hematopoietic tissue from the peripheral blood and bone marrow of patients and healthy individuals. Over the years, biomedical research has developed increasingly reliable study models, from immortalized cell lines to humanized animal models, that allowed us to deeply understand the cellular and molecular mechanisms of blood diseases.

More recently, advanced patient-derived models, such as conditionally reprogrammed cells, patient-derived tumor xenografts, 3D patient-derived organoid cell cultures, have attracted the interest of researchers, but the emergence of iPSC technology strongly contributed to providing an innovative study model. iPSCs are cells derived from somatic cells through a process of reprogramming, which with they are converted to pluripotent stem cell (PSC) state, silencing the somatic cell gene expression program and activating the network sustaining the self-renewing state. This process allows the generation of cell lines able to grow indefinitely and differentiate into all cell types of the human body. Brilliantly pioneered by Shinya Yamanaka (Takahashi et al., 2006) in 2006, this technology quickly spreads in biomedical laboratories and it currently represents the leading tool for the study of disease, thanks to its effectiveness and easy manufacture. Briefly, reprogramming of somatic cells to pluripotency requires the transient forced expression of four (or more) reprogramming factors (OCT4, SOX2, KLF4, and MYC), and more recently ameliorated with other factors (NANOG; LIN28) that enhance reprogramming efficiency (Yu et al., 2009). Several delivery methods were developed to introduce the RFs into cells (episomes, mRNA transfection, and Sendai Viruses) with different efficacy of reprogramming (generally lower than 0.1%).

Theoretically, any somatic cell type can be reprogrammed to pluripotency and, in the modeling of inherited genetic diseases, the choice of cell type is strictly related to its accessibility and availability.

For instance, the generation of HSCs from iPSCs is challenging for biomedical research, attempting to provide an experimental tool for studying developmental hematopoiesis, disease modeling, and drug discovery. The main efforts are focused to generate definitive HSCs with high proliferation capacity and able to give rise to all blood cell lineages. However, the scientific community is still debating about the optimal cell source to derive HSCs and specifically their stage of development.

Developmental hematopoiesis includes regulated sequential events occurring in spatiotemporally separated waves. Briefly, the first wave appears in the yolk sac and provides primitive blood cells (erythrocytes, megakaryocytes, macrophages) for the growing embryo, while the second wave generates myeloid- and lymphoid progenitors that migrate in the fetal liver. The final HSCs are generated in the third wave and localize in the bone marrow in the fourth wave when they are specialized. In this regard, it has been reported the discovery of a bone marrow hemogenic endothelium in adults, capable to generate HSCs de novo past embryonal stages (Yvernogeau et al., 2019), opening new perspectives in discovering the molecular mechanism of hematopoietic endothelium specification, such as transcription factor (i.e., Runx1, Sox17, Scl, Gfi1/Gfi1b, and Gata2) and signaling factor (i.e., Hedgehog, Bpm4, Notch ligands, and Wnt) modulation. Thus, the main goal in the field of HSC generation from iPSCs is to develop a protocol that generates bona fide HSCs with long-term engraftment potential. Despite huge efforts, *ex vivo* true HSCs generation (and therapeutic-grade HSCs) from iPSC without genetic manipulation remains theoric, and the main concerns are still related to their safety profile and high costs of production (Demirci et al., 2020).

One of the most intriguing challenges has involved the development of methods for hematopoietic differentiation of human iPSC, and, in this regard, bone marrow and peripheral blood represent the pivotal source for multiple blood cell types. Despite the limitations to achieving true HSC from iPSCs, the current differentiation protocols have improved efficiency, yield, and reproducibility, and they can be resumed in three methods:

- formation of embryoid bodies,
- co-cultures with stromal feeder cells,
- monolayer cultures.

HSCs can be further differentiated into specific cell blood lineages with appropriate media and cytokine cocktails. For instance, the generation of megakaryocyte and

platelets from iPSC was first developed by Takayama and coworkers in 2010 (Takayama et al., 2010), when they co-cultured human iPSCs with mouse cell line C3H10T1/2 for differentiation into hematopoietic progenitors and differentiate them in megakaryocyte with a specific differentiation medium, discovering the role of c-Myc in promoting Megakaryiopoiesis but inhibiting thrombopoiesis. Further, Nakamura and colleagues (Nakamura et al., 2014) developed inducible imMKCL lines by inducible overexpression of c-MYC, BMI1, and BCL-XL through the Tet-On system, and then the expression would be shut down when differentiation into platelets is needed. As mentioned before, Eto's group (Ito et al., 2018) has introduced a large scale platelet generation system from iPSC-derived Megakaryocytes: In this model, a bioreactor provides turbulent energy and shear stress which mimics the physiological shear stress of blood that helps to cut platelets from proplatelets tips, generating 100 billion platelets in an 8L tank bioreactor system. Notably, Ghevart's lab found that overexpression of FLI1, GATA1, and TAL1 IN ESC improved the generations of reprogrammed megakaryocytes, able to proliferate in culture for >90 days, maintaining the expression of typical markers (CD41/42a) and platelet production (Moureau et al, 2016) (**Figure 20**).

A

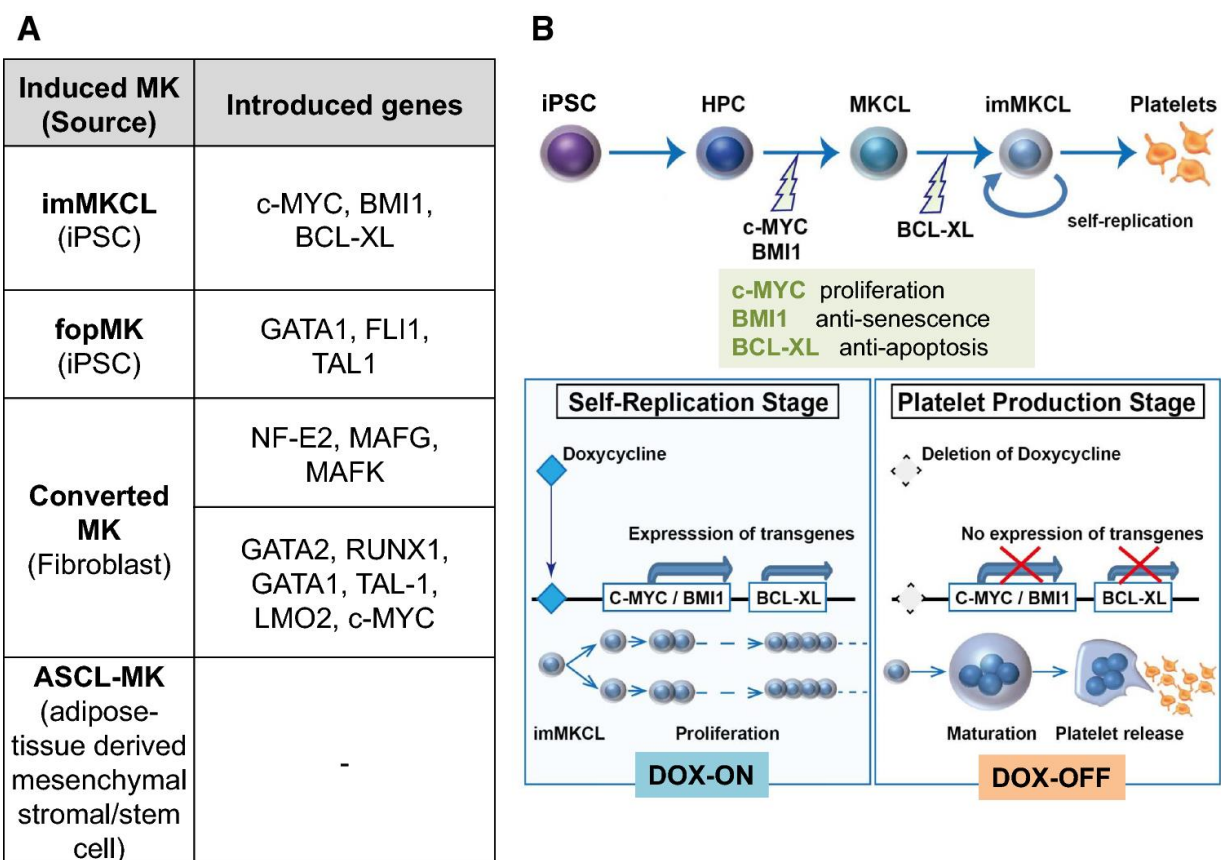| Induced MK (Source)	Introduced genes
imMKCL (iPSC)	c-MYC, BMI1, BCL-XL
fopMK (iPSC)	GATA1, FLI1, TAL1
Converted MK (Fibroblast)	NF-E2, MAFG, MAFK
	GATA2, RUNX1, GATA1, TAL-1, LMO2, c-MYC
ASCL-MK (adipose-tissue derived mesenchymal stromal/stem cell)	-

B

Fig.20 Different iPSC sources for megakaryocytes. (A) Various types of induced megakaryocytes were developed, providing an unlimited source of cells for studying

mechanisms of platelet production. **(B)** imMKCLs were obtained by introducing c-MYC and bone marrow in hematopoietic progenitors and BCL-XL in early megakaryocytes. Depletion of Doxycycline allows imMKCL maturation and differentiation.

To better investigate the pathogenetic mechanisms of disease and the response to therapy, iPSCs represent a fundamental model to study diseases. Human iPSC technology is an invaluable tool for the modeling of human diseases, especially in terms of rare diseases where access to patient material is limited, as it allows for the unlimited supply of undifferentiated patient-derived iPSCs to be frozen down and stored long term. Starting from the first brilliant results from Dimos and Park's groups (Dimos et al., 2008; Park et al., 2008) several iPSC models of disease were developed and this technology allowed for an almost unlimited amount of either healthy or disease-specific human pluripotent stem cells. In this regard, Hana Raslova's team first generated IPSCs from two pedigrees with germline *RUNX1* mutations associated with thrombocytopenia, elucidating the cellular and molecular mechanisms underlying the different pathological phenotypes in different mutations (Anthony-Debrè et al.; 2015). Another useful cell model of thrombocytopenia has been obtained in 2013 by Hirata and colleagues (Hirata et al., 2013) when they established an iPS cell line derived from a patient diagnosed with CAMT. This model proved useful to understand the role of c-Mpl signaling, and particularly, the fate decision leading to aberrant megakaryocyte differentiation in CAMT, probably related to modulation of *FLI1* expression. In 2019, Donada used an isogenic iPSCs model from 2 female patients with different Filamin A mutations, causing thrombocytopenia along with other malformations. This approach allowed to deeply investigate the mechanism of megakaryocyte differentiation and Filamin A expression, discovering that the loss of interaction of αIIβ3 with Filamin A led to RhoA activation, proplatelet formation defects, and macrothrombocytopenia (Donada et al., 2019). A recent work by Sara Borst (Borst et al., 2021) reported the generation of two different sets of iPSC lines: (1) patient-derived iPSCs harboring monoallelic germline *ETV6* or *RUNX1* mutations and (2) a wild-type (WT) iPSC line with the *ETV6* or *RUNX1* patient mutations introduced through CRISPR-Cas9 technology. Particularly, the gene-editing approach is useful to obtain isogenic patient-derived iPSCs and allows for analysis of how pathogenic mutations affect specific cell types (Musunuru, 2013). *RUNX1* and *ETV6* mutant cell lines were differentiated and displayed disparate phenotypes: *ETV6* mutant lines generated increased numbers of immature megakaryocytes, while *RUNX1* generated a decreased number of

megakaryocytes expressing normal maturation markers. Moreover, they both showed impaired proplatelet formation, suggesting that these iPSCs cell lines can represent a reliable model for studying molecular mechanisms of Inherited Thrombocytopenia.

Aim

In Inherited Thrombocytopenias the bone marrow fails to produce enough platelets and this leaves patients extremely susceptible to bruising, bleeding, and poor clotting after an injury or surgery. The treatment of these patients is facing a new era thanks to the development of Thrombopoietin Receptor Agonists (TPO-RAs). However, preliminary testing during different Phase II clinical trials demonstrated that some patients respond well to pharmacological treatments, while others do not. Why these differences exist could be investigated by designing new test systems that recreate the structure and function of bone marrow in the laboratory to study the mechanisms of the diseases and test drug efficacy on an individual scale.

My Ph.D. program aimed to model silk fibroin to develop an *ex vivo* miniaturized 3D bone marrow tissue model that recapitulates platelet biogenesis of patients with different forms of Inherited Thrombocytopenias. The technology has been validated with stem cell progenitors derived from a small volume of patient peripheral blood and/or iPSC lines. Eltrombopag has been used as a proof of concept for the applicability of this system as a laboratory tool for the development of personalized treatments for Inherited Thrombocytopenias or other hematological disorders.

Materials and Methods

Materials

B. mori silkworm cocoons were supplied by Tajima Shoji Co., Ltd. (Yokohama, Japan). Pharmed tubing was from Cole-Parmer (Vernon Hills, IL, USA). Immunomagnetic separation system was from Miltenyi Biotech (Bergisch Gladbach, Germany and Bologna, Italy). Recombinant human thrombopoietin (TPO), interleukin-6 (IL-6), interleukin-11 (IL-11), human bone morphogenetic protein 4 (BMP4), human vascular endothelial growth factor (VEGF), human fibroblast growth factor (FGF), human Fms-related tyrosine kinase 3 ligand (Flt3L), human stem cell factor (SCF) were from Peprotech (London, UK). CHiR 99021 was from TOCRIS. TruCount tubes and human fibronectin were from Becton Dickinson (S. Jose, CA, USA). The following antibodies were used: mouse monoclonal anti-CD61, clone SZ21, from Immunotech (Marseille, France); rabbit monoclonal anti-β1-tubulin was from Abcam. Alexa Fluor-conjugated secondary antibodies and Hoechst 33258 were from Life Technologies (Monza, Italy).

Production of the drug-testing device

The chamber was manufactured using 3D FDM printing technology and biocompatible silicon molding approach. The modeling of the bioreactor was created using CAD software and used to generate 3D negative mold components exported as STL (Standard Triangulation Language) files, sliced with Slic3R PE and exported to the FDM 3D printer Prusa i3 MK3S (Prusa Research, Czech Republic). The printing is done using a poly(lactic acid) (PLA) high-temperature filament of 1,75 mm (FormFutura, Netherland) deployed in layers of 100 μm by a 0.25 mm nozzle. After printing, the mold was cured in an oven at 100°C for 20 min to increase mechanical properties. To produce the perfusion channel, 21G needles were disposed in the dedicated holes and sealed with a gel of 25% Pluronic F-127. The molding was performed using a polydimethylsiloxane (PDMS) (Sylgard®184, Dow Corning), mixed in a 10:1 ratio of base material and curing agent. The selected material is stable both at low and high temperatures (45°C to 200°C) and it is resistant to UV, water, and solvents. The PDMS was poured into the 3D printed molds that were positioned in a vacuum chamber to remove all the air bubbles. The curing of the PDMS was performed in a dried oven 70°C for 4 hours; the molds were then dissociated from the final silicon models sterilizable by autoclave. The chamber consisted of two wells of 22x10 mm, having a hollow cavity of 15x2 mm enclosed in a block of 30x30 mm and connected to

the outside of the chamber through channels of 0.9 mm diameter. The luer adaptors for the inlet and outlet were mounted in the channel and sealed with biocompatible silicone adhesive MD7-4502 (Dow Corning, USA). Then, the modular flow chamber was equipped with a silk fibroin sponge functionalized with fibronectin as described previously (Christian A. Di Buduo et al., 2017).

Preparation of the silk fibroin solution

Silk fibroin aqueous solution was obtained from *B. mori* silkworm cocoons according to previously published literature (C. A. Di Buduo et al., 2018). Briefly, dewormed cocoons were boiled in 0.02 M Na_2CO_3. The fibers were rinsed in ultrapure water and dried overnight. The dried fibers were solubilized for 4 h at 60°C LiBr. The solubilized silk solution was dialyzed against distilled water using a Slide-A-Lyzer cassette (Thermo Scientific, Waltham, MA, USA) with a 3500 MW cutoff for three days and changing the water a total of eight times.

Silk bone marrow fabrication and assembly

Silk solution (8% w/v) (Lovett et al., 2007) was mixed with 25 µg/mL fibronectin and dispensed into the modular chamber. $NaCl_2$ particles (approximately 500 µm in diameter) were then sifted into the solution. The scaffolds were then placed at room temperature for 48 hours and then soaked in distilled water for 48 hours to leach out the $NaCl_2$ particles. The scaffolds were sterilized in ethanol and finally rinsed in PBS over 24 hours. Perfusion of the silk scaffold has been tested at different flow rates by using a peristaltic pump (ShenChen Flow Rates Peristaltic Pump - LabV1, China). The total volume collected after each test corresponded to that injected into the system by the pump.

Patients

Human peripheral blood samples were obtained from healthy controls and thrombocytopenic patients after informed consent. All samples were processed following the ethical committee of the I.R.C.C.S. Policlinico San Matteo Foundation and the principles of the Helsinki Declaration. The main features of the 24 investigated samples from 20 different patients are reported in Table 1. For 4 patients, the analysis

was performed on two different occasions, with very similar results. Diagnosis of *MYH9*-RD or *ANKRD26*-RT had been confirmed by genetic analysis in all the cases. All patients provided written informed consent for this study, which was approved by the Institutional Review Board of the I.R.C.C.S. Policlinico San Matteo Foundation, Pavia, Italy. A sample of 15 mL of peripheral venous blood anticoagulated with ACD was collected for the analysis in the 3D bone marrow system. 13 patients had previously received a short-term course of Eltrombopag either within a phase 2 clinical trial (Zaninetti, Gresele, et al., 2019) (n = 11) or in preparation for elective surgery (Zaninetti, Barozzi, et al., 2019) (n = 2). In any case, Eltrombopag was given at the dose of 50 or 75 mg/day for 3 or 6 weeks (Zaninetti, Barozzi, et al., 2019; Zaninetti, Gresele, et al., 2019). The *in vivo* clinical response to the drug was expressed as the absolute increase in platelet count at the end of Eltrombopag treatment with respect to baseline. Blood samples for this study were collected when patients were out of Eltrombopag therapy and had platelet count at their baseline levels.

Human megakaryocytes differentiation within the silk bone marrow

CD45^{+} hematopoietic stem cells from peripheral blood samples were separated by immunomagnetic bead selection kit (Miltenyi Biotec, Bologna, Italy) and cultured for 6 days in the flask in Stem Span medium (StemCell Technologies, Canada) supplemented with 1% penicillin-streptomycin, 1% L-glutamine, 10 ng/mL TPO, IL-6 and IL-11 in the presence or not of 500 ng/mL Eltrombopag (kind gift from Novartis) at 37°C in a 5% CO_2 fully humidified atmosphere, as previously described (Bluteau et al., 2014; Pecci et al., 2009). After 1 week, megakaryocytic progenitors were seeded in the silk bone marrow model in presence of 10 ng/mL TPO supplemented or not with 500 ng/mL Eltrombopag.

On day 14 of differentiation, the chamber was sealed, and the outlet ports were connected to the outlet needles. Culture media-filled tubes were connected to the inlet needles. The medium was pumped for 4 hours at a flow rate of 10 µL/min.

Induced Pluripotent Stem Cells generation

iPSCs were derived from one *MYH9*-RD patient with heterozygous g.103845T>A mutation and one healthy control providing their informed consent before the

participation in this study and in accordance with the local ethical committee and the Declaration of Helsinki. These experiments were performed by the group of Hana Raslova from the Institute Gustave Russie, as part of the consortium of the H2020-FetOpen-SilkFusion project coordinated by Prof. Alessandra Balduini.

CD34$^+$ cells were isolated from peripheral blood of patient using an immunomagnetic beads cell-sorting system (AutoMacs; Miltenyi Biotec, Paris, France) collected at diagnosis and amplified in serum-free media containing EPO (1 U/mL), FLT3l (10 ng/mL), G-CSF (20 ng/mL), IL-3 (10 ng/mL), IL-6 (10 ng/mL), SCF (25 ng/mL), TPO (10 ng/mL) and GM-CSF (10 ng/mL) for 6 days. Cells were then transduced with the CytoTune iPS 2.0 Sendai Reprogramming Kit (Thermo Fisher, Villebon-sur-Yvette, France) and the reprogramming was performed according to the manufacturer instructions. Colonies with an ES-like morphology were manually isolated, expanded for a small number of passages and frozen. iPSCs were maintained on Essential 8 or Essential 8 Flex media (Gibco/Thermo Fisher), on plates coated with N-truncated human recombinant vitronectin (Gibco). All derived clones were organized in colonies with defined edges and characterized by prominent nucleolus with a high nucleus to cytoplasm ratio. Cell passages were performed using a solution of EDTA 0.5 mM in PBS 1X, or TrypLE 1X (Gibco).

induced Pluripotent Stem Cells hematopoietic differentiation

At day -1, colonies of pluripotent stem cells were seeded on Geltrex (12 ug/cm2)-coated 100 mm dish plates, in mTeSR1 (STEMCELL™ Technologies) with 10 μM ROCK Inhibitor (Millipore). The starting cell concentration was adjusted for each cell line at 10-15% confluency range ($5x10^5$ cells/dish). After 4 hours, media was replaced with fresh mTeSR1. At Day 0, cells were transferred in a xeno-free media based on StemPro-34 SFM (ThermoFischer Scientific), supplemented with Penicillin/Streptomycin 0.5% v/v (Sigma), L-Glutamine 1% v/v (Gibco), 1- Thioglycerol 0.04 mg/mL (Sigma) and ascorbic acid 50 mg/mL (Sigma). This media was retained for the entire experiment and supplemented with different cytokines, small molecules and growth factors, according to the following schedule (Donada et al., 2019): days 0-2: BMP4 (10 ng/mL), VEGF (50 ng/mL) and CHIR99021 (2 μM). Days 2-4: BMP4 (10 ng/mL), VEGF (50 ng/mL) and FGF2 (20 ng/mL). Days 4-6: VEGF (15 ng/mL) and FGF2 (5 ng/mL). Day 6: VEGF (50 ng/mL), FGF2 (50 ng/mL), SCF (50 ng/mL) and

FLT3L (5 ng/mL). Days 7-10: VEGF (50 ng/mL), FGF2 (50 ng/mL), SCF (50 ng/mL), FLT3L (5 ng/mL), TPO (50 ng/mL) and IL-6 (10 ng/mL). Days 10-14: SCF (50 ng/mL), FLT3L (5 ng/mL), TPO (50 ng/mL) and IL-6 (10 ng/mL). Starting from day 14, megakaryocytic progenitors were seeded for additional 5 days within the silk bone marrow model in presence of TPO (50 ng/mL) supplemented or not with 500 ng/mL Eltrombopag.

Evaluation of differentiation and proplatelet formation by *ex vivo* differentiated megakaryocytes

Megakaryocyte differentiation and proplatelet yields were evaluated by adhesion on fibronectin at the end of the culture (14th day), as previously described (Di Buduo et al., 2014; Pecci et al., 2009). Briefly, 12 mm glass cover-slips were coated with 25 µg/ml human fibronectin (Merck-Millipore, Milan, Italy), for 24 hours at 4°C. Megakaryocytes were harvested from the silk bone marrow scaffold by extensive washing and seeded in a 24-well plate, at 37°C in a 5% CO_2 fully humidified atmosphere. After 16 hours, adhering cells were fixed in 4% paraformaldehyde (PFA), permeabilized with 0.1% Triton X-100 (Sigma Aldrich, Milan, Italy), and stained for immunofluorescence evaluation with rabbit anti-β1-tubulin primary antibody (1:700) or anti-mouse CD61 (1:100) and Alexa Fluor-conjugated secondary antibodies (1:500) (Invitrogen, Milan, Italy). Nuclei were stained with Hoechst 33258 (1:10,000) (Sigma Aldrich, Milan, Italy). The cover-slips were mounted onto glass slides with ProLong Gold antifade reagent (Invitrogen, Milan, Italy) and imaged by an Olympus BX51 microscope (Olympus, Deutschland GmbH, Hamburg, Germany).

Imaging of megakaryocyte cultures within the 3D silk bone marrow model

For immunofluorescence imaging of megakaryocyte cultures within the silk bone marrow tissue model, samples were fixed in 4% paraformaldehyde (PFA) for 20 minutes and then blocked with 5% bovine serum albumin (BSA, Sigma) for 30 minutes at room temperature. Samples were probed with anti-CD61, and then immersed in Alexa Fluor secondary antibody at room temperature. Nuclei were stained with Hoechst. Samples were imaged by a TCS SP8 confocal laser scanning microscope (Leica, Heidelberg, Germany). For silk fibroin scaffolds imaging, we took advantage of

silk auto-fluorescence in UV light (Talukdar et al., 2011). For all immunofluorescence imaging, the acquisition parameters were set on the negative controls. 3D reconstruction and image processing were performed using Leica licensed software or Image J software.

Evaluation of platelet morphology

For analysis of peripheral blood and *ex vivo* collected platelet morphology, different approaches were used. First, megakaryocytes at the end of differentiation and platelets from peripheral blood or perfused media were visualized by light microscopy with an Olympus IX53 (Olympus Deutschland GmbH, Hamburg, Germany). For analysis of cytoskeleton components, cells were stained as previously described (Di Buduo, Alberelli, et al., 2016). To visualize microtubule organization, samples were probed with anti-β1-tubulin and then immersed in Alexa Fluor secondary antibody at room temperature. Samples were mounted onto glass slides with ProLong Gold antifade reagent (Invitrogen, Milan, Italy) and then imaged by an Olympus BX51 fluorescence microscope (Olympus, Deutschland GmbH, Hamburg, Germany). For all immunofluorescence imaging, the acquisition parameters were set on the negative controls, which were routinely performed by omitting the primary antibody.

Flow cytometry

Flow cytometry settings for analysis of megakaryocytes and *ex vivo* generated platelets were established, as previously described (Abbonante et al., 2016; Cramer et al., 1997; Fujimoto et al., 2003; Nakamura et al., 2014; Takayama et al., 2008). For analysis of the percentage of fully differentiated megakaryocytes at the end of the culture (14th day), cells were suspended in phosphate buffer saline (PBS) and stained with a FITC-conjugated antibody against human CD41 and human CD42b (PE) (eBioscience, Milan, Italy) at room temperature in the dark for 30 minutes and then analyzed. *Ex vivo* collected platelets were analyzed using the same forward, and side scatter pattern as human peripheral blood and identified as CD41$^+$CD42b$^+$ events. Isotype controls were used as negative controls to exclude non-specific background signals. The platelet number was calculated using a TruCount bead standard.

Statistics

Values were expressed as mean plus or minus the standard deviation (mean±SD). A two-tailed paired t-test was performed for statistical analysis of data from samples tested in parallel under different experimental conditions. A two-tailed unpaired t-test was performed for statistical analysis of data from different samples. Statistical analysis was performed with GraphPad Software. A p-value of less than 0.05 was considered statistically significant.

Results

Device design and prototyping

In adults, hematopoietic bone marrow is located in the medullary cavity of flat and long bones, served by blood vessels that branch out into millions of small thin-walled arterioles and sinusoids allowing mature blood cells to enter the bloodstream. To mimic such a structure, a device prototype of a rectangular shape with 30x30 mm size and hollow cavities of 15x2 mm was developed (**Figure 21**). The printing process for the negative mold of our device has been created by an FDM 3d printer using a polylactic acid (PLA High temperature).
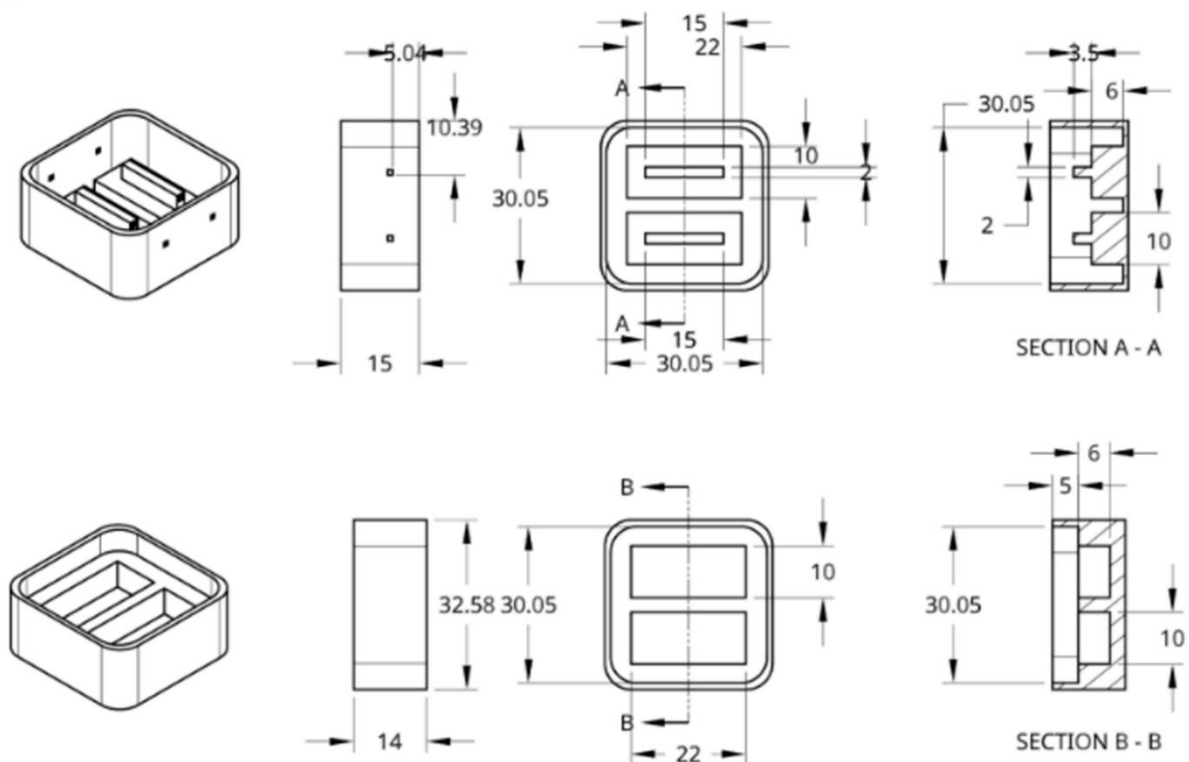

Fig.21 Designing the negative mold. Drawing of negative molds for the core device (upper panel) and the cover tap (lower panel) are respectively disposed in isometric view, right view, top view and transversal section view. Dimensions are in millimeters.

Once obtained the negative mold, needles are inserted in hollow cavities and a non-toxic polymeric organosilicon, Polydimethylsiloxane (PDMS) has been cast and cured (**Figure 22**). The final result is an optically clear, reusable, and autoclavable device.
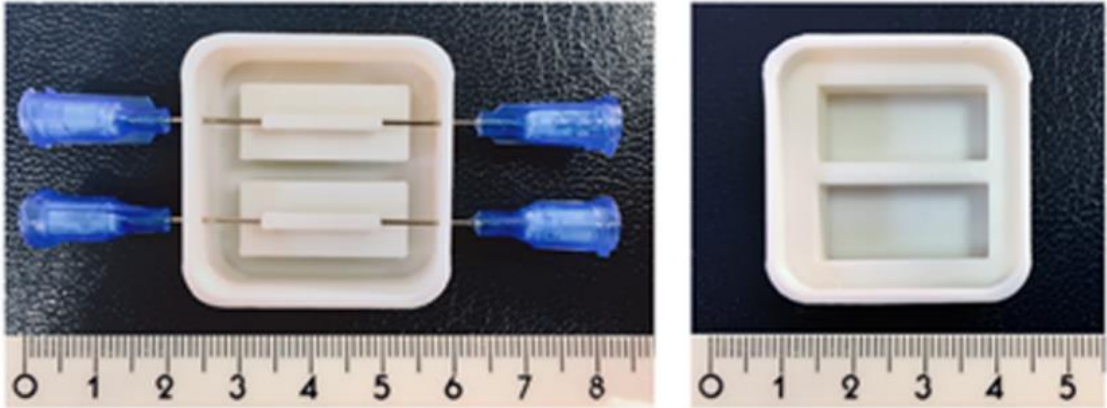
Fig.22. Shaping the PDMS device. Needles are inserted in the negative mold and PDMS is cast and cured in hallow spaces to obtain the final shape of the device.

To mimic the vascularized bone marrow structure, the flow chamber was designed in two parts: a cover top and a core device, containing two separate flow channels. This part is dedicated to the perfusion through the inlet port and outlet port where needles allow the connection to a perfusion system (**Figure 23**).

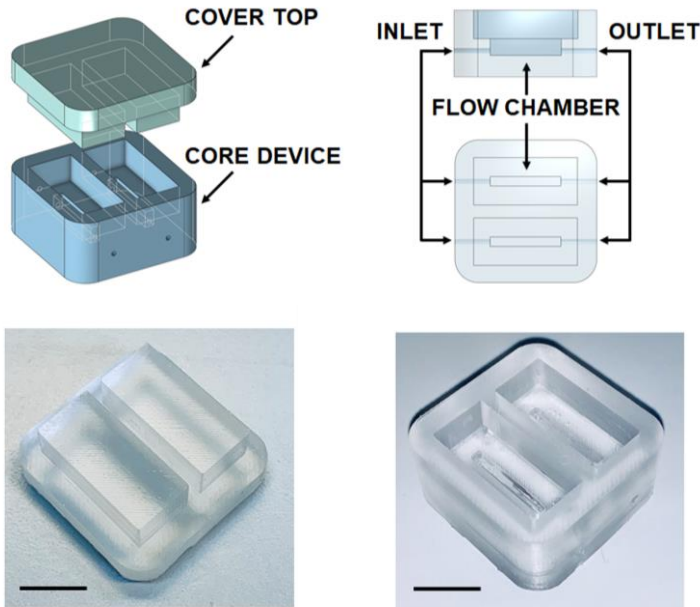**Fig.23. Functional designing of miniaturized bone marrow model.** The bone marrow model is composed of a Cover Top and a Core Device, with two chambers connected to a perfusion pump through an inlet port and an outlet port. Scale Bar: 1 cm.

The device was connected to an outside peristaltic electronic pump through 0.9 mm diameter channels equipped with luer lock adaptors. Crosstalk between channels inside the device was eliminated by appropriate spatial separation and independent perfusion to allow assessment of patient-specific responses, following simultaneous exposure to TPO alone and TPO in combination with the tested drug.

Assembly and characterization of silk-based bone marrow model

A silk fibroin structure functionalized with fibronectin was prepared with the salt leaching method and inserted into the device to model a spongy scaffold that reproduces bone marrow architecture, composition, and microcirculation. The silk scaffold was connected to gas-permeable tubing allowing perfusion of the media with a peristaltic pump (ShenChen Flow Rates Peristaltic Pump - LabV1, China) through the use of two needles plunged into inlet and outlet ports. A cover cap closes the system before starting perfusion.

The 3D reconstruction of the silk scaffold revealed the presence of multiple spatially-distinct niches and also demonstrated the homogeneous distribution of pores from top to bottom of the scaffold. This arrangement efficiently supported the diffusion of cells and media outflow without altering the shape and integrity of the silk. Importantly, the total volume collected after perfusion corresponded to that injected into the system by the pump (**Figure 24**).
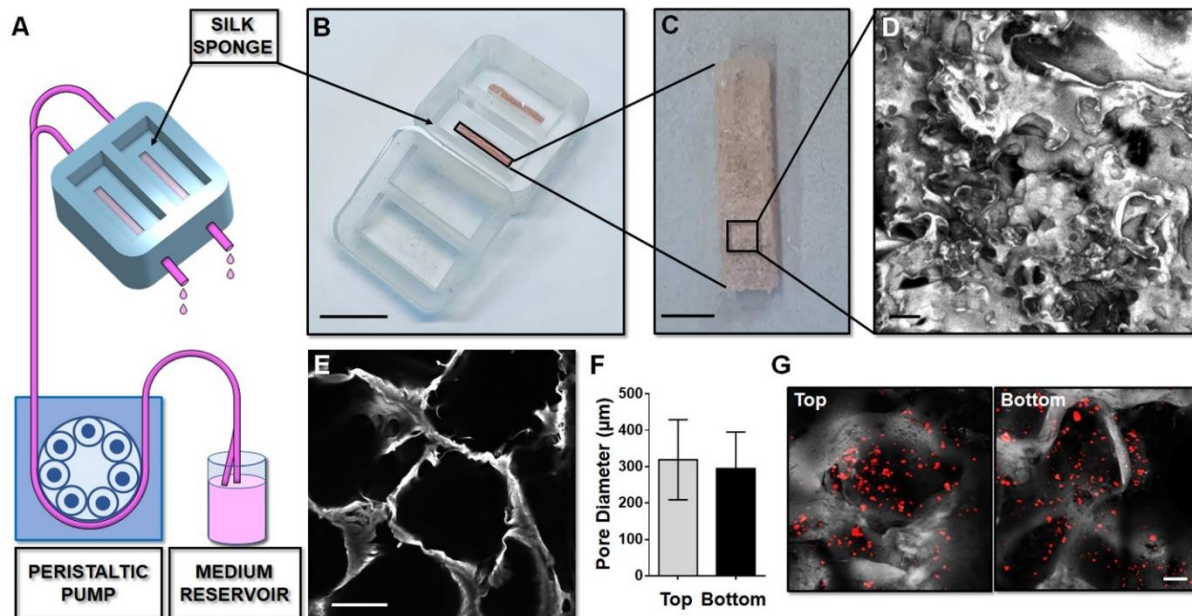
Fig.24. Silk sponge bone marrow perfusion system.

(**A-C**) A peristaltic pump drives perfusion of the cell culture medium from a reservoir to the device equipped with a silk fibroin sponge prepared directly inside the chamber by dispensing an aqueous silk solution mixed with salt particles (scale bar B = 1.5 cm; scale bar C = 2 mm). After leaching out the salt, the resulting porous silk sponge can be sterilized. (**D, E**) Confocal microscopy reconstruction of the silk sponge showed the presence of an interconnected alveolar network (scale bar D = 200 μm; scale bar E = 200 μm). (**F**) The analysis of pore diameters measured on top and bottom of the scaffold demonstrated no significant differences throughout the scaffold. Results are presented as mean±SD (n=150 pore/condition, p=NS). (**G**) Confocal microscopy analysis of CFSE+ cells cultured within the silk scaffold (red = CFSE; grey = silk; scale bar = 50 μm).

Evaluation of *ex vivo* drug response in thrombocytopenic patients through the silk-based bone marrow Model

Haematopoietic stem and progenitors cells were selected from the peripheral blood of healthy controls and patients affected by two forms of Inherited Thrombocytopenia: *ANKRD26*-RT and *MYH9*-RD, and cultured according to established protocols (Currao et al., 2015; Di Buduo, Currao, et al., 2016; Di Buduo et al., 2015).

The bone marrow device was able to support the efficient differentiation of mature megakaryocytes from both healthy controls and patients in the presence of TPO. However patient-derived megakaryocytes displayed a decreased percentage of

proplatelet formation by about 80%, accompanied by less branching of proplatelet shafts due to a significantly lower number of bifurcations (Healthy Control: 9±2; *ANKRD26*-RT: 1.9±0.7; *MYH9*-RD 1.8±0.9) as compared to healthy controls (**Figure 25**).
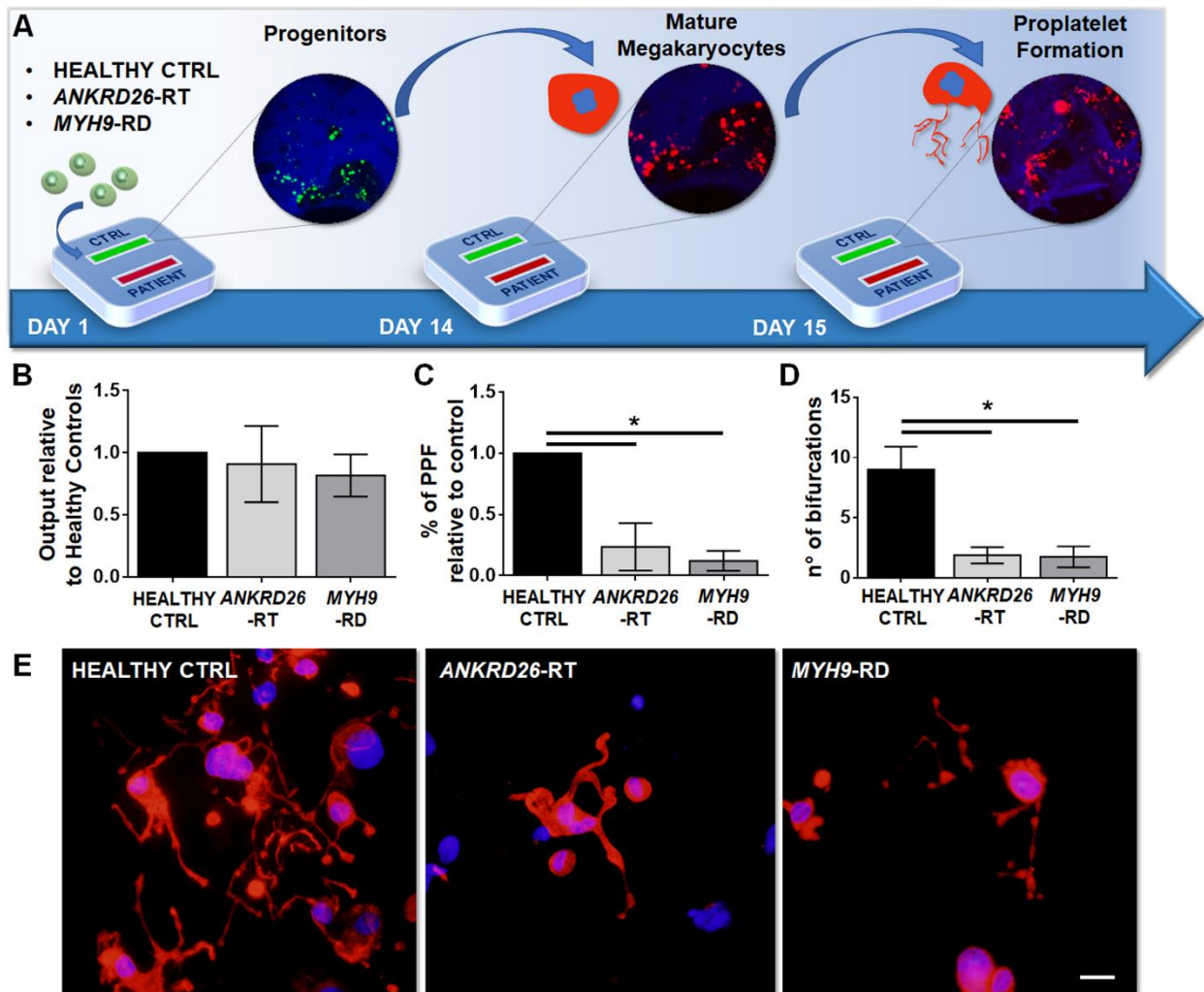
Fig. 25. Reproducing physiological and pathological megakaryopoiesis in a 3D scaffold.

(**A**) Megakaryocytes were differentiated from healthy controls and patients affected by *MYH9*-RD and *ANKRD26*-RT patients and cultured into the bone marrow device in presence of 10 ng/mL TPO. (**B**) Output of CD41$^+$CD42b$^+$ megakaryocyte at the end of differentiation relative to healthy controls (n=12 Healthy Controls, n=12 *MYH9*-RD; n=12 *ANKRD26*-RT; p=NS) (**C**) Percentage of proplatelet formation relative to healthy controls (n=12 Healthy Controls, n=12 *MYH9*-RD; n=12 *ANKRD26*-RT; *p<0.01). (**D**) The number of proplatelet bifurcation per single megakaryocytes in healthy controls and patients (n=12 Healthy Controls, n=12 *MYH9*-RD; n=12 *ANKRD26*-RT; *p<0.01). (**E**) Representative immunofluorescence staining of proplatelet

structure (red=β1-tubulin; blue=nuclei; scale bar=20 μm). All results are presented as mean±SD.

Collecting *ANKRD26*-RT and *MYH9*-RD patients samples

To validate the predictive value of the bone marrow response to drugs specifically targeting hematopoiesis, we chose Eltrombopag as the model compound since Eltrombopag represents to date the only tested drug shown to increase platelet count of patients with Inherited Thrombocytopenias.

First, the system was preliminarily validated with healthy control samples to explore the efficacy of Eltrombopag to stimulate megakaryocyte differentiation and proplatelet formation *ex vivo*. The results showed a significant increase of CD41$^+$CD42b$^+$ megakaryocytes in the presence of Eltrombopag with respect to TPO alone. Also, the drug was able to promote a higher percentage of proplatelet formation (**Figure 26**).
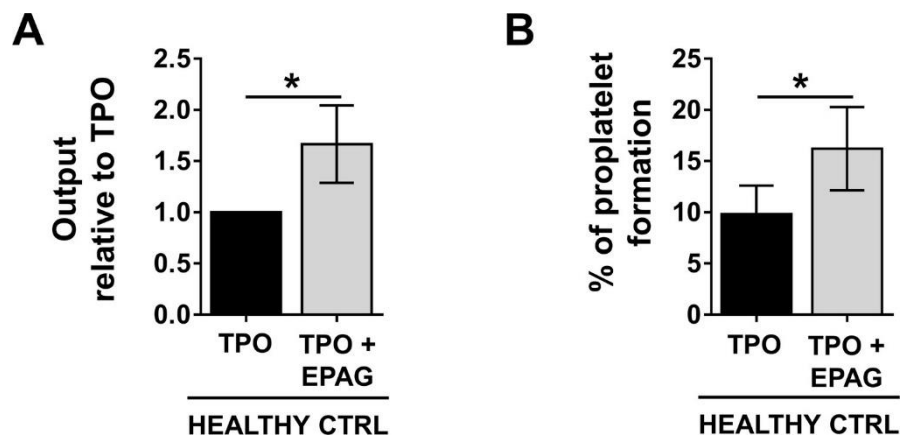
Fig.26. Evaluation of *ex vivo* efficacy of Eltrombopag in promoting thrombopoiesis in healthy controls. (**A**) Output of CD41$^+$CD42b$^+$ healthy control megakaryocytes at the end of differentiation cultured in the presence of TPO +EPAG, with respect to TPO alone (n = 6, *p<0.01). (**B**) The percentage of proplatelet forming-megakaryocytes was calculated as the number of cells displaying long filamentous pseudopods with respect to the total number of round megakaryocytes per analyzed field (n = 6; *p<0.01). All results are presented as mean ± SD.

Then, we tested the sensitivity of pathologic samples specifically regarding megakaryocyte differentiation and platelet production among 24 cultures using samples from *ANKRD26*-RT and *MYH9*-RD patients (**Table 1**). This cohort included

11 patients previously treated with Eltrombopag in a recent phase 2 clinical trial (Zaninetti, Gresele, et al., 2019) and 2 patients previously treated in preparation for elective surgery (Zaninetti, Barozzi, et al., 2019).

Table 1. Main features of the study population.

	ANKRD26-RT	*MYH9*-RD
Total samples, no.	12	12
M/F	9/3	5/7
Age - mean (range), years	46 [22-67]	48 [26-59]
Platelet count - mean (range) x10^9/L	32 [9-75]	29 [5-69]
Patients treated with Eltrombopag *in vivo*, no.	6[¥¥]	7[¥]
M/F	6/3	2/6
Age - mean (range),years	47 [22-67]	45 [31-59]
Platelet count at baseline - mean (range), x10^9/L	35 [12-75]	24 [5-69]
Increase of platelet count after Eltrombopag treatment* - mean (range), x10^9/L	34 [7-64]	88 [5-231]

*   Increase of platelet count at the end of Eltrombopag treatment with respect to baseline.

¥   of whom 1 patient repeated two times

¥¥   of whom 3 patients repeated two times

Blood samples for this study were collected when patients were out of Eltrombopag therapy and had platelet counts at their baseline levels.

Ex vivo drug testing on *ANKRD26*-RT and *MYH9*-RD patients samples

CD45^{+} hematopoietic stem cells from the 15 mL peripheral blood were harvested by an immunomagnetic separations kit (Miltenyi Biotec, Bologna, Italy) and cultured for 6 days in a flask in presence in Stem Span media (StemCell Technologies, Canada) supplemented with 1% penicillin-streptomycin, 1% L-glutamine, 10 ng/mL TPO, IL-6 and IL-11 in the presence or not of 500 ng/mL Eltrombopag (kindly provided by Novartis) at 37°C in a 5% CO_2 fully humidified atmosphere. After 1 week, early megakaryocytic progenitors were seeded for additional 8 days within the silk bone marrow model in presence of 10 ng/mL TPO supplemented or not with 500 ng/mL Eltrombopag.

Insights into the efficacy of Eltrombopag effects *ex vivo* were gained by simultaneously analyzing megakaryocyte differentiation at day 14 for each disorder.

For analysis of the percentage of fully differentiated megakaryocytes at the end of the culture (14th day), cells were washed out of the device, suspended in phosphate buffer saline (PBS), and stained with a FITC-conjugated antibody against human CD41 and human CD42b (PE) (eBioscience, Milan, Italy) at room temperature in the dark for 30 minutes and then analyzed.

To evaluate cell differentiation and morphology, megakaryocytes were coated on fibronectin coverslips and stained for megakaryocyte marker, CD61, and assessed through immunofluorescence analysis. For analysis of megakaryocyte ploidy, cells were fixed in ice-cold 70% ethanol overnight at −20°C and resuspended in PBS with 100 mg/mL of RNAse and propidium iodide solution and stained with FITC anti-CD41. We observed comparable megakaryocyte maturation in terms of cell size (**Figure 27-B**), ploidy profile (**Figure 27-C**), and expression of lineage-specific markers (**Figure 27-D and 27-E**), with and without Eltrombopag. However, the combination of TPO and Eltrombopag resulted in a significant two-fold increase in the output of mature megakaryocytes with respect to TPO alone for both *ANKRD26*-RT and *MYH9*-RD patients (**Figure 27-F**).
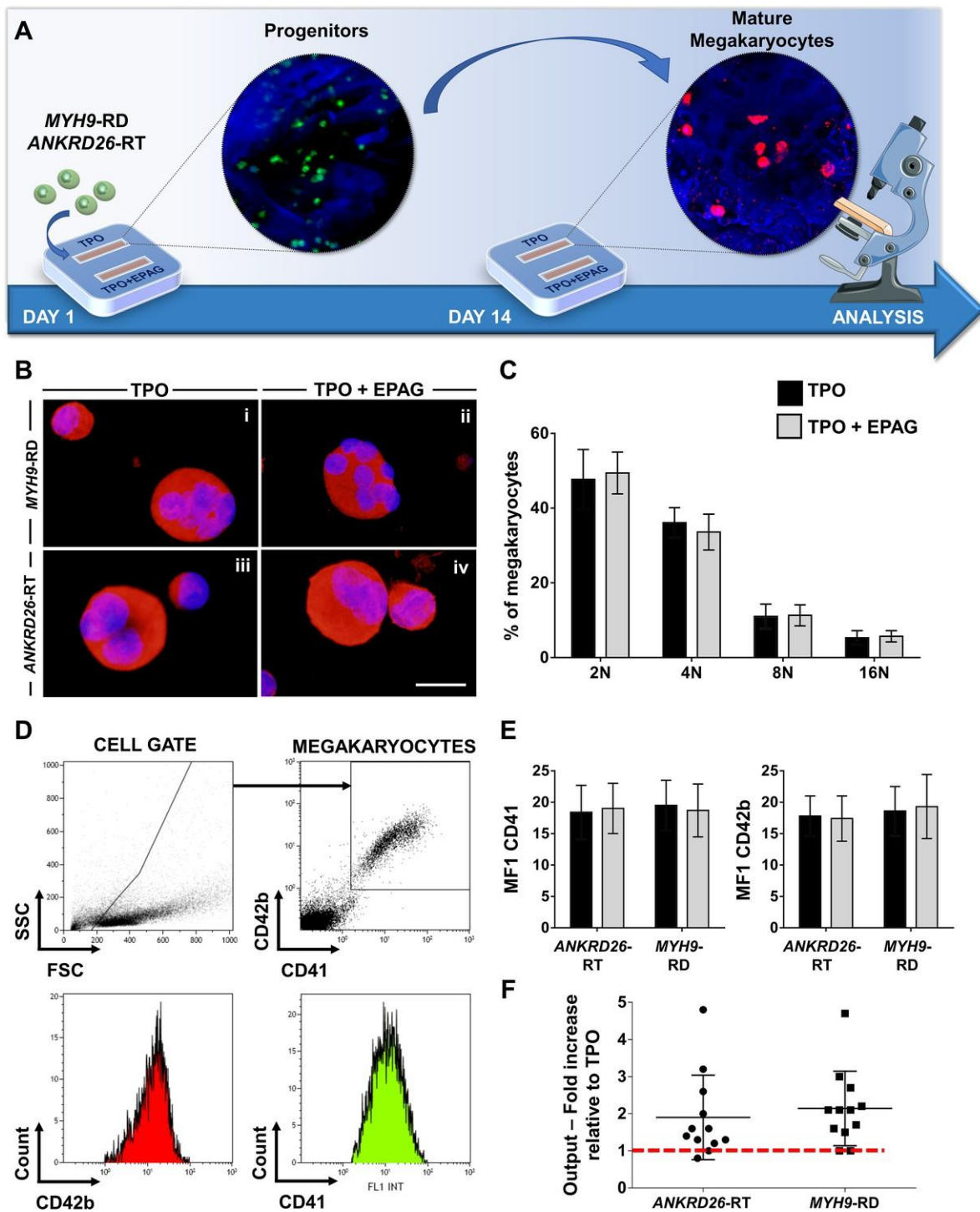
Fig. 27. Evaluation of *ex vivo* megakaryocyte differentiation in response to Eltrombopag

(**A**) Megakaryocytes were differentiated from peripheral blood progenitors of patients affected by *MYH9*-RD or *ANKRD26*-RT and cultured in the silk bone marrow tissue device in the presence of 10 ng/mL TPO supplemented or not with 500 ng/mL Eltrombopag (EPAG) and analyzed. (**B**) Representative immunofluorescence staining of CD61 (red=CD61; blue=nuclei; scale bar=25 μm) and (**C**) analysis of ploidy levels at the end of the culture (TPO: n=3 *MYH9*-RD; n=3 *ANKRD26*-RT; TPO+EPAG: n=3 *MYH9*-RD; n=3 *ANKRD26*-RT; p=NS). (**D**) Representative flow cytometry analysis of CD41$^+$CD42b$^+$ megakaryocytes at the end of the

culture and (**E**) statistical analysis of mean fluorescence intensity (MFI) of the markers (TPO: n=12 *MYH9*-RD; n=12 *ANKRD26*-RT; TPO+EPAG: n=12 *MYH9*-RD; n=12 *ANKRD26*-RT; p=NS). (**F**) Output was calculated as the fold increase in the percentage of CD41+CD42b+ cells in presence of TPO +EPAG with respect to the percentage of double-positive cells in presence of TPO alone (ANKRD26-RT: n = 12, $p<0.05$; MYH9-RD: n = 12, $p<0.01$). All results are presented as mean ± SD.

Assessment of *ex vivo* proplatelet formation in response to Eltrombopag

To evaluate the ability of Eltrombopag in sustaining the last steps of thrombopoiesis, cultured cells in a 3D scaffold were analyzed by confocal microscopy. For immunofluorescence imaging of megakaryocyte cultures within the silk bone marrow tissue model, samples were probed with anti-CD61 or β1-tubulin. Confocal microscopy analysis of 3D scaffolds revealed a homogeneous distribution of CD61$^+$ megakaryocytes throughout the entire construct in both culture conditions, with more clusters in the presence of Eltrombopag, from both *ANKRD26*-RT and *MYH9*-RD (**Figure 28Ai-iv**). Further, in the presence of Eltrombopag, megakaryocytes underwent characteristic cytoplasmic rearrangements typical of proplatelets (**Figure 28 Aii,iv**). β1-tubulin staining of megakaryocytes harvested from the device and seeded onto fibronectin-coated coverslips consistently highlighted that TPO in combination with Eltrombopag supported the extension of multiple branched shafts resembling nascent platelets at their terminal ends (**Figure 28 Av-viii**) and a significant increase in the percentage of proplatelet-forming megakaryocytes in both *ANKRD26*-RT (TPO: 3±2.6%; TPO plus Eltrombopag: 7.7±4.4%) and *MYH9*-RD (TPO: 1.5±1%; TPO plus Eltrombopag: 4.4±4.3%) (**Figure 28 B**).
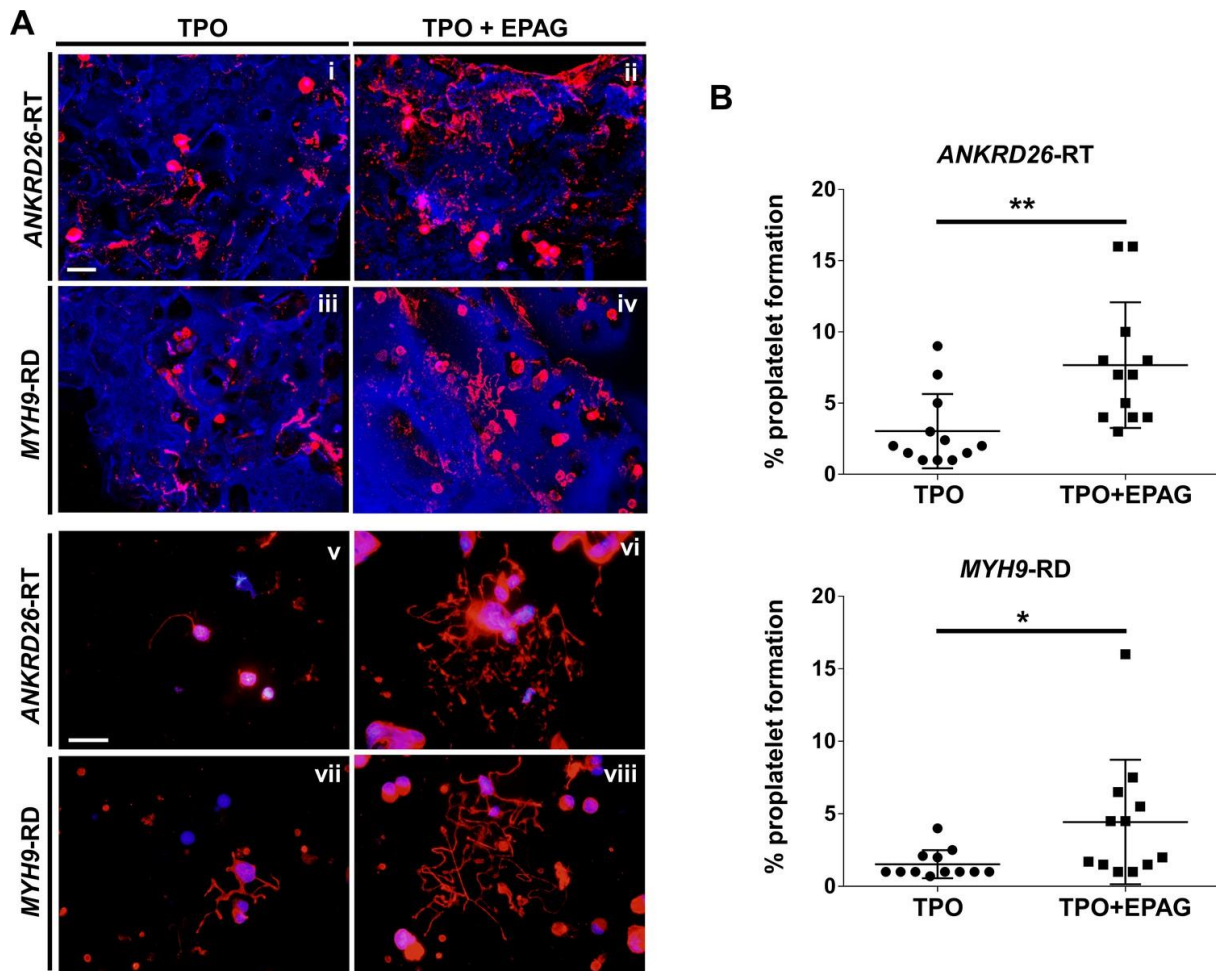
Fig.28. Evaluation of Eltrombopag effect on *ex vivo* proplatelet formation.

(**A**) Confocal microscopy analysis of 3D megakaryocyte culture imaged at the end of differentiation. Megakaryocytes were elongating proplatelet shafts, which assemble nascent platelets at their terminal ends, within the hollow space of silk pores (red=CD61, blue=silk) (scale bars = 50 μm). (**Av-viii**) Analysis of proplatelet structure was performed by immunofluorescence staining of the megakaryocyte-specific cytoskeleton component β1-tubulin (red=β1-tubulin; blue=nuclei; scale bar=25 μm). In both diseases, the representative pictures show increased elongation and branching of proplatelet shafts in presence of TPO+EPAG with respect to TPO alone. (**B**) The percentage of proplatelet forming megakaryocytes was calculated as the number of cells displaying long filamentous pseudopods with respect to the total number of round megakaryocytes per analyzed field (TPO: n=12 *MYH9*-RD; n=12 *ANKRD26*-RT; TPO+EPAG: n=12 *MYH9*-RD; n=12 *ANKRD26*-RT; **p<0.01; *p<0.05).

Evaluation of *ex vivo* platelet in response to Eltrombopag

Finally, the model was tested to evaluate the ability to mimic the dynamic blood flow and generate the shear forces needed to promote the *ex vivo* platelet production and release. Moreover, it has been evaluated the ability of this device to predict the patient-specific response to Eltrombopag by performing a systematic study comparing the extent of platelet production *ex vivo* with *in vivo* platelet response observed in the same patients (Zaninetti, Barozzi, et al., 2019; Zaninetti, Gresele, et al., 2019).

On day 15 of differentiation, each channel of the device was connected to a peristaltic pump at the inlet and a gas-permeable collection bag at the outlet. The number of *ex vivo* produced platelets was evaluated by flow cytometry after 4 hours of perfusion at 37°C and 5% CO_2 (**Figure 29-A**). *Ex vivo* collected platelets exhibited the β1-tubulin coil at their periphery, typically present in physiologic peripheral blood platelets (**Figure 29-B**), further supporting the physiological relevance of the reproduced bone marrow environment for replicating *in vivo* thrombopoiesis. *Ex vivo* collected platelets were double-stained with anti-CD41 and anti-CD42b antibodies and counted by flow cytometry with a bead standard (**Figure 29-C**). The number of $CD41^+CD42b^+$ platelets collected per single channel was globally increased under treatment with TPO in combination with Eltrombopag with respect to TPO alone, in both *ANKRD26*-RT and *MYH9*-RD groups. Platelet response was variable, with some samples demonstrating slight or no increase in *ex vivo* platelet production, as observed *in vivo*. However, a statistically significant correlation (R square = 0.78; p<0.0001) was observed when the increase of *ex vivo* platelet count in response to Eltrombopag is compared to the increase of in vivo treatment in the same patients (**Figure 29-D**).

Finally, *in vivo* platelet count in response to Eltrombopag was correlated with the *ex vivo* Megakaryocyte output. This interpolation didn't show the same correlation (R square = 0.35), suggesting that ex vivo platelet count is the ideal parameter to evaluate the patients' response to the drug treatment (**Figure 29-E**).
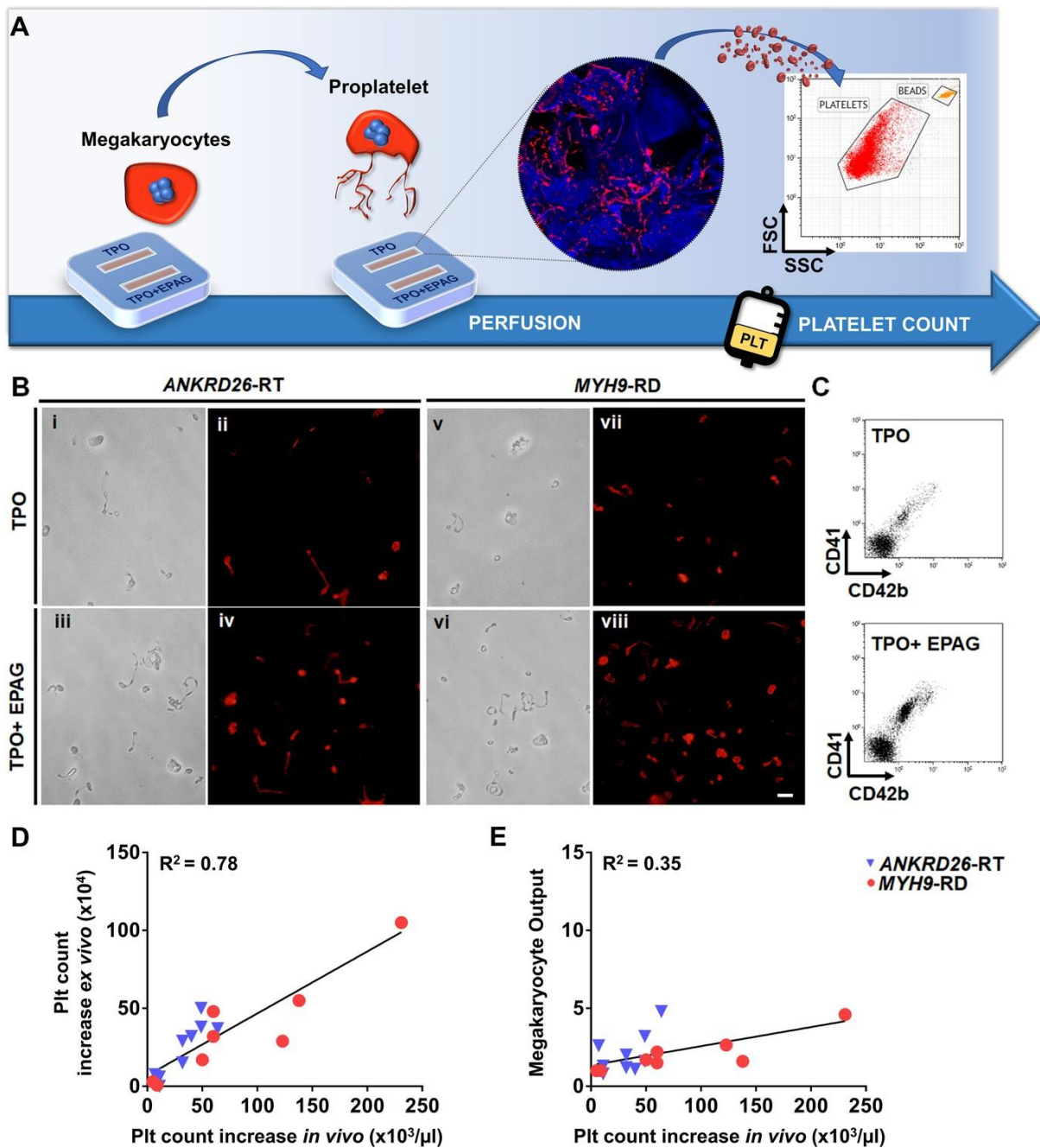
Fig.29. *Ex vivo* **platelet count for predicting response to treatments.**

(**A**) The flow chamber was perfused with culture media and released platelets collected into gas-permeable bags before counting by flow cytometry. (**B**) Light microscopy and immunofluorescent analysis of the collected medium demonstrated the presence of large pre-platelets, dumbbells, and little discoid platelets having the microtubule coil typically present in resting platelets (red=β1-tubulin, scale bars = 10 μm). (**C**) Representative flow cytometry analysis of expression of CD41 and CD42b surface markers. (**D**) Analysis of the correlation between the increase of platelet count analyzed ex vivo and the increase of platelet count observed in vivo from the same patients. For the ex vivo analysis, platelet count was calculated by flow cytometry with counting beads (n = 8 MYH9-RD; n = 9 ANKRD26-RT). (**E**) Analysis of

the correlation between ex vivo megakaryocyte output and the increase of platelet count observed in vivo from the same patients. (n = 8 MYH9-RD; n = 9 ANKRD26-RT).

Generation and differentiation of iPSCs from patients

Finally, the ultimate validation of this miniaturized bone marrow model has been performed through the use of the cell disease model represented by iPSC. Human iPSC disease modeling has emerged as an alternative modeling method for obtaining both important human pathology data and unlimited resources. In the last decade, the breakthrough of this technology paved the way in understanding the hidden pathogenetic mechanism of several pathologies, including Thrombocytopenias. For this project, iPSC clones were generated from one *MYH9*-RD patient and one healthy control. These cells were generated by Prof. Hana Raslova's group and gently provided for this project.

To evaluate iPSCs quality standard among different clones, cells were tested for pluripotency and found positive for OCT4, NANOG, and SOX2 by qRT-PCR analysis. SOX2, OCT4, NANOG, TRA 1-81, and SSEA4 marker expression was also confirmed by immunofluorescence analysis. Both control and patient clones displayed a normal diploid karyotype (control: 46,XX; patient: 46,XY) without noticeable abnormalities. These tests were gently performed by ISENET Engineering Srl.

MYH9-RD and healthy control iPSC clones were cultured and differentiated over 14 days in presence of SCF (50 ng/mL), FLT3L (5 ng/mL), TPO (50 ng/mL), and IL-6 (10 ng/mL). iPSCs-derived megakaryocytes were analyzed by flow cytometry to assess the expression of typical megakaryocyte markers (CD42a, CD42b, CD41, CD61) (**Figure 30-A**).

Megakaryocyte differentiation of iPSC clones was also confirmed in liquid culture conditions (**Figure 30-B**) and demonstrated that *MYH9*-RD iPSCs present a severe defect in proplatelet formation (control: 4.8±2.2%; *MYH9*-RD: 3.2±1.7%) and branching (n° of bifurcations: control: 6.3±2.8; *MYH9*-RD: 1.5±1) with respect to control iPSCs (**Figure 30-C and 30-D**).
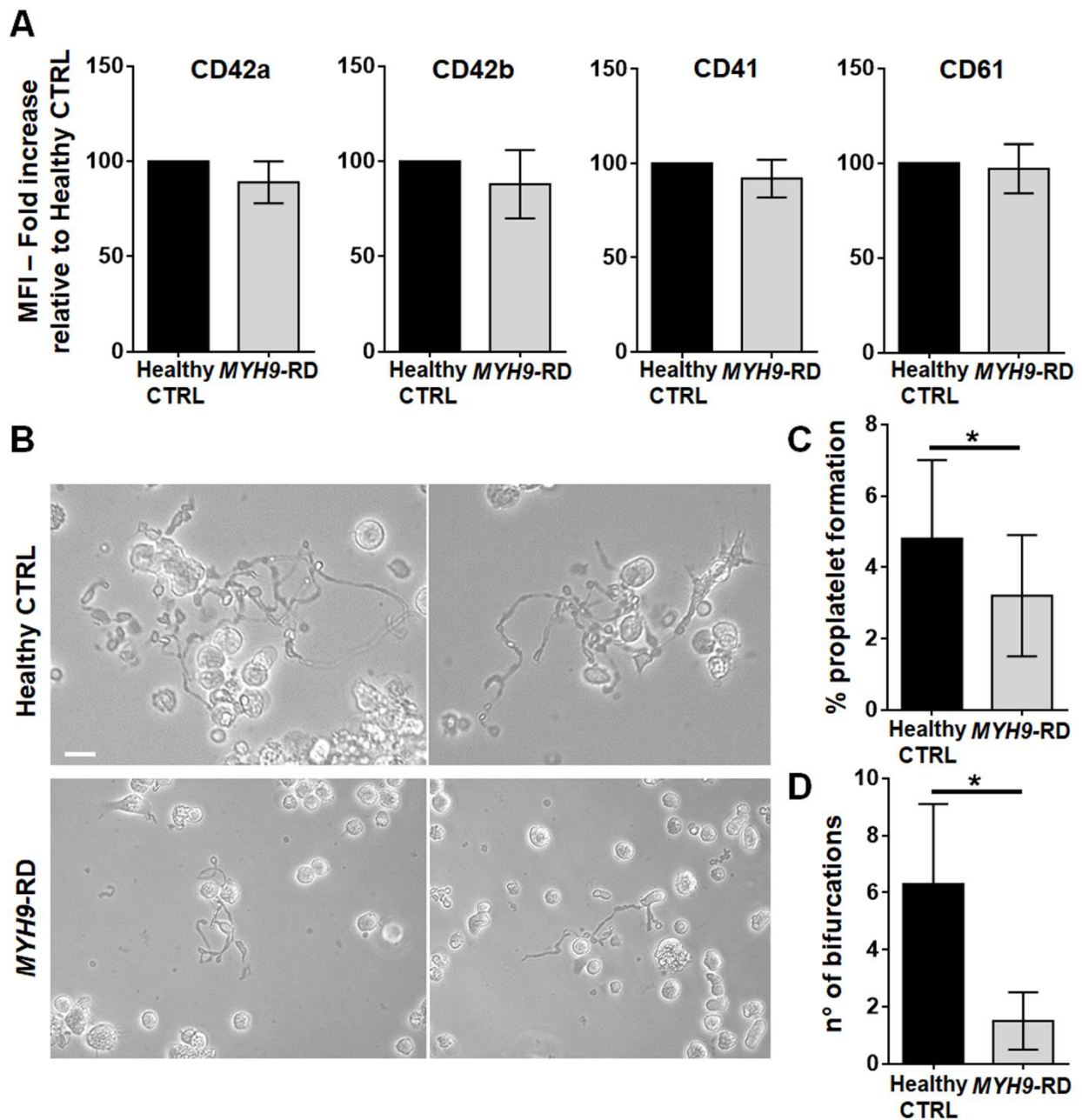
Fig. 30. Assessment of iPSC megakaryocyte differentiation.

(**A**) iPSC clones were cultured for 18 days and analyzed by flow cytometry to assess megakaryocytes differentiation. Histograms show the mean fluorescence intensity (MFI) of *MYH9*-RD clones for CD42a, CD42b, CD41, and CD61 markers, relative to healthy controls (n=3 Healthy Controls, n=3 *MYH9*-RD; p=NS). (**B**) Representative images of proplatelet forming-megakaryocytes at day 19 of culture. (**C**) Percentage of proplatelet formation from the different genotypes. (n=3 Healthy Controls, n=3 *MYH9*-RD; *p<0.05). (**D**) Number of bifurcation per single megakaryocyte from the different genotypes (*p<0.01). All results are presented as mean±SD.

Device validation with iPSCs from thrombocytopenic patients

To validate their use within the bone marrow tissue bioreactor, megakaryocyte progenitors from iPSC clones were sorted at day 14 of differentiation based on the expression of CD61$^+$, an early progenitor lineage-specific marker, and cultured for an additional 5 days within the device in the presence of 50 ng/mL TPO supplemented or not with 500 ng/mL Eltrombopag (**Figure 31-A**).

To evaluate the profile of megakaryocyte maturation and differentiation, *MYH9*-RD and Healthy Controls clones were analyzed by immunofluorescence after seeding on coverslips coated with Fibronectin, and by confocal microscopy after seeding in the silk sponge. Morphological analysis showed that MYH9-RD clones revealed a comparable megakaryocyte maturation in terms of cell size (**Figure 31-Bi-ii**). Cytofluorymetric analysis of expression of CD41 and CD42b (**Figure 31-C and 31-D**) in the presence of TPO or TPO plus Eltrombopag confirmed this data.

3D reconstruction of cell cultures from different *MYH9*-mutated clones revealed an increased number of megakaryocytes throughout the scaffold in the presence of TPO plus Eltrombopag (**Figure 31- Biii-iv**), paralleled by an increased percentage of proplatelets (**Figure 31- Biii-iv**) having more branches with respect to TPO alone (**Figure 31-Bv-viii**). Statistical analysis demonstrated a significant increase in cell proliferation in the presence of TPO plus Eltrombopag with respect to TPO alone (**Figure 31-E**).

Further, the miniaturized bone marrow silk model has been connected to a peristaltic pump and perfused to evaluate platelet release in both conditions. *Ex vivo* collected platelets were double-stained with anti-CD41 and anti-CD42b antibodies and counted by flow cytometry with a bead standard and significantly increased platelet count was observed under treatment with Eltrombopag (**Figure 31-F**).
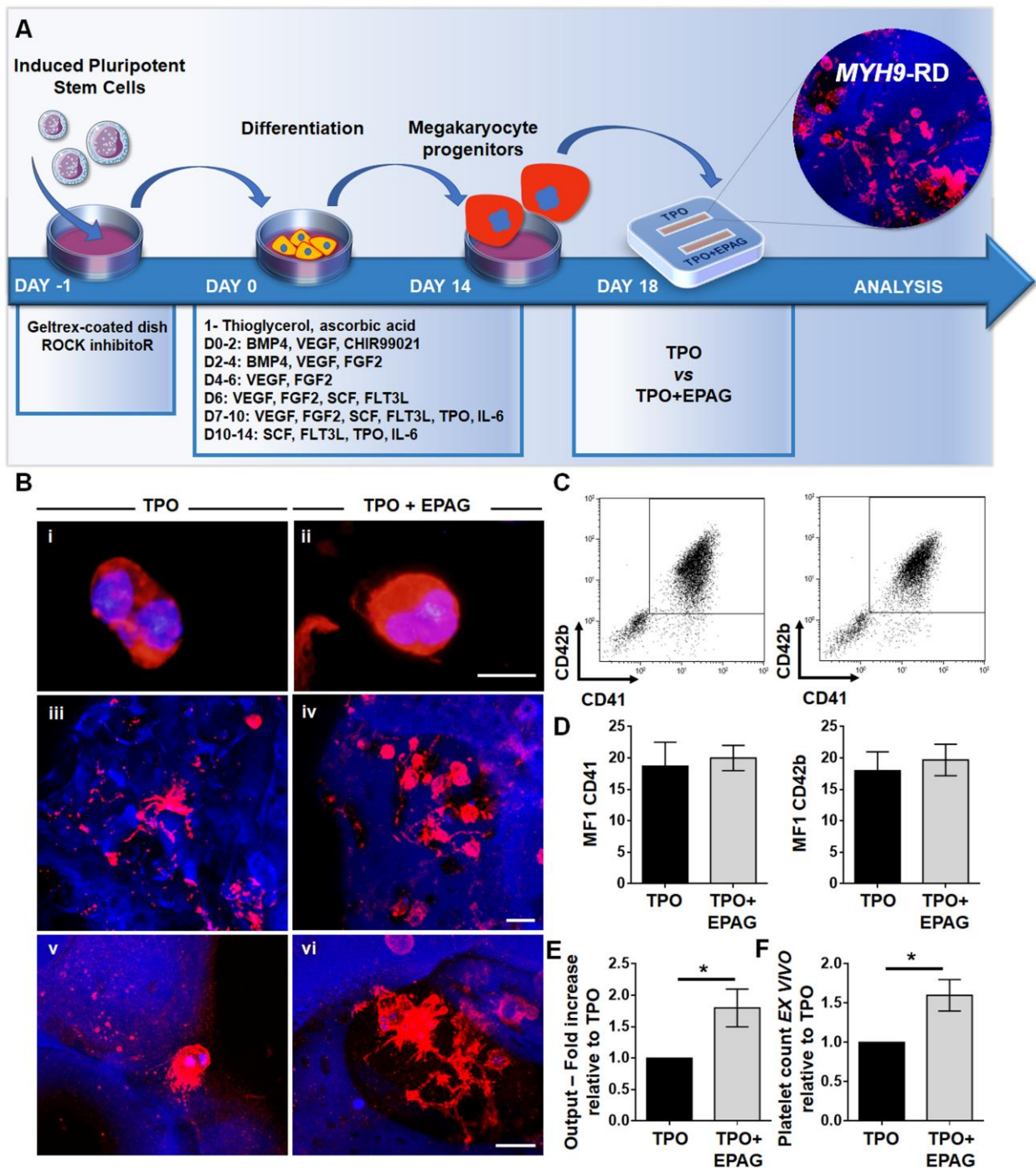
Fig. 31. Validation of the system with iPSC mutated clones.

(**A**) Megakaryocytes were differentiated from iPSCs of patients affected by *MYH9*-RD and cultured for 14 days in a petri dish before passing into the bone marrow device in presence of 10 ng/mL TPO supplemented or not with 500 ng/mL EPAG. (**B**) Representative immunofluorescence staining of CD61 megakaryocytes (i, ii) and confocal microscopy analysis (iii-vi) of 3D megakaryocyte culture imaged at the end of differentiation. Megakaryocytes are elongating proplatelet shafts, which assemble nascent platelets at their terminal ends, within the hollow space of silk pores (red=CD61, blue=silk, scale bars = 50 µm). (**C**) Representative

flow cytometry analysis of CD41$^+$CD42b$^+$ megakaryocytes at the end of the culture and (**D**) statistical analysis of mean fluorescence intensity (MFI) of the markers (n=3 TPO, n=3 TPO+EPAG; p=NS). (**E**) Output was calculated as the number of CD41$^+$CD42b$^+$ cells in presence of TPO+EPAG with respect to the percentage of double-positive cells in presence of TPO alone (n=3 TPO, n=3 TPO+EPAG; *p<0.05). (**F**) Platelet number was calculated with counting beads after perfusing the chamber. The fold increase was calculated as the number of *ex vivo* platelet counts in the presence of TPO+EPAG with respect to TPO alone (n=3 TPO, n=3 TPO+EPAG; *p<0.05). All results are presented as mean±SD.

Discussion

Bone marrow modeling still represents one of the most intriguing challenges in biomedical research. Located in the hollow spaces of bones, the cellular and matrix composition of this tissue has been explored and defined with surprising resolution in mice (Ito et al., 2018; Bornert et al., 2021). The generation of blood cells is an intricate process involving cell-cell interaction, ECM composition, and soluble factor networking, that contributes to orchestrating HSC fate (Malara et al., 2011). HSCs give rise to all blood cells and their tightly controlled balance is regulated by bone marrow niches, namely the osteoblastic and perivascular niches, which are responsible for the shift among quiescence, expansion, and differentiation (Schofield, 1978; Lo Celso et al., 2011). Despite the recent advances in bioengineering that have dramatically improved the ability of tissue and organ reconstruction, mimicking the bone marrow complexity remains unsatisfactory and incomplete.

Megakaryocytes represent a rare population of bone marrow cells, mainly involved in platelet production, but growing evidence is shedding light on their crucial role in the regulation of the whole bone marrow homeostasis. Following the cloning of TPO, the main regulator of thrombopoiesis (Kaushansky et al., 1994), major advances were made in the knowledge of the mechanisms underlying HSC differentiation, megakaryocyte maturation, and platelet production, but much remains to be clarified, both in physiological and pathological conditions. Bone marrow failure can result in defects of megakaryocyte function that can dramatically affect proplatelet elongation and platelet release, giving rise to a low blood platelet count and bleeding events. This condition, defined as Thrombocytopenia, arises from a plethora of factors, such as medical interventions (chemotherapy), autoimmunological responses, and abnormal platelet clearance

Next-Generation Sequencing (NGS) approach has brought a real breakthrough in genetic diagnostics of inherited thrombocytopenic disorders. Regardless of the severity of clinical manifestations, management of thrombocytopenic patients includes treatment and prevention of bleeding and other associated disorders. General treatment recommendations provide for the use of hemostatic agents, platelet concentrate transfusions, and allogeneic HSCT, but many concerns are addressed to their effectiveness and observed limitations due to adverse manifestations. Allogenic platelet transfusions are used to treat bleeding in a patient with thrombocytopenia but platelet concentrates administrations should be avoided to prevent hemorrhages because losing of efficacy due to alloimmunization, the onset of acute reactions, and

transmission of infectious disease. To date, platelet transfusions can't represent a reliable therapeutic approach for inherited thrombocytopenic patients unless the platelet count is significantly low. Therefore an urgent need for alternative medical approaches is still pressuring. In this regard, new therapeutical options are opening through the development of a new class of drugs, the TPO-RAs, able to stimulate the TPO receptor, c-Mpl, and enhance megakaryopoiesis and platelet production. Among these, Eltrombopag, Avatrombopag, and Romiplostim currently represent the most promising TPO-RAs and received the Food and Drug Administration (FDA) and European Medicine Agency (EMA) approvals for the treatment of primary immune thrombocytopenia in adults and children (Bussel et al., 2009), thrombocytopenia related to liver disease if a procedure is needed, and severe acquired aplastic anemia (Olnes et al., 2012). Clinical trials and case studies have reported the effectiveness of some TPO-RAs in patients with Inherited Thrombocytopenia, in which an increase in blood platelet count was observed (Rodeghiero et al., 2018). Particularly, Eltrombopag was administered in patients harbouring *MYH9-RD* and *ANKRD26*-RT mutations with encouraging results (Zaninetti et al., 2019) but less is known about the response for long-term treatment. Moreover, platelet response to these drugs remains variable among patients, due to intrinsic biological and/or mutation-related variability.

Eltrombopag is a small peptide molecule with high binding specificity for human c-Mpl, making it difficult to investigate its effectiveness and safety profile in animal models. In this context, providing an *ex vivo* model able to predict the *in vivo* response of TPO-RAs becomes necessary for the understanding of the mechanisms of action and the optimization of personalized therapies.

In the last decade, several groups attempted to design *ex vivo* bone marrow models, but the main challenge in engineering a fully functional vascularized bone marrow is reproducing both the cellular heterogeneity and the compartmentalized organization found *in vivo*. Our group developed several bioreactors able to reproduce *ex vivo* megakaryocyte maturation and platelet biogenesis (Di Buduo et al., 2015; Di Buduo et al., 2017) through the use of silk fibroin. This biomaterial, obtained from *Bombyx Mori* silk cocoons, can resume the main biological and biophysical features of the bone marrow microenvironment, and provide a platform to investigate the unexplored mechanisms of haematopoiesis.

The purpose of my doctorate was to establish a new miniaturized silk-based bone marrow model that could permit to test and predict the response to TPO-RAs (Eltrombopag) *ex vivo* in inherited thrombocytopenic patients. The bioreactor model has been developed with two distinct and parallel perfusion chambers to perform and analyze simultaneously different experimental conditions, with a relatively low amount of cells embedded in the silk 3D microenvironment. This system has been applied to study the *ex vivo* response to Eltrombopag in patients affected by *ANKRD26*-RT and *MYH9*-RD, who have been previously enrolled in a clinical trial and treated with the same drug (Zaninetti et al., 2019). The results showed how this model can reproduce the main steps of megakaryocyte differentiation and platelet production and could represent a useful tool for drugs screening. Specifically, the significant correlation between *ex vivo* and *in vivo* platelet count response to the treatment with Eltrombopag proves the reliability of this system as a predictable tool for *in vivo* response to TPO-RA.

As observed in this project, the high variability of response to Eltrombopag still raises several issues related to the absence of knowledge about the mechanisms of action of this molecule, which can justify the lack of efficacy in some conditions. Thus, this system could replace *in vivo* animal models and provide pre-clinical data on drug efficacy to reduce the number of non-responders unnecessarily exposed to the treatment. We are aware that this project has investigated the effect of Eltrombopag only on patients affected by *ANKRD26*-RT and *MYH9*-RD. Thrombocytopenic patients harbouring other inherited genetic alterations should be included and tested with this *ex vivo* system to better validate its reliability.

To date, several protocols for megakaryocyte differentiation starting from cord blood and peripheral blood HSCs have been established. Moreover, our group has defined an *in vitro* protocol of HSC differentiation from peripheral blood of patients affected by several pathologies, such as ITs and myeloproliferative neoplasms, but the experimental process may be hindered by the limited access to patient blood samples. In this regard, iPSC technology provides a potentially unlimited source of cells to be used in biomedical research. Somatic reprogramming to iPSC was realized in 2006, in mice (Takahashi et al., 2006), and in 2007 in humans (Takahashi et al., 2007) by transiently forced expression of a combination of transcription factors (Oct4 (Pou5f1), Sox2, Klf4, and c-Myc (OSKM). iPSCs generation opened new perspectives to produce patient-specific pluripotent stem cells and are expected to contribute to the

investigation of pathogenic mechanisms of diseases, drug screening, and personalized therapy.

To investigate the reliability and efficacy of the 3D bone marrow tissue model in studying mechanisms of diseases and testing candidate drugs through the use of the iPSC cell model, we derived iPSCs from one *MYH9*-RD patient in collaboration with the Institute Gustave Russie, as part of the collaboration for the SilkFusion project. Different clones were cultured and analyzed to evaluate megakaryocyte differentiation and platelet production in response to the treatment with Eltrombopag. The results showed normal megakaryocyte differentiation, but an impaired proplatelet formation of *MYH9-RD* clones compared to controls. When cultured within the 3D silk bone marrow model, the diseased clones showed comparable megakaryocyte maturation in terms of cell size and expression of CD41 and CD42b in the presence of TPO or TPO plus Eltrombopag, but increased proplatelet elongation and platelet release in presence of the drug.

In conclusion, this model demonstrated its ability to reproduce *ex vivo* megakaryocyte differentiation and platelet production and release in a 3D dynamic system. In 2D cultures, cells are seeded in a monolayer in the presence of molecules and soluble factors diluted directly in a liquid medium without reproducing the complexity of 3D tissues. While, our 3D tissue bioengineering approach, mimicking bone marrow structure, composition and flow dynamics, represents a more comprehensive model. The perfusable 3D structure is the only model that allow the reproduction of all Mk development, including the production of functional platelets. We expect that this system will provide a useful pre-clinical platform for testing the efficacy of candidate molecules and drugs, exploring their safety profile and mechanisms of action.

Besides its ability to stimulate platelet production, Eltrombopag is also efficacious to restore hematopoiesis in patients with severe aplastic anemia (Desmond et al., 2014; Drexler et al., 2021) and with low to intermediate-risk myelodysplastic syndrome (Vicente et al., 2020). Recently, Kao and colleagues (Kao et al., 2018) showed that Eltrombopag is also able to stimulate HSC self-renewal in ITP patients through iron-chelation dependent mechanism. A deep investigation of the mechanisms of action of Eltrombopag, and other TPO-RA, in the 3D cell culture system, may shed light on their mechanisms of action directly on human samples. Indeed, we expect that in the future, this miniaturized 3D silk-based bone marrow system may offer the opportunity to

overcome ethical and safety concerns regarding the use of animal models in pre-clinical investigations, avoiding the intrinsic biological variability of animal models.

Further, potential applications and developments of this technology may include its scaling-up for the *ex vivo* generation of blood components. Large-scale production of platelets remains an unsatisfied need for the scientific community facing the challenge of donor blood shortages, and many efforts are focused to develop a system that permits the generation of a significant amount of blood cells similar to native cells. Beyond regulatory and Good Manufacturing Practice issues, this silk-based bioreactor may represent the basis for a future approach of *ex vivo* production of all blood cells for transfusions.

References

- Abbonante V, Di Buduo CA, Gruppi C, De Maria C, Spedden E, De Acutis A, Staii C, Raspanti M, Vozzi G, Kaplan DL, Moccia F, Ravid K, Balduini A. A new path to platelet production through matrix sensing. Haematologica. 2017 Jul;102(7):1150-1160. doi: 10.3324/haematol.2016.161562. Epub 2017 Apr 14. PMID: 28411253; PMCID: PMC5566016.

- Afdhal NH, Giannini EG, Tayyab G, Mohsin A, Lee JW, Andriulli A, Jeffers L, McHutchison J, Chen PJ, Han KH, Campbell F, Hyde D, Brainsky A, Theodore D; ELEVATE Study Group. Eltrombopag before procedures in patients with cirrhosis and thrombocytopenia. N Engl J Med. 2012 Aug 23;367(8):716-24. doi: 10.1056/NEJMoa1110709. PMID: 22913681.

- Aguilar A, Pertuy F, Eckly A, Strassel C, Collin D, Gachet C, Lanza F, Léon C. Importance of environmental stiffness for megakaryocyte differentiation and proplatelet formation. Blood. 2016 Oct 20;128(16):2022-2032. doi: 10.1182/blood-2016-02-699959. Epub 2016 Aug 8. PMID: 27503502.

- Alexander WS. Thrombopoietin and the c-Mpl receptor: insights from gene targeting. Int J Biochem Cell Biol. 1999 Oct;31(10):1027-35. doi: 10.1016/s1357-2725(99)00079-5. PMID: 10582337.

- Al-Samkari H, Kuter DJ. Thrombopoietin level predicts response to treatment with eltrombopag and romiplostim in immune thrombocytopenia. Am J Hematol. 2018 Dec;93(12):1501-1508. doi: 10.1002/ajh.25275. Epub 2018 Sep 26. PMID: 30187942.

- Antony-Debré I, Manchev VT, Balayn N, Bluteau D, Tomowiak C, Legrand C, Langlois T, Bawa O, Tosca L, Tachdjian G, Leheup B, Debili N, Plo I, Mills JA, French DL, Weiss MJ, Solary E, Favier R, Vainchenker W, Raslova H. Level of RUNX1 activity is critical for leukemic predisposition but not for thrombocytopenia. Blood. 2015 Feb 5;125(6):930-40. doi: 10.1182/blood-2014-06-585513. Epub 2014 Dec 9. PMID: 25490895; PMCID: PMC4347283.

- Avecilla ST, Hattori K, Heissig B, Tejada R, Liao F, Shido K, Jin DK, Dias S, Zhang F, Hartman TE, Hackett NR, Crystal RG, Witte L, Hicklin DJ, Bohlen P, Eaton D, Lyden D, de Sauvage F, Rafii S. Chemokine-mediated interaction of hematopoietic progenitors with the bone marrow vascular niche is required for thrombopoiesis. Nat Med. 2004 Jan;10(1):64-71. doi: 10.1038/nm973. Epub 2003 Dec 21. PMID: 14702636.

- Baccin C, Al-Sabah J, Velten L, Helbling PM, Grünschläger F, Hernández-Malmierca P, Nombela-Arrieta C, Steinmetz LM, Trumpp A, Haas S. Combined single-cell and spatial transcriptomics reveal the molecular, cellular and spatial bone marrow niche organization. Nat Cell Biol. 2020 Jan;22(1):38-48. doi: 10.1038/s41556-019-0439-6. Epub 2019 Dec 23. PMID: 31871321; PMCID: PMC7610809.

- Balduini CL, Melazzini F, Pecci A. Inherited thrombocytopenias-recent advances in clinical and molecular aspects. Platelets. 2017 Jan;28(1):3-13. doi: 10.3109/09537104.2016.1171835. Epub 2016 May 9. PMID: 27161842.

- Balduini CL, Pecci A, Noris P. Inherited thrombocytopenias: the evolving spectrum. Hamostaseologie. 2012;32(4):259-70. doi: 10.5482/ha12050001. Epub 2012 Sep 13. PMID: 22972471.

- Basser RL, Underhill C, Davis I, Green MD, Cebon J, Zalcberg J, MacMillan J, Cohen B, Marty J, Fox RM, Begley CG. Enhancement of platelet recovery after myelosuppressive chemotherapy by recombinant human megakaryocyte growth and development factor in patients with advanced cancer. J Clin Oncol. 2000 Aug;18(15):2852-61. doi: 10.1200/JCO.2000.18.15.2852. PMID: 10920133.

- Battinelli EM, Thon JN, Okazaki R, Peters CG, Vijey P, Wilkie AR, Noetzli LJ, Flaumenhaft R, Italiano JE. Megakaryocytes package contents into separate α-granules that are differentially distributed in platelets. Blood Adv. 2019 Oct 22;3(20):3092-3098. doi: 10.1182/bloodadvances.2018020834. PMID: 31648331; PMCID: PMC6849942.

- Becker RP, De Bruyn PP. The transmural passage of blood cells into myeloid sinusoids and the entry of platelets into the sinusoidal circulation; a scanning electron microscopic investigation. Am J Anat. 1976 Feb;145(2):183-205. doi: 10.1002/aja.1001450204. PMID: 1258805.

- Bera TK, Liu XF, Yamada M, Gavrilova O, Mezey E, Tessarollo L, Anver M, Hahn Y, Lee B, Pastan I. A model for obesity and gigantism due to disruption of the Ankrd26 gene. Proc Natl Acad Sci U S A. 2008 Jan 8;105(1):270-5. doi: 10.1073/pnas.0710978105. Epub 2007 Dec 27. PMID: 18162531; PMCID: PMC2224199.

- Bera TK, Zimonjic DB, Popescu NC, Sathyanarayana BK, Kumar V, Lee B, Pastan I. POTE, a highly homologous gene family located on numerous chromosomes and expressed in prostate, ovary, testis, placenta, and prostate cancer. Proc Natl Acad Sci U S A. 2002 Dec 24;99(26):16975-80. doi: 10.1073/pnas.262655399. Epub 2002 Dec 10. Erratum in: Proc Natl Acad Sci U S A. 2003 Feb 4;100(3):1462. PMID: 12475935; PMCID: PMC139254.

- Blin A, Le Goff A, Magniez A, Poirault-Chassac S, Teste B, Sicot G, Nguyen KA, Hamdi FS, Reyssat M, Baruch D. Microfluidic model of the platelet-generating organ: beyond bone marrow biomimetics. Sci Rep. 2016 Feb 22;6:21700. doi: 10.1038/srep21700. PMID: 26898346; PMCID: PMC4761988.

- Bluteau D, Balduini A, Balayn N, Currao M, Nurden P, Deswarte C, Leverger G, Noris P, Perrotta S, Solary E, Vainchenker W, Debili N, Favier R, Raslova H. Thrombocytopenia-associated mutations in the ANKRD26 regulatory region induce MAPK hyperactivation. J Clin Invest. 2014 Feb;124(2):580-91. doi: 10.1172/JCI71861. Epub 2014 Jan 16. PMID: 24430186; PMCID: PMC3904625.

- Bolton-Maggs PH, Chalmers EA, Collins PW, Harrison P, Kitchen S, Liesner RJ, Minford A, Mumford AD, Parapia LA, Perry DJ, Watson SP, Wilde JT, Williams MD; UKHCDO. A review of inherited platelet disorders with guidelines for their management on behalf of the UKHCDO. Br J Haematol. 2006 Dec;135(5):603-33. doi: 10.1111/j.1365-2141.2006.06343.x. PMID: 17107346.

- Bornert A, Pertuy F, Lanza F, Gachet C, Léon C. In Vivo Two-photon Imaging of Megakaryocytes and Proplatelets in the Mouse Skull Bone Marrow. J Vis Exp. 2021 Jul 28;(173). doi: 10.3791/62515. PMID: 34398145.

- Borst S, Nations CC, Klein JG, Pavani G, Maguire JA, Camire RM, Drazer MW, Godley LA, French DL, Poncz M, Gadue P. Study of inherited thrombocytopenia resulting from mutations in ETV6 or RUNX1 using a human pluripotent stem cell

model. Stem Cell Reports. 2021 Jun 8;16(6):1458-1467. doi: 10.1016/j.stemcr.2021.04.013. Epub 2021 May 20. PMID: 34019812; PMCID: PMC8190596.

- Boulais PE, Frenette PS. Making sense of hematopoietic stem cell niches. Blood. 2015 Apr 23;125(17):2621-9. doi: 10.1182/blood-2014-09-570192. Epub 2015 Mar 11. PMID: 25762174; PMCID: PMC4408288.

- Broudy VC, Lin NL. AMG531 stimulates megakaryopoiesis in vitro by binding to Mpl. Cytokine. 2004 Jan 21;25(2):52-60. doi: 10.1016/j.cyto.2003.05.001. PMID: 14693160.

- Bruns I, Lucas D, Pinho S, Ahmed J, Lambert MP, Kunisaki Y, Scheiermann C, Schiff L, Poncz M, Bergman A, Frenette PS. Megakaryocytes regulate hematopoietic stem cell quiescence through CXCL4 secretion. Nat Med. 2014 Nov;20(11):1315-20. doi: 10.1038/nm.3707. Epub 2014 Oct 19. PMID: 25326802; PMCID: PMC4258871.

- Bussel JB, Cheng G, Saleh MN, Psaila B, Kovaleva L, Meddeb B, Kloczko J, Hassani H, Mayer B, Stone NL, Arning M, Provan D, Jenkins JM. Eltrombopag for the treatment of chronic idiopathic thrombocytopenic purpura. N Engl J Med. 2007 Nov 29;357(22):2237-47. doi: 10.1056/NEJMoa073275. PMID: 18046028.

- Bussel JB, Kuter DJ, George JN, McMillan R, Aledort LM, Conklin GT, Lichtin AE, Lyons RM, Nieva J, Wasser JS, Wiznitzer I, Kelly R, Chen CF, Nichol JL. AMG 531, a thrombopoiesis-stimulating protein, for chronic ITP. N Engl J Med. 2006 Oct 19;355(16):1672-81. doi: 10.1056/NEJMoa054626. Erratum in: N Engl J Med. 2006 Nov 9;355(19):2054. PMID: 17050891.

- Bussel JB, Kuter DJ, Pullarkat V, Lyons RM, Guo M, Nichol JL. Safety and efficacy of long-term treatment with romiplostim in thrombocytopenic patients with chronic ITP. Blood. 2009 Mar 5;113(10):2161-71. doi: 10.1182/blood-2008-04-150078. Epub 2008 Nov 3. Erratum in: Blood. 2009 May 7;113(19):4822. PMID: 18981291.

- Bussel JB, Provan D, Shamsi T, Cheng G, Psaila B, Kovaleva L, Salama A, Jenkins JM, Roychowdhury D, Mayer B, Stone N, Arning M. Effect of eltrombopag on platelet counts and bleeding during treatment of chronic idiopathic thrombocytopenic purpura: a randomised, double-blind, placebo-controlled trial. Lancet. 2009 Feb 21;373(9664):641-8. doi: 10.1016/S0140-6736(09)60402-5. PMID: 19231632.

- Buxboim A, Rajagopal K, Brown AE, Discher DE. How deeply cells feel: methods for thin gels. J Phys Condens Matter. 2010 May 19;22(19):194116. doi: 10.1088/0953-8984/22/19/194116. PMID: 20454525; PMCID: PMC2864502.

- Calvi LM, Adams GB, Weibrecht KW, Weber JM, Olson DP, Knight MC, Martin RP, Schipani E, Divieti P, Bringhurst FR, Milner LA, Kronenberg HM, Scadden DT. Osteoblastic cells regulate the haematopoietic stem cell niche. Nature. 2003 Oct 23;425(6960):841-6. doi: 10.1038/nature02040. PMID: 14574413.

- Cao TT, Zhang YQ. Processing and characterization of silk sericin from Bombyx mori and its application in biomaterials and biomedicines. Mater Sci Eng C Mater Biol Appl. 2016 Apr 1;61:940-52. doi: 10.1016/j.msec.2015.12.082. Epub 2015 Dec 30. PMID: 26838924.

- Chatterjee C, Schertl P, Frommer M, Ludwig-Husemann A, Mohra A, Dilger N, Naolou T, Meermeyer S, Bergmann TC, Alonso Calleja A, Lee-Thedieck C. Rebuilding the hematopoietic stem cell niche: Recent developments and future prospects. Acta Biomater. 2021 Sep 15;132:129-148. doi: 10.1016/j.actbio.2021.03.061. Epub 2021 Apr 1. PMID: 33813090.

- Chen Y, Aardema J, Kale S, Whichard ZL, Awomolo A, Blanchard E, Chang B, Myers DR, Ju L, Tran R, Reece D, Christensen H, Boukour S, Debili N, Strom TS, Rawlings D, Vázquez FX, Voth GA, Zhu C, Kahr WH, Lam WA, Corey SJ. Loss of the F-BAR protein CIP4 reduces platelet production by impairing membrane-cytoskeleton remodeling. Blood. 2013 Sep 5;122(10):1695-706. doi: 10.1182/blood-2013-03-484550. Epub 2013 Jul 23. PMID: 23881916; PMCID: PMC3765055.

- Choi ES, Nichol JL, Hokom MM, Hornkohl AC, Hunt P. Platelets generated in vitro from proplatelet-displaying human megakaryocytes are functional. Blood. 1995 Jan 15;85(2):402-13. PMID: 7529062.

- Choi JS, Harley BA. The combined influence of substrate elasticity and ligand density on the viability and biophysical properties of hematopoietic stem and progenitor cells. Biomaterials. 2012 Jun;33(18):4460-8. doi: 10.1016/j.biomaterials.2012.03.010. Epub 2012 Mar 22. PMID: 22444641.

- Chung S, Sudo R, Mack PJ, Wan CR, Vickerman V, Kamm RD. Cell migration into scaffolds under co-culture conditions in a microfluidic platform. Lab Chip. 2009 Jan 21;9(2):269-75. doi: 10.1039/b807585a. Epub 2008 Oct 31. PMID: 19107284.

- Craig R, Smith R, Kendrick-Jones J. Light-chain phosphorylation controls the conformation of vertebrate non-muscle and smooth muscle myosin molecules. Nature. 1983 Mar 31-Apr 6;302(5907):436-9. doi: 10.1038/302436a0. PMID: 6687627.

- Cramer EM, Norol F, Guichard J, Breton-Gorius J, Vainchenker W, Massé JM, Debili N. Ultrastructure of platelet formation by human megakaryocytes cultured with the Mpl ligand. Blood. 1997 Apr 1;89(7):2336-46. PMID: 9116277.

- Currao M, Balduini CL, Balduini A. High doses of romiplostim induce proliferation and reduce proplatelet formation by human megakaryocytes. PLoS One. 2013;8(1):e54723. doi: 10.1371/journal.pone.0054723. Epub 2013 Jan 24. PMID: 23359807; PMCID: PMC3554640.

- Currao M, Malara A, Di Buduo CA, Abbonante V, Tozzi L, Balduini A. Hyaluronan based hydrogels provide an improved model to study megakaryocyte-matrix interactions. Exp Cell Res. 2016 Aug 1;346(1):1-8. doi: 10.1016/j.yexcr.2015.05.014. Epub 2015 May 29. PMID: 26027944; PMCID: PMC5071306.

- Cwirla SE, Balasubramanian P, Duffin DJ, Wagstrom CR, Gates CM, Singer SC, Davis AM, Tansik RL, Mattheakis LC, Boytos CM, Schatz PJ, Baccanari DP, Wrighton NC, Barrett RW, Dower WJ. Peptide agonist of the thrombopoietin receptor as potent as the natural cytokine. Science. 1997 Jun 13;276(5319):1696-9. doi: 10.1126/science.276.5319.1696. PMID: 9180079.

- D. Woulfe, J. Yang, N. Prevost, P. O'Brien, L.F. Brass,Signal transduction during initiation, extension, and perpetuation of platelet plug formation, A.D. Michelson (Ed.), Platelets, Academic Press, San Diego (2002), pp. 197-213

- Dahlen DD, Broudy VC, Drachman JG. Internalization of the thrombopoietin receptor is regulated by 2 cytoplasmic motifs. Blood. 2003 Jul 1;102(1):102-8. doi: 10.1182/blood-2002-11-3468. Epub 2003 Mar 6. PMID: 12623841.

- de Sauvage FJ, Hass PE, Spencer SD, Malloy BE, Gurney AL, Spencer SA, Darbonne WC, Henzel WJ, Wong SC, Kuang WJ, et al. Stimulation of megakaryocytopoiesis and thrombopoiesis by the c-Mpl ligand. Nature. 1994 Jun 16;369(6481):533-8. doi: 10.1038/369533a0. PMID: 8202154.

- Demirci S, Leonard A, Tisdale JF. Hematopoietic stem cells from pluripotent stem cells: Clinical potential, challenges, and future perspectives. Stem Cells Transl Med. 2020 Dec;9(12):1549-1557. doi: 10.1002/sctm.20-0247. Epub 2020 Jul 29. PMID: 32725882; PMCID: PMC7695636.

- Desmond R, Townsley DM, Dumitriu B, Olnes MJ, Scheinberg P, Bevans M, Parikh AR, Broder K, Calvo KR, Wu CO, Young NS, Dunbar CE. Eltrombopag restores trilineage hematopoiesis in refractory severe aplastic anemia that can be sustained on discontinuation of drug. Blood. 2014 Mar 20;123(12):1818-25. doi: 10.1182/blood-2013-10-534743. Epub 2013 Dec 17. PMID: 24345753; PMCID: PMC3962161.

- Dewair M, Baur X, Ziegler K. Use of immunoblot technique for detection of human IgE and IgG antibodies to individual silk proteins. J Allergy Clin Immunol. 1985 Oct;76(4):537-42. doi: 10.1016/0091-6749(85)90772-9. PMID: 4056241.

- Di Buduo CA, Aguilar A, Soprano PM, Bocconi A, Miguel CP, Mantica G, Balduini A. Latest culture techniques: cracking the secrets of bone marrow to mass-produce erythrocytes and platelets *ex vivo*. Haematologica. 2021 Apr 1;106(4):947-957. doi: 10.3324/haematol.2020.262485. PMID: 33472355; PMCID: PMC8017859. Ferreira LP, Gaspar VM, Mano JF. Design of spherically structured 3D in vitro tumor models -Advances and prospects. Acta Biomater. 2018 Jul 15;75:11-34. doi: 10.1016/j.actbio.2018.05.034. Epub 2018 May 23. PMID: 29803007.

- Di Buduo CA, Moccia F, Battiston M, De Marco L, Mazzucato M, Moratti R, Tanzi F, Balduini A. The importance of calcium in the regulation of megakaryocyte function. Haematologica. 2014 Apr;99(4):769-78. doi: 10.3324/haematol.2013.096859. Epub 2014 Jan 24. PMID: 24463213; PMCID: PMC3971088.

- Di Buduo CA, Soprano PM, Miguel CP, Perotti C, Del Fante C, Balduini A. A Gold Standard Protocol for Human Megakaryocyte Culture Based on the Analysis of 1,500 Umbilical Cord Blood Samples. Thromb Haemost. 2021 Apr;121(4):538-542. doi: 10.1055/s-0040-1719028. Epub 2020 Nov 7. PMID: 33160288.

- Di Buduo CA, Soprano PM, Tozzi L, Marconi S, Auricchio F, Kaplan DL, Balduini A. Modular flow chamber for engineering bone marrow architecture and function. Biomaterials. 2017 Nov;146:60-71. doi: 10.1016/j.biomaterials.2017.08.006. Epub 2017 Aug 8. PMID: 28898758; PMCID: PMC6056889.

- Di Buduo CA, Wray LS, Tozzi L, Malara A, Chen Y, Ghezzi CE, Smoot D, Sfara C, Antonelli A, Spedden E, Bruni G, Staii C, De Marco L, Magnani M, Kaplan DL, Balduini A. Programmable 3D silk bone marrow niche for platelet generation ex vivo and modeling of megakaryopoiesis pathologies. Blood. 2015 Apr 2;125(14):2254-

64. doi: 10.1182/blood-2014-08-595561. Epub 2015 Jan 9. PMID: 25575540; PMCID: PMC4383799.

- Dimos JT, Rodolfa KT, Niakan KK, Weisenthal LM, Mitsumoto H, Chung W, Croft GF, Saphier G, Leibel R, Goland R, Wichterle H, Henderson CE, Eggan K. Induced pluripotent stem cells generated from patients with ALS can be differentiated into motor neurons. Science. 2008 Aug 29;321(5893):1218-21. doi: 10.1126/science.1158799. Epub 2008 Jul 31. PMID: 18669821.

- Ding L, Saunders TL, Enikolopov G, Morrison SJ. Endothelial and perivascular cells maintain haematopoietic stem cells. Nature. 2012 Jan 25;481(7382):457-62. doi: 10.1038/nature10783. PMID: 22281595; PMCID: PMC3270376.

- Donada A, Balayn N, Sliwa D, Lordier L, Ceglia V, Baschieri F, Goizet C, Favier R, Tosca L, Tachdjian G, Denis CV, Plo I, Vainchenker W, Debili N, Rosa JP, Bryckaert M, Raslova H. Disrupted filamin A/$\alpha_{IIb}\beta_3$ interaction induces macrothrombocytopenia by increasing RhoA activity. Blood. 2019 Apr 18;133(16):1778-1788. doi: 10.1182/blood-2018-07-861427. Epub 2019 Jan 2. PMID: 30602618; PMCID: PMC6484462.

- Dong C, Li WD, Geller F, Lei L, Li D, Gorlova OY, Hebebrand J, Amos CI, Nicholls RD, Price RA. Possible genomic imprinting of three human obesity-related genetic loci. Am J Hum Genet. 2005 Mar;76(3):427-37. doi: 10.1086/428438. Epub 2005 Jan 12. PMID: 15647995; PMCID: PMC1196395.

- Dova Pharmaceuticals Inc, Doptelet: Prescribing information. https://www.accessdata.fda.gov/drugsatfda_docs/label/2019/210238s001lbl.pdf; (2019)

- Drachman JG, Kaushansky K. Dissecting the thrombopoietin receptor: functional elements of the Mpl cytoplasmic domain. Proc Natl Acad Sci U S A. 1997 Mar 18;94(6):2350-5. doi: 10.1073/pnas.94.6.2350. PMID: 9122198; PMCID: PMC20091.

- Drexler B, Passweg J. Current evidence and the emerging role of eltrombopag in severe aplastic anemia. Ther Adv Hematol. 2021 Mar 3;12:2040620721998126. doi: 10.1177/2040620721998126. PMID: 33747425; PMCID: PMC7940771.

- Ebbe S. Biology of megakaryocytes. Prog Hemost Thromb. 1976;3:211-29. PMID: 781731.

- Eicke D, Baigger A, Schulze K, Latham SL, Halloin C, Zweigerdt R, Guzman CA, Blaszczyk R, Figueiredo C. Large-scale production of megakaryocytes in microcarrier-supported stirred suspension bioreactors. Sci Rep. 2018 Jul 5;8(1):10146. doi: 10.1038/s41598-018-28459-x. PMID: 29977045; PMCID: PMC6033877.

- Erhardt J, Erickson-Miller CL, Tapley P; SB 497115-GR, a Low Molecular Weight TPOR Agonist, Does Not Induce Platelet Activation or Enhance Agonist-Induced Platelet Aggregation in Vitro.. *Blood* 2004; 104 (11): 3888.

- Evans LT, Anglen T, Scott P, Lukasik K, Loncarek J, Holland AJ. ANKRD26 recruits PIDD1 to centriolar distal appendages to activate the PIDDosome following centrosome amplification. EMBO J. 2021 Feb 15;40(4):e105106. doi:

10.15252/embj.2020105106. Epub 2020 Dec 22. PMID: 33350495; PMCID: PMC7883295.

- Fava LL, Schuler F, Sladky V, Haschka MD, Soratroi C, Eiterer L, Demetz E, Weiss G, Geley S, Nigg EA, Villunger A. The PIDDosome activates p53 in response to supernumerary centrosomes. Genes Dev. 2017 Jan 1;31(1):34-45. doi: 10.1101/gad.289728.116. PMID: 28130345; PMCID: PMC5287111.

- Fei Z, Bera TK, Liu X, Xiang L, Pastan I. Ankrd26 gene disruption enhances adipogenesis of mouse embryonic fibroblasts. J Biol Chem. 2011 Aug 5;286(31):27761-8. doi: 10.1074/jbc.M111.248435. Epub 2011 Jun 13. PMID: 21669876; PMCID: PMC3149366.

- Fielder PJ, Hass P, Nagel M, Stefanich E, Widmer R, Bennett GL, Keller GA, de Sauvage FJ, Eaton D. Human platelets as a model for the binding and degradation of thrombopoietin. Blood. 1997 Apr 15;89(8):2782-8. PMID: 9108396.

- Fiore M, Saut N, Alessi MC, Viallard JF. Successful use of eltrombopag for surgical preparation in a patient with ANKRD26-related thrombocytopenia. Platelets. 2016 Dec;27(8):828-829. doi: 10.1080/09537104.2016.1190446. Epub 2016 Jun 8. PMID: 27276516.

- Food and Drug Administration (FDA) https://www.fda.gov/media/97633/download

- Fuentes R, Wang Y, Hirsch J, Wang C, Rauova L, Worthen GS, Kowalska MA, Poncz M. Infusion of mature megakaryocytes into mice yields functional platelets. J Clin Invest. 2010 Nov;120(11):3917-22. doi: 10.1172/JCI43326. Epub 2010 Oct 25. PMID: 20972336; PMCID: PMC2964983.

- Fujimoto TT, Kohata S, Suzuki H, Miyazaki H, Fujimura K. Production of functional platelets by differentiated embryonic stem (ES) cells in vitro. Blood. 2003 Dec 1;102(12):4044-51. doi: 10.1182/blood-2003-06-1773. Epub 2003 Aug 14. PMID: 12920021.

- Fukushima-Shintani M, Suzuki K, Iwatsuki Y, Abe M, Sugasawa K, Hirayama F, Kawasaki T, Nakahata T. AKR-501 (YM477) a novel orally-active thrombopoietin receptor agonist. Eur J Haematol. 2009 Apr;82(4):247-54. doi: 10.1111/j.1600-0609.2008.01198.x. Epub 2009 Jan 16. PMID: 19183407.

- Gandhi MJ, Cummings CL, Drachman JG. FLJ14813 missense mutation: a candidate for autosomal dominant thrombocytopenia on human chromosome 10. Hum Hered. 2003;55(1):66-70. doi: 10.1159/000071812. PMID: 12890928.

- Giannini EG, Greco A, Savarino V. A Review on the Use of Eltrombopag in Patients with Advanced Liver Disease. *Clinical Medicine Therapeutics*. January 2009. doi:10.4137/CMT.S2267

- González-Porras JR, Godeau B, Carpenedo M. Switching thrombopoietin receptor agonist treatments in patients with primary immune thrombocytopenia. Ther Adv Hematol. 2019 May 9;10:2040620719837906. doi: 10.1177/2040620719837906. PMID: 31156798; PMCID: PMC6515841.

- Gröpper S, Althaus K, Najm J, Haase S, Aul C, Greinacher A, Giagounidis A. A patient with Fechtner syndrome successfully treated with romiplostim. Thromb

Haemost. 2012 Mar;107(3):590-1. doi: 10.1160/TH11-07-0474. Epub 2012 Jan 25. PMID: 22273764.

- Guillemot F, Guillotin B, Fontaine A, Ali M, Catros S, Kériquel V, Fricain J-C, Rémy M, Bareille R, Amédée-Vilamitjana J (2011) Laser-assisted bioprinting to deal with tissue complexity in regenerative medicine. MRS Bull 36:1015–1019

- Gurney AL, Carver-Moore K, de Sauvage FJ, Moore MW. Thrombocytopenia in c-mpl-deficient mice. Science. 1994 Sep 2;265(5177):1445-7. doi: 10.1126/science.8073287. PMID: 8073287.

- Gurney AL, de Sauvage FJ. Dissection of c-Mpl and thrombopoietin function: studies of knockout mice and receptor signal transduction. Stem Cells. 1996;14 Suppl 1:116-23. doi: 10.1002/stem.5530140715. PMID: 11012211.

- Harrison DE, Jordan CT, Zhong RK, Astle CM. Primitive hemopoietic stem cells: direct assay of most productive populations by competitive repopulation with simple binomial, correlation and covariance calculations. Exp Hematol. 1993 Feb;21(2):206-19. PMID: 8425559.

- Hirata S, Takayama N, Jono-Ohnishi R, Endo H, Nakamura S, Dohda T, Nishi M, Hamazaki Y, Ishii E, Kaneko S, Otsu M, Nakauchi H, Kunishima S, Eto K. Congenital amegakaryocytic thrombocytopenia iPS cells exhibit defective MPL-mediated signaling. J Clin Invest. 2013 Sep;123(9):3802-14. doi: 10.1172/JCI64721. Epub 2013 Aug 1. PMID: 23908116; PMCID: PMC3754238.

- Hoffman RC, Andersen H, Walker K, Krakover JD, Patel S, Stamm MR, Osborn SG. Peptide, disulfide, and glycosylation mapping of recombinant human thrombopoietin from ser1 to Arg246. Biochemistry. 1996 Nov 26;35(47):14849-61. doi: 10.1021/bi961075b. PMID: 8942648.

- Imbach P, Crowther M. Thrombopoietin-receptor agonists for primary immune thrombocytopenia. N Engl J Med. 2011 Aug 25;365(8):734-41. doi: 10.1056/NEJMct1014202. PMID: 21864167.

- Ingavle G, Shabrani N, Vaidya A, Kale V. Mimicking megakaryopoiesis in vitro using biomaterials: Recent advances and future opportunities. Acta Biomater. 2019 Sep 15;96:99-110. doi: 10.1016/j.actbio.2019.07.025. Epub 2019 Jul 15. PMID: 31319203.

- Italiano JE Jr, Lecine P, Shivdasani RA, Hartwig JH. Blood platelets are assembled principally at the ends of proplatelet processes produced by differentiated megakaryocytes. J Cell Biol. 1999 Dec 13;147(6):1299-312. doi: 10.1083/jcb.147.6.1299. PMID: 10601342; PMCID: PMC2168104.

- Italiano JE Jr, Patel-Hett S, Hartwig JH. Mechanics of proplatelet elaboration. J Thromb Haemost. 2007 Jul;5 Suppl 1:18-23. doi: 10.1111/j.1538-7836.2007.02487.x. PMID: 17635704.

- Itkin T, Gur-Cohen S, Spencer JA, Schajnovitz A, Ramasamy SK, Kusumbe AP, Ledergor G, Jung Y, Milo I, Poulos MG, Kalinkovich A, Ludin A, Kollet O, Shakhar G, Butler JM, Rafii S, Adams RH, Scadden DT, Lin CP, Lapidot T. Distinct bone marrow blood vessels differentially regulate haematopoiesis. Nature. 2016 Apr

21;532(7599):323-8. doi: 10.1038/nature17624. Epub 2016 Apr 13. PMID: 27074509; PMCID: PMC6450701.

- Ito Y, Nakamura S, Sugimoto N, Shigemori T, Kato Y, Ohno M, Sakuma S, Ito K, Kumon H, Hirose H, Okamoto H, Nogawa M, Iwasaki M, Kihara S, Fujio K, Matsumoto T, Higashi N, Hashimoto K, Sawaguchi A, Harimoto KI, Nakagawa M, Yamamoto T, Handa M, Watanabe N, Nishi E, Arai F, Nishimura S, Eto K. Turbulence Activates Platelet Biogenesis to Enable Clinical Scale Ex Vivo Production. Cell. 2018 Jul 26;174(3):636-648.e18. doi: 10.1016/j.cell.2018.06.011. Epub 2018 Jul 12. PMID: 30017246.

- J.H. Hartwig Platelet structure A.D. Michelson (Ed.), Platelets, Academic Press, San Diego (2002), pp. 37-52

- Jiao Z, Song Y, Jin Y, Zhang C, Peng D, Chen Z, Chang P, Kundu SC, Wang G, Wang Z, Wang L. In Vivo Characterizations of the Immune Properties of Sericin: An Ancient Material with Emerging Value in Biomedical Applications. Macromol Biosci. 2017 Dec;17(12). doi: 10.1002/mabi.201700229. Epub 2017 Oct 17. PMID: 29045024.

- Junt T, Schulze H, Chen Z, Massberg S, Goerge T, Krueger A, Wagner DD, Graf T, Italiano JE Jr, Shivdasani RA, von Andrian UH. Dynamic visualization of thrombopoiesis within bone marrow. Science. 2007 Sep 21;317(5845):1767-70. doi: 10.1126/science.1146304. PMID: 17885137.

- Kanazawa S, Okada H, Hojo H, Ohba S, Iwata J, Komura M, Hikita A, Hoshi K. Mesenchymal stromal cells in the bone marrow niche consist of multi-populations with distinct transcriptional and epigenetic properties. Sci Rep. 2021 Aug 4;11(1):15811. doi: 10.1038/s41598-021-94186-5. PMID: 34349154; PMCID: PMC8338933.

- Kao YR, Chen J, Narayanagari SR, Todorova TI, Aivalioti MM, Ferreira M, Ramos PM, Pallaud C, Mantzaris I, Shastri A, Bussel JB, Verma A, Steidl U, Will B. Thrombopoietin receptor-independent stimulation of hematopoietic stem cells by eltrombopag. Sci Transl Med. 2018 Sep 12;10(458):eaas9563. doi: 10.1126/scitranslmed.aas9563. PMID: 30209246.

- Kaushansky K, Lok S, Holly RD, Broudy VC, Lin N, Bailey MC, Forstrom JW, Buddle MM, Oort PJ, Hagen FS, et al. Promotion of megakaryocyte progenitor expansion and differentiation by the c-Mpl ligand thrombopoietin. Nature. 1994 Jun 16;369(6481):568-71. doi: 10.1038/369568a0. PMID: 8202159.

- Kelley MJ, Jawien W, Ortel TL, Korczak JF. Mutation of MYH9, encoding non-muscle myosin heavy chain A, in May-Hegglin anomaly. Nat Genet. 2000 Sep;26(1):106-8. doi: 10.1038/79069. PMID: 10973260.

- Kim MJ, Park SH, Opella SJ, Marsilje TH, Michellys PY, Seidel HM, Tian SS. NMR structural studies of interactions of a small, nonpeptidyl Tpo mimic with the thrombopoietin receptor extracellular juxtamembrane and transmembrane domains. J Biol Chem. 2007 May 11;282(19):14253-61. doi: 10.1074/jbc.M611616200. Epub 2007 Mar 16. PMID: 17369254.

- Knowlton S, Anand S, Shah T, Tasoglu S. Bioprinting for Neural Tissue Engineering. Trends Neurosci. 2018 Jan;41(1):31-46. doi: 10.1016/j.tins.2017.11.001. Epub 2017 Dec 6. PMID: 29223312.

- Kumagai Y, Fujita T, Ozaki M, Sahashi K, Ohkura M, Ohtsu T, Arai Y, Sonehara Y, Nichol JL. Pharmacodynamics and pharmacokinetics of AMG 531, a thrombopoiesis-stimulating peptibody, in healthy Japanese subjects: a randomized, placebo-controlled study. J Clin Pharmacol. 2007 Dec;47(12):1489-97. doi: 10.1177/0091270007306563. Epub 2007 Oct 9. PMID: 17925591.

- Kunisaki Y, Bruns I, Scheiermann C, Ahmed J, Pinho S, Zhang D, Mizoguchi T, Wei Q, Lucas D, Ito K, Mar JC, Bergman A, Frenette PS. Arteriolar niches maintain haematopoietic stem cell quiescence. Nature. 2013 Oct 31;502(7473):637-43. doi: 10.1038/nature12612. Epub 2013 Oct 9. PMID: 24107994; PMCID: PMC3821873.

- Kuter DJ, Bussel JB, Lyons RM, Pullarkat V, Gernsheimer TB, Senecal FM, Aledort LM, George JN, Kessler CM, Sanz MA, Liebman HA, Slovick FT, de Wolf JT, Bourgeois E, Guthrie TH Jr, Newland A, Wasser JS, Hamburg SI, Grande C, Lefrère F, Lichtin AE, Tarantino MD, Terebelo HR, Viallard JF, Cuevas FJ, Go RS, Henry DH, Redner RL, Rice L, Schipperus MR, Guo DM, Nichol JL. Efficacy of romiplostim in patients with chronic immune thrombocytopenic purpura: a double-blind randomised controlled trial. Lancet. 2008 Feb 2;371(9610):395-403. doi: 10.1016/S0140-6736(08)60203-2. PMID: 18242413.

- Kuter DJ, Gernsheimer TB. Thrombopoietin and platelet production in chronic immune thrombocytopenia. Hematol Oncol Clin North Am. 2009 Dec;23(6):1193-211. doi: 10.1016/j.hoc.2009.09.001. PMID: 19932428; PMCID: PMC2789970.

- Kuter DJ, Rummel M, Boccia R, Macik BG, Pabinger I, Selleslag D, Rodeghiero F, Chong BH, Wang X, Berger DP. Romiplostim or standard of care in patients with immune thrombocytopenia. N Engl J Med. 2010 Nov 11;363(20):1889-99. doi: 10.1056/NEJMoa1002625. PMID: 21067381.

- Kuter DJ, Tarantino MD, Lawrence T. Clinical overview and practical considerations for optimizing romiplostim therapy in patients with immune thrombocytopenia. Blood Rev. 2021 Sep;49:100811. doi: 10.1016/j.blre.2021.100811. Epub 2021 Feb 27. PMID: 33781612.

- Kuter DJ. New thrombopoietic growth factors. Blood. 2007 Jun 1;109(11):4607-16. doi: 10.1182/blood-2006-10-019315. Epub 2007 Feb 8. PMID: 17289815; PMCID: PMC1885525.

- Kuter DJ. The biology of thrombopoietin and thrombopoietin receptor agonists. Int J Hematol. 2013 Jul;98(1):10-23. doi: 10.1007/s12185-013-1382-0. Epub 2013 Jul 3. PMID: 23821332.

- Lasky LC, Sullenbarger B. Manipulation of oxygenation and flow-induced shear stress can increase the in vitro yield of platelets from cord blood. Tissue Eng Part C Methods. 2011 Nov;17(11):1081-8. doi: 10.1089/ten.tec.2011.0108. Epub 2011 Aug 30. PMID: 21877917.

- Lee EJ, Godara P, Haylock D. Biomanufacture of human platelets for transfusion: Rationale and approaches. Exp Hematol. 2014 May;42(5):332-46. doi: 10.1016/j.exphem.2014.02.002. Epub 2014 Mar 22. PMID: 24667682.

- Lee KH, Kwon GH, Shin SJ, Baek JY, Han DK, Park Y, Lee SH. Hydrophilic electrospun polyurethane nanofiber matrices for hMSC culture in a microfluidic cell chip. J Biomed Mater Res A. 2009 Aug;90(2):619-28. doi: 10.1002/jbm.a.32059. PMID: 18546183.

- Lefrançais E, Ortiz-Muñoz G, Caudrillier A, Mallavia B, Liu F, Sayah DM, Thornton EE, Headley MB, David T, Coughlin SR, Krummel MF, Leavitt AD, Passegué E, Looney MR. The lung is a site of platelet biogenesis and a reservoir for haematopoietic progenitors. Nature. 2017 Apr 6;544(7648):105-109. doi: 10.1038/nature21706. Epub 2017 Mar 22. PMID: 28329764; PMCID: PMC5663284.

- Li J, Xia Y, Kuter DJ. Interaction of thrombopoietin with the platelet c-mpl receptor in plasma: binding, internalization, stability and pharmacokinetics. Br J Haematol. 1999 Aug;106(2):345-56. doi: 10.1046/j.1365-2141.1999.01571.x. PMID: 10460590.

- Li Z, Delaney MK, O'Brien KA, Du X. Signaling during platelet adhesion and activation. Arterioscler Thromb Vasc Biol. 2010 Dec;30(12):2341-9. doi: 10.1161/ATVBAHA.110.207522. Epub 2010 Nov 11. PMID: 21071698; PMCID: PMC3085271.

- Linden MD, Furman MI, Frelinger AL 3rd, Fox ML, Barnard MR, Li Y, Przyklenk K, Michelson AD. Indices of platelet activation and the stability of coronary artery disease. J Thromb Haemost. 2007 Apr;5(4):761-5. doi: 10.1111/j.1538-7836.2007.02462.x. Epub 2007 Feb 26. PMID: 17371489.

- Liu C, Wu D, Xia M, Li M, Sun Z, Shen B, Liu Y, Jiang E, Wang H, Su P, Shi L, Xiao Z, Zhu X, Zhou W, Wang Q, Gao X, Cheng T, Zhou J. Characterization of Cellular Heterogeneity and an Immune Subpopulation of Human Megakaryocytes. Adv Sci (Weinh). 2021 Aug;8(15):e2100921. doi: 10.1002/advs.202100921. Epub 2021 May 26. PMID: 34042332; PMCID: PMC8336508.

- Liu XF, Bera TK, Liu LJ, Pastan I. A primate-specific POTE-actin fusion protein plays a role in apoptosis. Apoptosis. 2009 Oct;14(10):1237-44. doi: 10.1007/s10495-009-0392-0. PMID: 19669888; PMCID: PMC7285894.

- Lo Celso C, Scadden DT. The haematopoietic stem cell niche at a glance. J Cell Sci. 2011 Nov 1;124(Pt 21):3529-35. doi: 10.1242/jcs.074112. PMID: 22083139; PMCID: PMC3215569.

- Lovett M, Cannizzaro C, Daheron L, Messmer B, Vunjak-Novakovic G, Kaplan DL. Silk fibroin microtubes for blood vessel engineering. Biomaterials. 2007 Dec;28(35):5271-9. doi: 10.1016/j.biomaterials.2007.08.008. Epub 2007 Aug 28. PMID: 17727944; PMCID: PMC2695960.

- Lu SJ, Li F, Yin H, Feng Q, Kimbrel EA, Hahm E, Thon JN, Wang W, Italiano JE, Cho J, Lanza R. Platelets generated from human embryonic stem cells are functional in vitro and in the microcirculation of living mice. Cell Res. 2011 Mar;21(3):530-45. doi: 10.1038/cr.2011.8. Epub 2011 Jan 11. PMID: 21221130; PMCID: PMC3193430.

- Luengo JI, Duffy KJ, Shaw AN, Delorme E, Wiggall KJ, Giampa L, Liu N, Smith H, Tian S, Miller SG, Keenan RM, Rosen J, Dillon SB, Lamb P, Erickson-Miller CL;

Discovery of SB-497115, a Small-Molecule Thrombopoietin (TPO) Receptor Agonist for the Treatment of Thrombocytopenia.. *Blood* 2004; 104 (11): 2910.

- Luoh SM, Stefanich E, Solar G, et al. Role of the distal half of the c-Mpl intracellular domain in control of platelet production by thrombopoietin in vivo. Molecular and Cellular Biology. 2000 Jan;20(2):507-515. DOI: 10.1128/mcb.20.2.507-515.2000. PMID: 10611229; PMCID: PMC85116.

- Macaulay IC, Tijssen MR, Thijssen-Timmer DC, Gusnanto A, Steward M, Burns P, Langford CF, Ellis PD, Dudbridge F, Zwaginga JJ, Watkins NA, van der Schoot CE, Ouwehand WH. Comparative gene expression profiling of in vitro differentiated megakaryocytes and erythroblasts identifies novel activatory and inhibitory platelet membrane proteins. Blood. 2007 Apr 15;109(8):3260-9. doi: 10.1182/blood-2006-07-036269. Epub 2006 Dec 27. PMID: 17192395; PMCID: PMC6485507.

- Makar RS, Zhukov OS, Sahud MA, Kuter DJ. Thrombopoietin levels in patients with disorders of platelet production: diagnostic potential and utility in predicting response to TPO receptor agonists. Am J Hematol. 2013 Dec;88(12):1041-4. doi: 10.1002/ajh.23562. Epub 2013 Sep 12. PMID: 23913253.

- Malara A, Gruppi C, Rebuzzini P, Visai L, Perotti C, Moratti R, Balduini C, Tira ME, Balduini A. Megakaryocyte-matrix interaction within bone marrow: new roles for fibronectin and factor XIII-A. Blood. 2011 Feb 24;117(8):2476-83. doi: 10.1182/blood-2010-06-288795. Epub 2010 Dec 3. PMID: 21131589.

- Marconi C, Canobbio I, Bozzi V, Pippucci T, Simonetti G, Melazzini F, Angori S, Martinelli G, Saglio G, Torti M, Pastan I, Seri M, Pecci A. 5'UTR point substitutions and N-terminal truncating mutations of ANKRD26 in acute myeloid leukemia. J Hematol Oncol. 2017 Jan 18;10(1):18. doi: 10.1186/s13045-016-0382-y. PMID: 28100250; PMCID: PMC5242010.

- Martinez A, McMahon R, Jenkins K, Miller WM; Using Computational Fluid Dynamics (CFD) to Enhance Ex Vivo Platelet Production Via Shear Forces within Microfluidic Bioreactors. Blood 2016; 128 (22)

- Mazharian A, Mori J, Wang YJ, Heising S, Neel BG, Watson SP, Senis YA. Megakaryocyte-specific deletion of the protein-tyrosine phosphatases Shp1 and Shp2 causes abnormal megakaryocyte development, platelet production, and function. Blood. 2013 May 16;121(20):4205-20. doi: 10.1182/blood-2012-08-449272. Epub 2013 Mar 18. PMID: 23509158; PMCID: PMC3656453.

- McHutchison JG, Dusheiko G, Shiffman ML, Rodriguez-Torres M, Sigal S, Bourliere M, Berg T, Gordon SC, Campbell FM, Theodore D, Blackman N, Jenkins J, Afdhal NH; TPL102357 Study Group. Eltrombopag for thrombocytopenia in patients with cirrhosis associated with hepatitis C. N Engl J Med. 2007 Nov 29;357(22):2227-36. doi: 10.1056/NEJMoa073255. PMID: 18046027.

- Meinel L, Karageorgiou V, Fajardo R, Snyder B, Shinde-Patil V, Zichner L, Kaplan D, Langer R, Vunjak-Novakovic G. Bone tissue engineering using human mesenchymal stem cells: effects of scaffold material and medium flow. Ann Biomed Eng. 2004 Jan;32(1):112-22. doi: 10.1023/b:abme.0000007796.48329.b4. PMID: 14964727.

- Moreau T, Evans AL, Vasquez L, Tijssen MR, Yan Y, Trotter MW, Howard D, Colzani M, Arumugam M, Wu WH, Dalby A, Lampela R, Bouet G, Hobbs CM, Pask DC, Payne H, Ponomaryov T, Brill A, Soranzo N, Ouwehand WH, Pedersen RA, Ghevaert C. Large-scale production of megakaryocytes from human pluripotent stem cells by chemically defined forward programming. Nat Commun. 2016 Apr 7;7:11208. doi: 10.1038/ncomms11208. Erratum in: Nat Commun. 2017 Jul 28;8:15076. PMID: 27052461; PMCID: PMC4829662.

- Mostafa SS, Miller WM, Papoutsakis ET. Oxygen tension influences the differentiation, maturation and apoptosis of human megakaryocytes. Br J Haematol. 2000 Dec;111(3):879-89. PMID: 11122151.

- Musunuru K. Genome editing of human pluripotent stem cells to generate human cellular disease models. Dis Model Mech. 2013 Jul;6(4):896-904. doi: 10.1242/dmm.012054. Epub 2013 Jun 10. PMID: 23751357; PMCID: PMC3701209.

- Nakamura S, Takayama N, Hirata S, Seo H, Endo H, Ochi K, Fujita K, Koike T, Harimoto K, Dohda T, Watanabe A, Okita K, Takahashi N, Sawaguchi A, Yamanaka S, Nakauchi H, Nishimura S, Eto K. Expandable megakaryocyte cell lines enable clinically applicable generation of platelets from human induced pluripotent stem cells. Cell Stem Cell. 2014 Apr 3;14(4):535-48. doi: 10.1016/j.stem.2014.01.011. Epub 2014 Feb 13. PMID: 24529595.

- Nakamura-Ishizu A, Matsumura T, Stumpf PS, Umemoto T, Takizawa H, Takihara Y, O'Neil A, Majeed ABBA, MacArthur BD, Suda T. Thrombopoietin Metabolically Primes Hematopoietic Stem Cells to Megakaryocyte-Lineage Differentiation. Cell Rep. 2018 Nov 13;25(7):1772-1785.e6. doi: 10.1016/j.celrep.2018.10.059. PMID: 30428347.

- Necchi V, Balduini A, Noris P, Barozzi S, Sommi P, di Buduo C, Balduini CL, Solcia E, Pecci A. Ubiquitin/proteasome-rich particulate cytoplasmic structures (PaCSs) in the platelets and megakaryocytes of ANKRD26-related thrombo-cytopenia. Thromb Haemost. 2013 Feb;109(2):263-71. doi: 10.1160/TH12-07-0497. Epub 2012 Dec 6. PMID: 23223974.

- Nelson MR , Roy K . Bone-marrow mimicking biomaterial niches for studying hematopoietic stem and progenitor cells. J Mater Chem B. 2016 May 28;4(20):3490-3503. doi: 10.1039/c5tb02644j. Epub 2016 Apr 15. PMID: 32263382.

- Newland A, Caulier MT, Kappers-Klunne M, Schipperus MR, Lefrere F, Zwaginga JJ, Christal J, Chen CF, Nichol JL. An open-label, unit dose-finding study of AMG 531, a novel thrombopoiesis-stimulating peptibody, in patients with immune thrombocytopenic purpura. Br J Haematol. 2006 Nov;135(4):547-53. doi: 10.1111/j.1365-2141.2006.06339.x. PMID: 17061981.

- Nilsson SK, Debatis ME, Dooner MS, Madri JA, Quesenberry PJ, Becker PS. Immunofluorescence characterization of key extracellular matrix proteins in murine bone marrow in situ. J Histochem Cytochem. 1998 Mar;46(3):371-7. doi: 10.1177/002215549804600311. PMID: 9487119.

- Noris P, Favier R, Alessi MC, Geddis AE, Kunishima S, Heller PG, Giordano P, Niederhoffer KY, Bussel JB, Podda GM, Vianelli N, Kersseboom R, Pecci A, Gnan C, Marconi C, Auvrignon A, Cohen W, Yu JC, Iguchi A, Miller Imahiyerobo A, Boehlen F, Ghalloussi D, De Rocco D, Magini P, Civaschi E, Biino G, Seri M, Savoia A, Balduini CL. ANKRD26-related thrombocytopenia and myeloid malignancies. Blood. 2013 Sep 12;122(11):1987-9. doi: 10.1182/blood-2013-04-499319. PMID: 24030261.

- Noris P, Pecci A. Hereditary thrombocytopenias: a growing list of disorders. Hematology Am Soc Hematol Educ Program. 2017 Dec 8;2017(1):385-399. doi: 10.1182/asheducation-2017.1.385. PMID: 29222283; PMCID: PMC6142591.

- Noris P, Perrotta S, Seri M, Pecci A, Gnan C, Loffredo G, Pujol-Moix N, Zecca M, Scognamiglio F, De Rocco D, Punzo F, Melazzini F, Scianguetta S, Casale M, Marconi C, Pippucci T, Amendola G, Notarangelo LD, Klersy C, Civaschi E, Balduini CL, Savoia A. Mutations in ANKRD26 are responsible for a frequent form of inherited thrombocytopenia: analysis of 78 patients from 21 families. Blood. 2011 Jun 16;117(24):6673-80. doi: 10.1182/blood-2011-02-336537. Epub 2011 Apr 5. PMID: 21467542.

- Nurden AT, Nurden P. Inherited thrombocytopenias: history, advances and perspectives. Haematologica. 2020 Aug;105(8):2004-2019. doi: 10.3324/haematol.2019.233197. Epub 2020 Jun 11. PMID: 32527953; PMCID: PMC7395261.

- Olnes MJ, Scheinberg P, Calvo KR, Desmond R, Tang Y, Dumitriu B, Parikh AR, Soto S, Biancotto A, Feng X, Lozier J, Wu CO, Young NS, Dunbar CE. Eltrombopag and improved hematopoiesis in refractory aplastic anemia. N Engl J Med. 2012 Jul 5;367(1):11-9. doi: 10.1056/NEJMoa1200931. Erratum in: N Engl J Med. 2012 Jul 19;367(3):284. PMID: 22762314; PMCID: PMC3422737.

- Omenetto FG, Kaplan DL. New opportunities for an ancient material. Science. 2010 Jul 30;329(5991):528-31. doi: 10.1126/science.1188936. PMID: 20671180; PMCID: PMC3136811.

- Pal K, Nowak R, Billington N, Liu R, Ghosh A, Sellers JR, Fowler VM. Megakaryocyte migration defects due to nonmuscle myosin IIA mutations underlie thrombocytopenia in MYH9-related disease. Blood. 2020 May 21;135(21):1887-1898. doi: 10.1182/blood.2019003064. Erratum in: Blood. 2020 Aug 6;136(6):771. PMID: 32315395; PMCID: PMC7243143.

- Pallotta I, Lovett M, Kaplan DL, Balduini A. Three-dimensional system for the in vitro study of megakaryocytes and functional platelet production using silk-based vascular tubes. Tissue Eng Part C Methods. 2011 Dec;17(12):1223-32. doi: 10.1089/ten.tec.2011.0134. Epub 2011 Sep 6. PMID: 21895494; PMCID: PMC3226422.

- Panilaitis B, Altman GH, Chen J, Jin HJ, Karageorgiou V, Kaplan DL. Macrophage responses to silk. Biomaterials. 2003 Aug;24(18):3079-85. doi: 10.1016/s0142-9612(03)00158-3. PMID: 12895580.

- Park IH, Arora N, Huo H, Maherali N, Ahfeldt T, Shimamura A, Lensch MW, Cowan C, Hochedlinger K, Daley GQ. Disease-specific induced pluripotent stem cells. Cell.

2008 Sep 5;134(5):877-86. doi: 10.1016/j.cell.2008.07.041. Epub 2008 Aug 7. PMID: 18691744; PMCID: PMC2633781.

- Patel SR, Hartwig JH, Italiano JE Jr. The biogenesis of platelets from megakaryocyte proplatelets. J Clin Invest. 2005 Dec;115(12):3348-54. doi: 10.1172/JCI26891. PMID: 16322779; PMCID: PMC1297261.

- Pecci A, Balduini CL. Inherited thrombocytopenias: an updated guide for clinicians. Blood Rev. 2021 Jul;48:100784. doi: 10.1016/j.blre.2020.100784. Epub 2020 Dec 1. PMID: 33317862.

- Pecci A, Gresele P, Klersy C, Savoia A, Noris P, Fierro T, Bozzi V, Mezzasoma AM, Melazzini F, Balduini CL. Eltrombopag for the treatment of the inherited thrombocytopenia deriving from MYH9 mutations. Blood. 2010 Dec 23;116(26):5832-7. doi: 10.1182/blood-2010-08-304725. Epub 2010 Sep 15. PMID: 20844233.

- Pecci A, Ma X, Savoia A, Adelstein RS. MYH9: Structure, functions and role of non-muscle myosin IIA in human disease. Gene. 2018 Jul 20;664:152-167. doi: 10.1016/j.gene.2018.04.048. Epub 2018 Apr 19. PMID: 29679756; PMCID: PMC5970098.

- Pecci A, Malara A, Badalucco S, Bozzi V, Torti M, Balduini CL, Balduini A. Megakaryocytes of patients with MYH9-related thrombocytopenia present an altered proplatelet formation. Thromb Haemost. 2009 Jul;102(1):90-6. doi: 10.1160/TH09-01-0068. PMID: 19572073.

- Pertuy F, Eckly A, Weber J, Proamer F, Rinckel JY, Lanza F, Gachet C, Léon C. Myosin IIA is critical for organelle distribution and F-actin organization in megakaryocytes and platelets. Blood. 2014 Feb 20;123(8):1261-9. doi: 10.1182/blood-2013-06-508168. Epub 2013 Nov 15. PMID: 24243973.

- Pippucci T, Savoia A, Perrotta S, Pujol-Moix N, Noris P, Castegnaro G, Pecci A, Gnan C, Punzo F, Marconi C, Gherardi S, Loffredo G, De Rocco D, Scianguetta S, Barozzi S, Magini P, Bozzi V, Dezzani L, Di Stazio M, Ferraro M, Perini G, Seri M, Balduini CL. Mutations in the 5' UTR of ANKRD26, the ankirin repeat domain 26 gene, cause an autosomal-dominant form of inherited thrombocytopenia, THC2. Am J Hum Genet. 2011 Jan 7;88(1):115-20. doi: 10.1016/j.ajhg.2010.12.006. PMID: 21211618; PMCID: PMC3014357.

- Porcelijn L, Folman CC, Bossers B, Huiskes E, Overbeeke MA, v d Schoot CE, de Haas M, von dem Borne AE. The diagnostic value of thrombopoietin level measurements in thrombocytopenia. Thromb Haemost. 1998 Jun;79(6):1101-5. PMID: 9657431.

- Provan D., Saleh M, Goodison S., Rafi R. Stone N., Hamilton JM, Hassani H, Mayer B, Uhl J, Jenkins J. The safety profile of eltrombopag, a novel oral platelet growth factor, in thrombocytopenic patients and healthy subjects. Journal of Clinical Oncology 2006 24:18_suppl, 18596-18596

- Punzo F, Mientjes EJ, Rohe CF, Scianguetta S, Amendola G, Oostra BA, Bertoli-Avella AM, Perrotta S. A mutation in the acyl-coenzyme A binding domain-containing protein 5 gene (ACBD5) identified in autosomal dominant

thrombocytopenia. J Thromb Haemost. 2010 Sep;8(9):2085-7. doi: 10.1111/j.1538-7836.2010.03979.x. PMID: 20626622.

- Qian H, Buza-Vidas N, Hyland CD, Jensen CT, Antonchuk J, Månsson R, Thoren LA, Ekblom M, Alexander WS, Jacobsen SE. Critical role of thrombopoietin in maintaining adult quiescent hematopoietic stem cells. Cell Stem Cell. 2007 Dec 13;1(6):671-84. doi: 10.1016/j.stem.2007.10.008. Epub 2007 Nov 20. PMID: 18371408.

- Raciti GA, Bera TK, Gavrilova O, Pastan I. Partial inactivation of Ankrd26 causes diabetes with enhanced insulin responsiveness of adipose tissue in mice. Diabetologia. 2011 Nov;54(11):2911-22. doi: 10.1007/s00125-011-2263-9. Epub 2011 Aug 13. PMID: 21842266; PMCID: PMC3881194.

- Radley JM, Scurfield G. The mechanism of platelet release. Blood. 1980 Dec;56(6):996-9. PMID: 7437520.

- Rockwood DN, Preda RC, Yücel T, Wang X, Lovett ML, Kaplan DL. Materials fabrication from Bombyx mori silk fibroin. Nat Protoc. 2011 Sep 22;6(10):1612-31. doi: 10.1038/nprot.2011.379. PMID: 21959241; PMCID: PMC3808976.

- Rodeghiero F, Pecci A, Balduini CL. Thrombopoietin receptor agonists in hereditary thrombocytopenias. J Thromb Haemost. 2018 Sep;16(9):1700-1710. doi: 10.1111/jth.14217. Epub 2018 Jul 27. PMID: 29956472.
- Roth M, Will B, Simkin G, Narayanagari S, Barreyro L, Bartholdy B, Tamari R, Mitsiades CS, Verma A, Steidl U. Eltrombopag inhibits the proliferation of leukemia cells via reduction of intracellular iron and induction of differentiation. Blood. 2012 Jul 12;120(2):386-94. doi: 10.1182/blood-2011-12-399667. Epub 2012 May 24. PMID: 22627766; PMCID: PMC3398759.

- Sakabe H., Ito H., Miyamoto T., Noishiki Y., Ha W.S. In vivo blood compatibility of regenerated silk fibroin. Sen'i Gakkaishi. 1989;45:487–490. doi: 10.2115/fiber.45.11_487.

- Sanjuan-Pla A, Macaulay IC, Jensen CT, Woll PS, Luis TC, Mead A, Moore S, Carella C, Matsuoka S, Bouriez Jones T, Chowdhury O, Stenson L, Lutteropp M, Green JC, Facchini R, Boukarabila H, Grover A, Gambardella A, Thongjuea S, Carrelha J, Tarrant P, Atkinson D, Clark SA, Nerlov C, Jacobsen SE. Platelet-biased stem cells reside at the apex of the haematopoietic stem-cell hierarchy. Nature. 2013 Oct 10;502(7470):232-6. doi: 10.1038/nature12495. Epub 2013 Aug 11. PMID: 23934107.

- Santin M, Motta A, Freddi G, Cannas M. In vitro evaluation of the inflammatory potential of the silk fibroin. J Biomed Mater Res. 1999 Sep 5;46(3):382-9. doi: 10.1002/(sici)1097-4636(19990905)46:3<382::aid-jbm11>3.0.co;2-r. PMID: 10397996.

- Schofield R. The relationship between the spleen colony-forming cell and the haemopoietic stem cell. Blood Cells. 1978;4(1-2):7-25. PMID: 747780.

- Schulze H, Korpal M, Hurov J, Kim SW, Zhang J, Cantley LC, Graf T, Shivdasani RA. Characterization of the megakaryocyte demarcation membrane system and its

role in thrombopoiesis. Blood. 2006 May 15;107(10):3868-75. doi: 10.1182/blood-2005-07-2755. Epub 2006 Jan 24. PMID: 16434494; PMCID: PMC1895279.

- Sellers T, Hart T, Semanik M, Murthy K; Pharmacology and Safety of SB-497115-GR, an Orally Active Small Molecular Weight TPO Receptor Agonist, in Chimpanzees, Rats and Dogs.. *Blood* 2004; 104 (11): 2063.

- Seri M, Pecci A, Di Bari F, Cusano R, Savino M, Panza E, Nigro A, Noris P, Gangarossa S, Rocca B, Gresele P, Bizzaro N, Malatesta P, Koivisto PA, Longo I, Musso R, Pecoraro C, Iolascon A, Magrini U, Rodriguez Soriano J, Renieri A, Ghiggeri GM, Ravazzolo R, Balduini CL, Savoia A. MYH9-related disease: May-Hegglin anomaly, Sebastian syndrome, Fechtner syndrome, and Epstein syndrome are not distinct entities but represent a variable expression of a single illness. Medicine (Baltimore). 2003 May;82(3):203-15. doi: 10.1097/01.md.0000076006.64510.5c. PMID: 12792306.

- Shin JW, Buxboim A, Spinler KR, Swift J, Christian DA, Hunter CA, Léon C, Gachet C, Dingal PC, Ivanovska IL, Rehfeldt F, Chasis JA, Discher DE. Contractile forces sustain and polarize hematopoiesis from stem and progenitor cells. Cell Stem Cell. 2014 Jan 2;14(1):81-93. doi: 10.1016/j.stem.2013.10.009. Epub 2013 Nov 21. PMID: 24268694; PMCID: PMC3969018.

- Shin JY, Hu W, Naramura M, Park CY. High c-Kit expression identifies hematopoietic stem cells with impaired self-renewal and megakaryocytic bias. J Exp Med. 2014 Feb 10;211(2):217-31. doi: 10.1084/jem.20131128. Epub 2014 Jan 20. PMID: 24446491; PMCID: PMC3920569.

- Shiozawa Y, Havens AM, Pienta KJ, Taichman RS. The bone marrow niche: habitat to hematopoietic and mesenchymal stem cells, and unwitting host to molecular parasites. Leukemia. 2008 May;22(5):941-50. doi: 10.1038/leu.2008.48. Epub 2008 Feb 28. PMID: 18305549; PMCID: PMC5944299.

- Sofia S, McCarthy MB, Gronowicz G, Kaplan DL. Functionalized silk-based biomaterials for bone formation. J Biomed Mater Res. 2001 Jan;54(1):139-48. doi: 10.1002/1097-4636(200101)54:1<139::aid-jbm17>3.0.co;2-7. PMID: 11077413.

- Soong HK, Kenyon KR. Adverse reactions to virgin silk sutures in cataract surgery. Ophthalmology. 1984 May;91(5):479-83. doi: 10.1016/s0161-6420(84)34273-7. PMID: 6377167.

- Staubitz JI, Musholt TJ, Schad A, Springer E, Lang H, Rajalingam K, Roth W, Hartmann N. ANKRD26-RET - A novel gene fusion involving RET in papillary thyroid carcinoma. Cancer Genet. 2019 Oct;238:10-17. doi: 10.1016/j.cancergen.2019.07.002. Epub 2019 Jul 5. PMID: 31425920.

- Stegner D, Nieswandt B. Platelet receptor signaling in thrombus formation. J Mol Med (Berl). 2011 Feb;89(2):109-21. doi: 10.1007/s00109-010-0691-5. Epub 2010 Nov 7. PMID: 21058007.

- Stegner D, vanEeuwijk JMM, Angay O, Gorelashvili MG, Semeniak D, Pinnecker J, Schmithausen P, Meyer I, Friedrich M, Dütting S, Brede C, Beilhack A, Schulze H, Nieswandt B, Heinze KG. Thrombopoiesis is spatially regulated by the bone marrow vasculature. Nat Commun. 2017 Jul 25;8(1):127. doi: 10.1038/s41467-017-00201-7. PMID: 28743899; PMCID: PMC5527048.

- Suki B, Bates JH. Extracellular matrix mechanics in lung parenchymal diseases. Respir Physiol Neurobiol. 2008 Nov 30;163(1-3):33-43. doi: 10.1016/j.resp.2008.03.015. Epub 2008 Apr 8. PMID: 18485836; PMCID: PMC2666313.

- Sullenbarger B, Bahng JH, Gruner R, Kotov N, Lasky LC. Prolonged continuous in vitro human platelet production using three-dimensional scaffolds. Exp Hematol. 2009 Jan;37(1):101-10. doi: 10.1016/j.exphem.2008.09.009. Epub 2008 Nov 13. PMID: 19013002; PMCID: PMC2676426.

- Sun S, Jin C, Si J, Lei Y, Chen K, Cui Y, Liu Z, Liu J, Zhao M, Zhang X, Tang F, Rondina MT, Li Y, Wang QF. Single-cell analysis of ploidy and the transcriptome reveals functional and spatial divergency in murine megakaryopoiesis. Blood. 2021 Oct 7;138(14):1211-1224. doi: 10.1182/blood.2021010697. PMID: 34115843; PMCID: PMC8499048.

- Suzuki A, Shin JW, Wang Y, Min SH, Poncz M, Choi JK, Discher DE, Carpenter CL, Lian L, Zhao L, Wang Y, Abrams CS. RhoA is essential for maintaining normal megakaryocyte ploidy and platelet generation. PLoS One. 2013 Jul 23;8(7):e69315. doi: 10.1371/journal.pone.0069315. PMID: 23935982; PMCID: PMC3720647.

- Takahashi K, Yamanaka S. Induction of pluripotent stem cells from mouse embryonic and adult fibroblast cultures by defined factors. Cell. 2006 Aug 25;126(4):663-76. doi: 10.1016/j.cell.2006.07.024. Epub 2006 Aug 10. PMID: 16904174.

- Takayama N, Nishimura S, Nakamura S, Shimizu T, Ohnishi R, Endo H, Yamaguchi T, Otsu M, Nishimura K, Nakanishi M, Sawaguchi A, Nagai R, Takahashi K, Yamanaka S, Nakauchi H, Eto K. Transient activation of c-MYC expression is critical for efficient platelet generation from human induced pluripotent stem cells. J Exp Med. 2010 Dec 20;207(13):2817-30. doi: 10.1084/jem.20100844. Epub 2010 Nov 22. PMID: 21098095; PMCID: PMC3005234.

- Takayama N, Nishikii H, Usui J, Tsukui H, Sawaguchi A, Hiroyama T, Eto K, Nakauchi H. Generation of functional platelets from human embryonic stem cells in vitro via ES-sacs, VEGF-promoted structures that concentrate hematopoietic progenitors. Blood. 2008 Jun 1;111(11):5298-306. doi: 10.1182/blood-2007-10-117622. Epub 2008 Apr 3. PMID: 18388179.

- Thon JN, Mazutis L, Wu S, Sylman JL, Ehrlicher A, Machlus KR, Feng Q, Lu S, Lanza R, Neeves KB, Weitz DA, Italiano JE Jr. Platelet bioreactor-on-a-chip. Blood. 2014 Sep 18;124(12):1857-67. doi: 10.1182/blood-2014-05-574913. PMID: 25606631; PMCID: PMC4168343.

- Torisawa YS, Spina CS, Mammoto T, Mammoto A, Weaver JC, Tat T, Collins JJ, Ingber DE. Bone marrow-on-a-chip replicates hematopoietic niche physiology in vitro. Nat Methods. 2014 Jun;11(6):663-9. doi: 10.1038/nmeth.2938. Epub 2014 May 4. PMID: 24793454.

- Tozzi L, Laurent PA, Di Buduo CA, Mu X, Massaro A, Bretherton R, Stoppel W, Kaplan DL, Balduini A. Multi-channel silk sponge mimicking bone marrow vascular niche for platelet production. Biomaterials. 2018 Sep;178:122-133. doi:

10.1016/j.biomaterials.2018.06.018. Epub 2018 Jun 17. PMID: 29920404; PMCID: PMC6082392.

- Triana S, Vonficht D, Jopp-Saile L, Raffel S, Lutz R, Leonce D, Antes M, Hernández-Malmierca P, Ordoñez-Rueda D, Ramasz B, Boch T, Jann JC, Nowak D, Hofmann WK, Müller-Tidow C, Hübschmann D, Alexandrov T, Benes V, Trumpp A, Paulsen M, Velten L, Haas S. Single-cell proteo-genomic reference maps of the hematopoietic system enable the purification and massive profiling of precisely defined cell states. Nat Immunol. 2021 Dec;22(12):1577-1589. doi: 10.1038/s41590-021-01059-0. Epub 2021 Nov 22. PMID: 34811546; PMCID: PMC8642243.

- Vepari C, Kaplan DL. Silk as a Biomaterial. Prog Polym Sci. 2007;32(8-9):991-1007. doi: 10.1016/j.progpolymsci.2007.05.013. PMID: 19543442; PMCID: PMC2699289.

- Vicente A, Patel BA, Gutierrez-Rodrigues F, Groarke E, Giudice V, Lotter J, Feng X, Kajigaya S, Weinstein B, Barranta E, Olnes MJ, Parikh AR, Albitar M, Wu CO, Shalhoub R, Calvo KR, Townsley DM, Scheinberg P, Dunbar CE, Young NS, Winkler T. Eltrombopag monotherapy can improve hematopoiesis in patients with low to intermediate risk-1 myelodysplastic syndrome. Haematologica. 2020 Dec 1;105(12):2785-2794. doi: 10.3324/haematol.2020.249995. PMID: 33256377; PMCID: PMC7716353.

- Vigon I, Mornon JP, Cocault L, Mitjavila MT, Tambourin P, Gisselbrecht S, Souyri M. Molecular cloning and characterization of MPL, the human homolog of the v-mpl oncogene: identification of a member of the hematopoietic growth factor receptor superfamily. Proc Natl Acad Sci U S A. 1992 Jun 15;89(12):5640-4. doi: 10.1073/pnas.89.12.5640. PMID: 1608974; PMCID: PMC49348.

- Vijayavenkataraman S, Yan WC, Lu WF, Wang CH, Fuh JYH. 3D bioprinting of tissues and organs for regenerative medicine. Adv Drug Deliv Rev. 2018 Jul;132:296-332. doi: 10.1016/j.addr.2018.07.004. Epub 2018 Jul 7. PMID: 29990578.

- Walker G, Beebe DJ. A passive pumping method for microfluidic devices. Lab Chip. 2002 Aug;2(3):131-4. doi: 10.1039/b204381e. Epub 2002 Aug 5. PMID: 15100822.

- Wang B, Nichol JL, Sullivan JT. Pharmacodynamics and pharmacokinetics of AMG 531, a novel thrombopoietin receptor ligand. Clin Pharmacol Ther. 2004 Dec;76(6):628-38. doi: 10.1016/j.clpt.2004.08.010. PMID: 15592334.

- Wang H, He J, Xu C, Chen X, Yang H, Shi S, Liu C, Zeng Y, Wu D, Bai Z, Wang M, Wen Y, Su P, Xia M, Huang B, Ma C, Bian L, Lan Y, Cheng T, Shi L, Liu B, Zhou J. Decoding Human Megakaryocyte Development. Cell Stem Cell. 2021 Mar 4;28(3):535-549.e8. doi: 10.1016/j.stem.2020.11.006. Epub 2020 Dec 18. PMID: 33340451.

- White ES. Lung extracellular matrix and fibroblast function. Ann Am Thorac Soc. 2015 Mar;12 Suppl 1(Suppl 1):S30-3. doi: 10.1513/AnnalsATS.201406-240MG. PMID: 25830832; PMCID: PMC4430981.

- Winkler IG, Barbier V, Nowlan B, Jacobsen RN, Forristal CE, Patton JT, Magnani JL, Lévesque JP. Vascular niche E-selectin regulates hematopoietic stem cell

dormancy, self renewal and chemoresistance. Nat Med. 2012 Nov;18(11):1651-7. doi: 10.1038/nm.2969. Epub 2012 Oct 21. PMID: 23086476.

- Woods K, Guezguez B. Dynamic Changes of the Bone Marrow Niche: Mesenchymal Stromal Cells and Their Progeny During Aging and Leukemia. Front Cell Dev Biol. 2021 Aug 10;9:714716. doi: 10.3389/fcell.2021.714716. PMID: 34447754; PMCID: PMC8383146.

- Yamamoto R, Morita Y, Ooehara J, Hamanaka S, Onodera M, Rudolph KL, Ema H, Nakauchi H. Clonal analysis unveils self-renewing lineage-restricted progenitors generated directly from hematopoietic stem cells. Cell. 2013 Aug 29;154(5):1112-1126. doi: 10.1016/j.cell.2013.08.007. PMID: 23993099.

- Yamanouchi J, Hato T, Kunishima S, Niiya T, Nakamura H, Yasukawa M. A novel MYH9 mutation in a patient with MYH9 disorders and platelet size-specific effect of romiplostim on macrothrombocytopenia. Ann Hematol. 2015 Sep;94(9):1599-600. doi: 10.1007/s00277-015-2416-x. Epub 2015 Jun 9. PMID: 26051904.

- Yang L, Bryder D, Adolfsson J, Nygren J, Månsson R, Sigvardsson M, Jacobsen SE. Identification of Lin(-)Sca1(+)kit(+)CD34(+)Flt3- short-term hematopoietic stem cells capable of rapidly reconstituting and rescuing myeloablated transplant recipients. Blood. 2005 Apr 1;105(7):2717-23. doi: 10.1182/blood-2004-06-2159. Epub 2004 Nov 30. PMID: 15572596.

- Yang Y, Liu C, Lei X, Wang H, Su P, Ru Y, Ruan X, Duan E, Feng S, Han M, Xu Y, Shi L, Jiang E, Zhou J. Integrated Biophysical and Biochemical Signals Augment Megakaryopoiesis and Thrombopoiesis in a Three-Dimensional Rotary Culture System. Stem Cells Transl Med. 2016 Feb;5(2):175-85. doi: 10.5966/sctm.2015-0080. Epub 2015 Dec 23. PMID: 26702125; PMCID: PMC4729548.

- Yu J, Hu K, Smuga-Otto K, Tian S, Stewart R, Slukvin II, Thomson JA. Human induced pluripotent stem cells free of vector and transgene sequences. Science. 2009 May 8;324(5928):797-801. doi: 10.1126/science.1172482. Epub 2009 Mar 26. PMID: 19325077; PMCID: PMC2758053.

- Yvernogeau L, Gautier R, Petit L, Khoury H, Relaix F, Ribes V, Sang H, Charbord P, Souyri M, Robin C, Jaffredo T. In vivo generation of haematopoietic stem/progenitor cells from bone marrow-derived haemogenic endothelium. Nat Cell Biol. 2019 Nov;21(11):1334-1345. doi: 10.1038/s41556-019-0410-6. Epub 2019 Nov 4. PMID: 31685991.

- Zaninetti C, Barozzi S, Bozzi V, Gresele P, Balduini CL, Pecci A. Eltrombopag in preparation for surgery in patients with severe MYH9-related thrombocytopenia. Am J Hematol. 2019 Aug;94(8):E199-E201. doi: 10.1002/ajh.25500. Epub 2019 May 8. PMID: 31034630.

- Zaninetti C, Gresele P, Bertomoro A, Klersy C, De Candia E, Veneri D, Barozzi S, Fierro T, Alberelli MA, Musella V, Noris P, Fabris F, Balduini CL, Pecci A. Eltrombopag for the treatment of inherited thrombocytopenias: a phase II clinical trial. Haematologica. 2020 Mar;105(3):820-828. doi: 10.3324/haematol.2019.223966. Epub 2019 Jul 4. PMID: 31273088; PMCID: PMC7049343.

- Zaoming W, Codina R, Fernández-Caldas E, Lockey RF. Partial characterization of the silk allergens in mulberry silk extract. J Investig Allergol Clin Immunol. 1996 Jul-Aug;6(4):237-41. PMID: 8844500.

- Zhang J, Niu C, Ye L, Huang H, He X, Tong WG, Ross J, Haug J, Johnson T, Feng JQ, Harris S, Wiedemann LM, Mishina Y, Li L. Identification of the haematopoietic stem cell niche and control of the niche size. Nature. 2003 Oct 23;425(6960):836-41. doi: 10.1038/nature02041. PMID: 14574412.